DISSERTATION

zum Thema

Effects of ultrarelativistic plasmas on cosmological perturbations

ausgeführt zum Zwecke der Erlangung des akademischen Grades
Doktor der technischen Wissenschaften

eingereicht an der Technischen Universität Wien
Technisch Naturwissenschaftliche Fakultät

von

Dipl.-Ing. Dominik J. Schwarz

Rochusgasse 6/8, A-1030 Wien
Matrikelnummer 8626486
geboren am 15. Jänner 1968 in Wien

Wien, im Mai 1995 ....

Abstract

The progenitors of large-scale structure, like clusters, voids or great walls, in the almost isotropic and homogeneous universe are described by linear perturbation theory at early times. The dynamics of density perturbations, rotational perturbations, and gravitational waves depends on the matter content of the universe. At high temperatures, close to the big bang, matter forms a relativistic plasma. Strongly interacting particles behave like a perfect fluid (e.g. photons and baryons). Other particles, which are weakly interacting or collisionless (e.g. neutrinos), give rise to anisotropic pressure and additional phenomena such as collisionless damping.

The aim of this work is to investigate the evolution of gauge-invariant cosmological perturbations during the radiation dominated epoch of the universe on a fundamental level. Therefore thermal field theory is used to describe a plasma of ultrarelativistic particles close to thermal equilibrium and to study its effects on the dynamics of the perturbations. From the thermal graviton self-energy the perturbation of the energy-momentum tensor is calculated in a manifest gauge-invariant manner. For a collisionless plasma it is shown that the high temperature limit of the field theoretic approach is equivalent to the kinetic approach. For a collisional plasma we go beyond the kinetic approach by performing a resummation of the hard thermal loops.

Exact (regular and singular) solutions are obtained for a collisionless gas mixed with a perfect fluid. The dependence on the initial conditions is studied in detail. Dimension dependent effects, such as directional dispersion, are investigated. A simple toy model is used to understand the effects of weak self-interactions in the plasma.

To Petra

I am thankful to my parents for rendering my studies possible and for their support during this time. I thank my wife for her love and patience and her interest in my work.

I like to thank Anton K. Rebhan for raising my interest in the subjects of cosmological perturbations and thermal field theory and for his collaboration and support. I benefitted much from collaboration with Herbert Nachbagauer.

I am grateful for discussions with Herbert Balasin, Ed Bertschinger, Franz Embacher, Julio Fabris, Maximilian Kreuzer, Jerome Martin, and Wolfgang Mödritsch. I thank Anton K. Rebhan, Herbert Nachbagauer, and Petra Lutter for proofreading and comments on the manuscript. My gratitude goes to the Institut für Theoretische Physik and all its members for providing good working conditions, especially to Wolfgang Kummer for his promotion.

My work was supported by the FWF projects P9005-PHY and P10063-PHY and the HCM network "Physics at high energy colliders".

Heinz Erhardt
Der rötliche Mars und die Venus

Früher zogen Mars und Venus —
wann es war, kann man nur ahnen —
eng beinander und in Liebe
ihre vorgeschriebnen Bahnen.

Plötzlich kam ein fremder Körper,
der sich zwischen beide zwängte
und den Mars von seiner Venus
oder umgekehrt — verdrängte.

Dieser Fremdling war die Erde!
Und sie machte sich noch breiter,
und der Mars entschwand der Venus
immer weiter, immer weiter.

Und die Sehnsucht nach der Freundin
hat den Mars schon fast getötet;
doch — erblickt er sie von ferne,
sehn wir, wie er zart errötet . . .

Contents

1 Introduction **2**
1.1 Isotropic cosmology 7
1.2 Evolution of fluctuations 14
1.3 Primordial fluctuations 17

2 Linear perturbations **19**
2.1 Gauge dependence 19
2.2 Bardeen's variables 22
2.3 Perfect fluid perturbations 25
2.3.1 Radiation dominated model 26
2.3.2 Matter dominated model 27
2.4 Perfect fluid plus relativistic plasma 28
2.4.1 Collisionless damping 29

3 Thermalized matter **31**
3.1 The thermal graviton self-energy 32
3.1.1 Scalar perturbations 36
3.1.2 Vector perturbations 36
3.1.3 Tensor perturbations 37
3.2 Collisional matter (n=3) 37
3.2.1 Scalar perturbations 41
3.2.2 Vector perturbations 42
3.2.3 Tensor perturbations 42
3.3 The Boltzmann equation (n=3) 43
3.3.1 Scalar perturbations 45
3.3.2 Vector perturbations 46
3.3.3 Tensor perturbations 47

4 Perturbations with relativistic plasmas **49**
4.1 Collisionless matter mixed with a perfect fluid 52
4.1.1 Scalar perturbations 52

4.1.2 Vector perturbations 56
4.1.3 Tensor perturbations 61
4.2 Dimension dependent effects 61
4.2.1 Scalar perturbations 63
4.2.2 Vector perturbations 63
4.2.3 Tensor perturbations 64
4.3 Weakly self-interacting matter 66

5 Conclusion and outlook 73

Appendix 76

A Notations 76

B Integrals 79
B.1 Collisionless matter 79
B.2 Collisional matter 80

C Recursion relations 84
C.1 Scalar perturbations 84
C.2 Vector perturbations 86
C.3 Tensor perturbations 87

Bibliography 89

Chapter 1

Introduction

In clear nights we face an astonishing amount of stars in the sky. Most of the stars we see by eye belong to the Milky Way ($\gamma\alpha\lambda\alpha\xi\acute{\iota}\varsigma$ as the old Greek said). We may even have a look at our neighbour galaxy, the Andromeda Nebula (M31 as the astronomers say). We are living at the edge of the Milky Way, about 8.5 kpc from its center, whereas our neighbour M31 is approximately 770 kpc away from us. These are incredible distances in comparison with our own size (1pc $= 3.086 \times 10^{16}$m ~ 3 light years). By means of modern telescopes a much larger part of the universe has been looked at. It turns out that the Milky Way and M31 are part of the so-called Local Group of galaxies, all within 1 Mpc.

The distance to stars far away and to galaxies cannot be measured directly. What can be measured is the redshift of light emitted by that objects. The relation between redshift and distance of an object is model dependent. The lack of our knowledge about the expansion rate of the universe is coded in the parameter h^{-1}, which is related to the distance by the Hubble law (see below). Exploring the universe more deeply, we find other groups and clusters of galaxies like the Coma cluster, which has a size of 15 h^{-1} Mpc and is about 70 h^{-1} Mpc away. The galaxy distribution in the region of the Coma cluster is shown in Fig. 1.1 [1] at 13^{h} right ascension. Each dot represents a galaxy. The linear structure across the whole slice is the so-called Great Wall. Its size exceeds 100 h^{-1} Mpc. The large regions containing almost no galaxies are called voids. For a more detailed review of the observed large-scale structure see the books by P.J.E. Peebles [2, 3]. On grounds of much deeper (but only angular) surveys (mainly in the infra-red and X-ray range of the spectrum) and by galaxy counts it is argued that, as smoothed over scales comparable with the Hubble scale (3 h^{-1} Gpc; see below), the distribution of matter is homogeneous. Of course, at scales of the Milky Way, the Local Group, or the Local Supercluster, the distribution of galaxies is

Figure 1.1: A cone diagram from the CfA survey of galaxies with blue magnitude smaller than 15.5 in the declination range 26.5° to 32.5° [1]. The dots show redshift versus right ascension for 1057 galaxies.

inhomogeneous.

A natural question to ask is whether the large-scale structure is just out there (placed there by a creator) or whether it has evolved and is still evolving. The observation that the redshift of starlight is related to the distance of the source led Hubble assume a linear relation between velocity v and distance d of galaxies, $v = H_0 d + v_{\mathrm{peculiar}}$, where H_0 is the Hubble constant (or expansion rate), convenient units are:

$$H_0 = 100\ h\ \mathrm{km\ s^{-1} Mpc^{-1}} \tag{1.1}$$

From observations the dimensionless quantity h is restricted to the intervall $(0.4, 1)$ [4]. The distance is related to the redshift for nonrelativistic velocity v by

$$d = \frac{cz}{H_0} + O\left((\frac{cz}{H_0})^2 \right) \ . \tag{1.2}$$

The distance where the redshift exceeds unity is called the Hubble length $\ell_{\mathrm{H}} = c/H_0 = 3\ h^{-1}$ Gpc. The Hubble relation indicates that all galaxies (exept the local ones) are moving away from us, thus supporting an evolving universe. The evolution of stars is in favour of an evolving universe, too.

Gravity is the only force acting on scales as large as the Hubble length (electrostatic forces cancel since the universe is neutral, magnetic forces are possible, they give rise to anisotropic models). Einstein's general relativity is a good description of gravity, at least for scales well above the Planck length $\ell_{\mathrm{Planck}} = 1.616 \times 10^{-35}$m. (Note that 1Gpc $= 1.91 \times 10^{60} \ell_{\mathrm{Planck}}$.) In order to solve the Einstein equations we need guiding principles to select the cosmologically relevant boundary conditions. First of all, we assume the Copernicanian Principle: We are not in any way privileged observers. The second assumption is the Relativity Principle: The laws of physics are the same everywhere in space-time. In its strongest versions these two may be summarized to the so-called Cosmological Principle [5] (although Einstein was guided to it by another argument [3]):

(i) The space-time manifold $\mathcal{M}$ has topology $\mathcal{M} = I \times \Sigma$, with Σ being space-like and maximally symmetric and $I \subseteq \mathrm{I\!R}$, i.e. the space is homogeneous and isotropic.

(ii) All observables respect this symmetry, i.e. the metric, the Riemann curvature, and other tensorfields.

The Cosmological Principle leads to the Friedmann-Lemaître-Robertson-Walker (FLRW) models, describing an expanding universe. These models explain the Hubble law by the expansion of space-time. Accordingly, the universe

Figure 1.2: Difference of the FIRAS spectrum of the cosmic microwave background radiation to a $T = 2.726$ K black body spectrum [6].

started in a space-time singularity, the big bang. All matter was thermalized in a primordial fireball, which cooled due to the expansion. The dominant matter contribution was radiation. During various transitions matter formed from fundamental particles. Some prominent transitions are the hadronization of the quarks and gluons followed by fusion of protons and neutrons to primodial nuclei (He, D, etc.) in nucleosynthesis. As time goes by, electrons and nuclei combine to atoms, and the universe becomes luminous. Strong support for isotropy on large scales comes from the cosmic background radiation (CBR), which is a perfect black body radiation (Fig. 1.2) at a temperature of 2.726 ± 0.017 K [6]. It is the redshifted radiation from the time when the universe got luminous ($z \sim 1000$). The temperature fluctuations across the sky have been measured by the COBE satellite to be $\delta T/T \sim 10^{-5}$ on large scales ($\sim 7°$) [7]. From the electroweak scale ($T \sim 100$ GeV) to the recombination of atoms ($T \sim 1\mathrm{eV} k_\mathrm{B}^{-1} = 1.161 \times 10^4$ K) the simple FLRW models together with particle physics are extremely successful in describing the early universe. Since the model is isotropic and homogeneous, it describes a structureless universe. Today, this universe would consist of a homogeneous, cold gas cloud of light atoms (H, He, etc.).

This gives rise to the question, *how did the large-scale structure of the universe form?* It is argued that there had been small primordial fluctuations, which oscillated during the radiation dominated epoch. While the universe cooled down, it became dominated by nonrelativistic matter (dust). Now the fluctuations are allowed to grow due to gravitational amplification. After exceeding a certain limit they are expected to collapse. Subsequently, matter heats up due to the interplay of gravitational attraction and pressure. From hot gas clouds, stars, and galaxies may form.

In this work we will deal with the evolution of fluctuations in the radiation dominated epoch of the early universe. Since the perturbations of FLRW models are small at this epoch, solutions to the linearized Einstein equations are studied. Matter is described by thermal quantum-field theory. We study the effects of relativistic plasmas and perfect fluids on density and pressure fluctuations, rotational perturbations, and gravitational waves. The number of spatial dimensions is $n \geq 3$. Higher dimensional spaces may be of interest for alternative cosmological models as Kaluza-Klein models [8] and will be useful to understand some dimension dependent features of cosmological perturbations.

In the following section (1.1) the isotropic FLRW models are introduced. We will also comment on alternative scenarios. The basic principles of structure formation from the generation of fluctuations to their collapse are explained in section 1.2. In the last section of this chapter (1.3) mechanisms for the generation of initial fluctuations are discussed.

In the second chapter the theory of linear perturbations and gauge-invariant metric potentials is set up. We discuss the linearization of the Einstein equations and related gauge problems. The linearized equations will be formulated in terms of gauge-invariant quantities and solved for perfect fluids in a flat FLRW model in the RD and MD regime. The third capter is devoted to the high-temperature evaluation of the thermal graviton self-energy (or polarization tensor). The graviton self-energy is used to calculate the perturbations of the energy-momentum tensor. This closes the linearized Einstein equations. Their solutions are obtained in the fourth chapter, where the effects of relativistic plasmas on cosmological perturbations are discussed. The last chapter contains a discussion of unsolved problems related to the thermal-field-theoretic approach to cosmological perturbations and a summary of our results.

Our notation is summarized in the appendix A. We use units $c = \hbar = k_B = 1$ and keep $G = m_{\rm Planck}^{1-n}$.

1.1 Isotropic cosmology

In general relativity space-time is defined by the topology of a differentiable manifold $\mathcal{M}$ and its causal and metric structure g [9]. The Cosmological Principle restricts the topology of space-time, such that space-like hypersurfaces have to exist at any time, i.e. $\mathcal{M} = I \times \Sigma^n$; n is the number of spatial dimensions. The metric has to be diffeomorphic to the Robertson-Walker (RW) metric. The line element associated with the RW metric reads:

$$ds^2 = -dt^2 + S^2(t)\left(\frac{dr^2}{1-\kappa r^2} + r^2 d\Omega_{n-1}^2\right) . \tag{1.3}$$

$S(t)$ is the cosmic scale factor, t is the cosmic time, and $d\Omega_{n-1}$ is the surface element of the $n-1$ dimensional Euclidian sphere. The RW metric describes space-times with hyperbolic ($\kappa = -1$), flat ($\kappa = 0$), or spherical ($\kappa = 1$) geometry, i.e. negative, zero, or positive spatial curvature ${}^nR = n(n-1)\kappa/S^2$. The enveloping spaces for the three cases are $\mathcal{U} \in \{\mathrm{H}^n, \mathrm{I\!R}^n, \mathrm{S}^n\}$. The isotropic and homogeneous space-times have $n(n+1)/2$ Killing vector-fields. They are in convolution and form a basis of the isometry group $\mathcal{G}$. All topologies compatible with the Cosmological Principle are given by the quotient spaces $\Sigma^n = \mathcal{U}/\mathcal{H}$ [10], where $\mathcal{H} \subseteq \mathcal{G}$. In the following we will be interested in the local structure of space-time only. Thus, we choose $\Sigma^n = \mathcal{U}$.

The RW coordinates behave singularly at $r = 1$ in the spherical case. This can be circumvented by the coordinate transformation $r = f(\chi)$, with

$$f(\chi) = \frac{\sin(\sqrt{\kappa}\chi)}{\sqrt{\kappa}} = \begin{cases} \sin(\chi) & \kappa = 1 \\ \chi & \kappa = 0 \\ \sinh(\chi) & \kappa = -1 \end{cases} .$$

Now $\chi \in [0, \infty)$ for hyperbolic or flat geometries, and $\chi \in [0, \pi)$ for spherical geometry. In the new coordinate χ the line element (1.3) reads:

$$ds^2 = -dt^2 + S^2(t)\left(d\chi^2 + f^2(\chi) d\Omega_{n-1}^2\right) . \tag{1.4}$$

Let us call these coordinates *comoving*, since they describe the universe for an observer whose proper time corresponds to the cosmic time. The dot will be used to denote derivatives with respect to cosmic time. The distance between two comoving galaxies at the time t is $d = S(t)\Delta\chi$. Its relative velocity is $v = Hd$, where $H := \dot{S}/S$ is the expansion rate. Its current value is called the Hubble constant H_0. Due to the time dependence of distances, the wavelength of light is shifted with time. The shift of spectral lines is given by

$$z := \frac{\lambda_{\mathrm{obs}} - \lambda_{\mathrm{em}}}{\lambda_{\mathrm{em}}} = \frac{S(t_{\mathrm{obs}})}{S(t_{\mathrm{em}})} - 1 .$$

For short time intervals $S(t_{\rm em}) \sim S(t_{\rm obs}) + (t_{\rm em} - t_{\rm obs})\dot{S}(t_{\rm obs})$. Therefore $(c = 1)$

$$z \sim H_0(t_{\rm obs} - t_{\rm em}) = H_0 d$$

with d being the distance between observer and source. This is the Hubble law. From observations it is evident that $z > 0$ for sources far away, thus the universe is expanding, i.e. $\dot{S}(t) > 0$. The expanding space volume reads in comoving coordinates:

$$V(\Sigma^n) = S^n(t)\frac{2\pi^{\frac{n}{2}}}{\Gamma(\frac{n}{2})}\int d\chi f^2(\chi)\ .$$

It is finite for the spherical geometry and infinite for the other cases.

To study the propagation of photons and other massless particles in the early universe *conformal* time $\tau = \int^t dt'/S(t')$ is introduced. The conformal line element reads:

$$ds^2 = S^2(\tau)\left(-d\tau^2 + d\chi^2 + f^2(\chi)d\Omega^2_{n-1}\right)\ . \tag{1.5}$$

Derivatives with respect to the conformal time will be denoted by primes. The conformal time interval $\Delta\tau$ from emission to observation of a light signal equals the coordinate distance $\Delta\chi$. Thus, the maximum coordinate distance from which light can reach us equals the conformal coordinate age of the universe. Our present state cannot be influenced by processes that occured outside our past light-cone. The proper distance to the particle horizon is given by

$$d_{\rm h} = S(\tau)(\tau - \tau_1(t_1)) = S(t)\int_{t_1}^t \frac{dt'}{S(t')}\ . \tag{1.6}$$

where t_1 is the value of cosmic time of the inital singularity. Events with spatial separation greater $d_{\rm h}$ have never been in causal contact during epochs with $0 < w < 1/n$.

The FLRW space-times have vanishing Weyl curvature. This means that they are conformally flat. This is manifest after the transformation:

$$\begin{aligned}
\tau &= \frac{1}{\sqrt{\kappa}}\left[\arctan\left(\frac{\sqrt{\kappa}}{2}(T+R)\right) + \arctan\left(\frac{\sqrt{\kappa}}{2}(T-R)\right)\right] \\
\chi &= \frac{1}{\sqrt{\kappa}}\left[\arctan\left(\frac{\sqrt{\kappa}}{2}(T+R)\right) - \arctan\left(\frac{\sqrt{\kappa}}{2}(T-R)\right)\right]\ . \qquad (1.7)
\end{aligned}$$

Let us call T, R the conformal-flat coordinates. Their line element reads:

$$\begin{aligned}
ds^2 &= F^2(T,R)\left(-dT^2 + dR^2 + R^2 d\Omega^2_{n-1}\right) \qquad (1.8)\\
F(T,R) &= S(\tau(T,R))\left[\left(1 + \frac{\kappa}{4}(T+R)^2\right)\left(1 + \frac{\kappa}{4}(T-R)^2\right)\right]^{-\frac{1}{2}}\ .
\end{aligned}$$

The evolution of the cosmic scale factor is not determined by the Comological Principle. In general relativity the evolution of the metric is determined by the Einstein equations:

$$G_{\mu\nu} = -8\pi G T_{\mu\nu} \ , \tag{1.9}$$

where $G_{\mu\nu} = R_{\mu\nu} - \frac{1}{2} g_{\mu\nu} R$. A possible cosmological constant Λ is absorbed into the energy-momentum tensor. Observational limits show that it may play a role on scales $\Lambda^{-\frac{1}{2}} > 1$ Gpc [11].

The Cosmological Principle restricts the form of the energy-momentum tensor as well:

$$T_{\mu\nu} = u_\mu u_\nu (E + P) + g_{\mu\nu} P \ , \tag{1.10}$$

where $E = E(t)$ and $P = P(t)$. Formally, this is the energy-momentum tensor of a perfect fluid with energy E and isotropic pressure P. u_μ is the velocity of a observer comoving with the fluid, i.e. $u_\mu = \delta^0_\mu$ in comoving coordinates, normalized to $u_\mu u^\mu = -1$.

From (1.9) and (1.10) the Friedmann equations are obtained, using comoving coordinates:

$$\begin{aligned}
\left(\frac{\dot S}{S}\right)^2 + \frac{\kappa}{S^2} &= \frac{16\pi G}{n(n-1)} E && (1.11)\\
\frac{\ddot S}{S} + \frac{n-2}{2}\left[\left(\frac{\dot S}{S}\right)^2 + \frac{\kappa}{S^2}\right] &= -\frac{8\pi G}{n-1} P && (1.12)\\
\dot E + n\left(\frac{\dot S}{S}\right)(E+P) &= 0 \ . && (1.13)
\end{aligned}$$

The last equation follows from the first two equations. It expresses the covariant conservation of the energy density. Instead of E the dimensionless variable Ω is often used. It is defined by

$$\Omega := \frac{E}{E_{\text{flat}}} \ , \text{with} \quad E_{\text{flat}} = \frac{n(n-1)H^2}{16\pi G} \ . \tag{1.14}$$

It takes values $0 < \Omega < 1$ for $\kappa = -1$, $\Omega = 1$ for $\kappa = 0$, and $\Omega > 1$ for $\kappa = 1$. The observed value Ω_0 lies between 0.1 and 0.3, but $\Omega_0 \sim 1$ cannot be excluded [11].

Supplemented with an equation of state $P = P(E)$ the Friedmann equations can be solved. There are three important cases:

(i) the radiation dominated (RD) state, $P = E/n$,

(ii) the dust or matter dominated (MD) state, $P = 0$,

(iii) and the vacuum dominated (VD) state, $P = -E$.

Let us write $P = wE$, with $w = 1/n, 0, -1$ for the RD, MD, and VD models.

From the covariant conservation of energy density the scale dependence of E follows:

$$\frac{E}{E(S=1)} = S^{-n(1+w)} \ . \tag{1.15}$$

Detailed discussions of the various solutions can be found in [4, 3, 11].

The equations of state can be derived from microphysics. The energy-momentum tensor for a free and massless scalar particle is given (in flat space-time) by:

$$T^{\mu\nu} = \int \frac{d^{n+1}K}{(2\pi)^{n+1}} \left(\frac{1}{2}\eta^{\mu\nu} - \frac{K^\mu K^\nu}{K^2} \right) \ . \tag{1.16}$$

At zero temperature (after renormalization) a contribution to the vacuum energy follows (and $\Lambda := 8\pi G E$). Usually the renormalization is chosen to set the vacuum energy to zero, but as several phase transitions occur during the evolution of the universe a nonvanishing cosmological constant has to play an important role in the early universe, from the particle physics' point of view.

At finite temperature the well defined leading contribution in T is

$$E = \varepsilon(n) T^{n+1} \qquad \text{with } \varepsilon(n) := \frac{n\zeta(n+1)}{\pi^{\frac{n+1}{2}}\Gamma(\frac{n+1}{2})} \tag{1.17}$$

and the energy-momentum tensor being traceless. (In three spatial dimensions $\varepsilon(3) = \pi^2/30$.) This leads to the equation of state for radiation. The generalization to the FLRW models is simple for the RD epoch. As the energy density scales with S^{-n-1}, we see that the temperature scales with S^{-1}.

For other fields, (1.17) has to be multiplied by the number of physical (thermal) modes [1]

$$g_* = g_b + \frac{2^n - 1}{2^n} g_f \ ,$$

where g_b and g_f are the bosonic and fermionic degrees of freedom that are thermalized (at the same temperature T). In the early universe this number depends on the temperature, $g_* = g_*(T)$. The reason is that relativistic particles contribute to g_* only. At the epach of recombination $g_* \sim 6$, whereas

[1] Usually g_* counts multiples of photon degrees of freedom. Because this is a dimension dependent quantity we prefere this definition.

above the electroweak scale $g_* \sim 200$ considering the particle content of the minimal standard model (n=3).

The simplest procedure to calculate (1.17) is the imaginary time formalism (e.g. [12, 13]). The exponentiated Euclidian action of any field theory resembles a statistical partition function. The fields are periodical in imaginary time, because the Boltzmann factor is rewritten into an imaginary time evolution operator. The inverse of the periodicity length is identified with the temperature of the system. Now only discrete frequencies are allowed (Matsubara frequencies), the integral over k_0 in (1.16) is replaced by a sum

$$\int \frac{dk_0}{2\pi} \rightarrow T \sum_{j=-\infty}^{\infty} ,$$

with $k_0 = 2j\pi\imath T$ for bosonic frequencies and $k_0 = (2j+1)\pi\imath T$ for fermionic frequencies.

A collection of mass points does not give rise to a pressure term, only the energy density is nonzero for dust.

We solve the Friedmann equations for conformal coordinates, because we will focus on relativistic matter later on. The equations (1.11) – (1.13) are transformed to conformal time by

$$\frac{d}{dt} \rightarrow \frac{1}{S(\tau)} \frac{d}{d\tau} .$$

The solutions of (1.13) are the same in both time coordinates. For ordinary matter ($w \in [0, 1/n]$) we expect that the conformal scale factor is increasing with time: $\dot{S} > 0 \Rightarrow S' > 0$, i.e. the proper distance to the particle horizon is growing. From the Friedmann equations follows $\ddot{S} < 0 \Rightarrow S'' < 0$ for dust or radiation. Therefore there had to be an initial singularity — we set: $S(\tau_{\text{BigBang}} = 0) = 0$. With this initial condition the solution to the Friedmann equations is:

$$S(\tau) = \left[\sqrt{\frac{16\pi G E(S=1)}{n(n-1)}} f\left(\frac{|n(1+w)-2|}{2} \tau \right) \right]^{\frac{2}{n(1+w)-2}} . \qquad (1.18)$$

f is the same function as in the conformal line element (1.5). (1.18) is valid for the VD model too, but with different initial conditions. For these solutions the particle horizon is at constant distance for $\kappa = 0$ and at shrinking distance for $\kappa = -1$. For $\kappa = 1$ it is growing slowly.

It is evident from (1.18) that for $\kappa = 1$ the universe does not expand forever. After reaching its maximal extension at $\tau = \pi/2$ it starts to collapse and will end up in a big chrunch at $\tau = \pi$.

With (1.18) the relation between conformal time and cosmic time $t = \int^{\tau} S(\bar{\tau})d\bar{\tau}$ can be evaluated, e.g. for $\kappa = 0$

$$t \sim \tau^{\frac{n(1+w)}{n(1+w)-2}}, \quad \text{and } S(t) \sim t^{\frac{2}{n(1+w)}} .$$

Today ($t = t_0$) the overall pressure in the universe is almost zero ($P_0/E_0 \leq 10^{-4}$ [11]). Therefore we may describe the present epoch of the universe by the MD model. As we follow time backwards, the energy density of the relic radiation (the photonic CBR and neutrino background radiation) increases with S^{-4}, whereas the energy density of the dust increases with S^{-3}. Thus, at a certain time $t_{\rm eq}$ the density in dust and radiation is equal, and before that time radiation dominates the universe. This happens at a redshift of $z_{\rm eq} \sim 10^4$. According to the relation (valid in the MD model)

$$\Omega(z) = \frac{\Omega_0(1+z)}{1+\Omega_0 z} ,$$

the value of Ω was very close to 1 at early times. At the time of matter-radiation equilibration $\Omega(z_{\rm eq} = 10^4) = 0.99996$ for $\Omega_0 = 0.2$. Thus, the Einstein-de Sitter model ($\kappa = 0$) is a good approximation for the early universe. With increasing temperature atoms, nuclei, and even hadrons disapear, near the singularity the universe gets so dense that even weakly interacting particles as neutrinos will be thermalized.

Up to now we have considered the cosmological standard model. There are several questions that cannot be answered by this model, some of them are:

- Why do we live in four space-time dimensions?
- What is the reason for the observed isotropy, e.g. why has the CBR the same temperature in all directions in the sky, although two opposite regions in the sky have never been in causal contact (horizon problem)?
- Who or what created all the large-scale structure?

The question of space-time dimensions may be treated within Kaluza-Klein models [8], the problem is to find a unique procedure to compactify the invisible dimensions. Higher dimensional physics may be essential in the unification of the fundamental forces. An example is the theory of superstrings. A Kaluza-Klein scenario, which is interesting for our purpose, starts with an isotropic big bang, but in $n > 3$ spatial dimensions. Due to some mechanism (for a more detailed discussion see [8] and references therein) $n - 3$ dimensions start to recollapse after some time (Fig. 1.3). Space-time

Figure 1.3: Time dependence of the scale factors of 3-space $(a(t))$ and $n-3$-space $(b(t))$ from [8].

becomes anisotropic till the $n-3$ dimensions disappear effectively and an isotropic 3-space remains.

Another scenario starts with an anisotropic big bang. During the early evolution of the universe $n-3$ dimensions shrink, whereas 3 spatial dimensions grow and become the observable part of the universe.

This leads us to the question of isotropy. If the universe was anisotropic at early times, there could have been several mechanisms to isotropize it. An old idea is the mixmaster universe, a universe filled with a viscous fluid [14] or a universe filled with collisionless particles [15]. But there is a family of more appealing models, the inflationary universes, e.g. [11, 4]. In these models the universe undergoes an inflational growth of the cosmic scale factor (about 60 e-folds). As a consequence, the particle horizon is at shrinking distance or slowly growing, and wiggles in the space-time will be pushed far outside the horizon. The basic problem with inflationary theories is that there is a plethora of them. These models provide a possibility to create seeds for large scale structure. A second way to create seeds are topological defects [11, 4].

1.2 Evolution of fluctuations

Let us assume that there were some tiny ripples and wiggles in the energy density inside the particle horizon in the early universe. We write $E = \tilde{E} + \delta E$, where the tilde denotes quantities of a cosmological background model. We define

$$\delta := \frac{\delta E}{\tilde{E}} \ , \tag{1.19}$$

the density contrast. To understand how gravity can amplify the tiny fluctuations around the background we follow an analysis by Jeans [16] using Newtonian gravity. The Newtonian gravity potential is denoted by ϕ. Matter is described by a perfect fluid. The three equations of motion for E, $\mathbf{v}$, and ϕ are the continuity equation, the Euler equation, and the Poisson equation.

$$\begin{aligned} \dot{E} + \nabla \cdot (E\mathbf{v}) &= 0 \\ \dot{\mathbf{v}} + \mathbf{v} \cdot \nabla \mathbf{v} &= -\frac{1}{E}\nabla P - \nabla \phi \\ \nabla^2 \phi = 4\pi G E \ . & \end{aligned} \tag{1.20}$$

$P(E)$ is given by an equation of state and

$$c_s^2 := \left(\frac{\partial P}{\partial E}\right)_{\text{isentropic}} \cong \frac{\delta P}{\delta E} \tag{1.21}$$

defines the sound velocity. Assume a flat homogeneous background with $\tilde{\mathbf{v}} = 0$ and $\tilde{E}$ being constant. Note that the observer is comoving with the background. The linearized equations (1.20) read:

$$\begin{aligned} \delta\dot{E} + \tilde{E}\nabla\cdot\delta\mathbf{v} &= 0 \\ \delta\dot{\mathbf{u}} + \frac{c_{\mathrm{s}}^2}{\tilde{E}}\nabla\delta E + \nabla\delta\phi &= 0 \\ \nabla^2\delta\phi = 4\pi G\delta E \ . \end{aligned} \tag{1.22}$$

The last equation involves the so-called Jeans swindle, i.e. $\nabla\tilde{\phi} = 0$ in the second equation of (1.22) implies $\nabla^2\tilde{\phi} = 0$ (!) instead of $\nabla^2\tilde{\phi} = 4\pi G\tilde{E}$. A constant energy-density of the background is not consistent with a constant Newtonian gravity potential. Nevertheless, the result of Jeans is useful, and it will turn out that it is almost correct. Eliminating $\delta\phi$ and $\delta\mathbf{v}$ in (1.22) we obtain:

$$-\delta\ddot{E} + c_{\mathrm{s}}^2\nabla^2\delta E + 4\pi G\tilde{E}\delta E = 0 \ . \tag{1.23}$$

With the ansatz $\delta E = A\exp\imath(\omega t - \mathbf{kx})$ we obtain the dispersion law

$$\omega^2 = c_{\mathrm{s}}^2 k^2 - 4\pi G\tilde{E} \ .$$

For $k > k_{\mathrm{J}}$, with

$$k_{\mathrm{J}} := \left(\frac{4\pi G\tilde{E}}{c_{\mathrm{s}}^2}\right)^{\frac{1}{2}} \ ,$$

the density fluctiations δE oscillate in time, whereas for $k < k_{\mathrm{J}}$ the density contrast δ can grow or decay exponentially. As soon as the density contrast approaches unity the linear analysis is no longer applicable and non-linear methods have to be invoked.

The Jeans swindle was necessary within flat space-time, because an infinite homogeneous filled space-time is inconsistent with Newtonian gravity, as well as with General Relativity. Taking the expansion of space-time into account solves this problem. With scale dependent $\tilde{E}(S)$, $\nabla\tilde{\phi}$ has no longer to be zero. Instead of redoing the Newtonian analysis in an expanding background [4] (with $w = 0$), we can guess the critical comoving wave number as

$$k_{\mathrm{J}} = \left(\frac{4\pi G\tilde{E}(S)}{c_{\mathrm{s}}^2}\right)^{\frac{1}{2}} S \ ,$$

because k is the comoving wavenumber and $k/S(t)$ is the physical wave number. In addition to the scale dependence of the critical (comoving) wavelength

$$\ell_{\mathrm{J}} := 2\pi S^{-1}\left(\frac{c_{\mathrm{s}}^2}{4\pi G\tilde{E}(S)}\right)^{\frac{1}{2}} \sim c_{\mathrm{s}} S^{\frac{n-2}{2}} \sim c_{\mathrm{s}}\tau \ , \tag{1.24}$$

the expansion of the universe slows the growing (decaying) rate of the supercritical scales ($\ell > \ell_{\mathrm{J}}$). The growth (decay) is no longer described by an exponential, it follows a power law. This result will be obtained in the next chapter within the fully relativistic theory. The generalization to more than three spatial dimensions is simple. Apart from the prefactor on the r.h.s. of the Poisson equation all manipulations are dimension independent.

It is useful to define the Jeans mass to be the mass contained within a sphere of radius $\ell_{\mathrm{J}}/2$, i.e.

$$M_{\mathrm{J}} := \frac{4\pi}{3}\left(\frac{\ell_{\mathrm{J}}}{2}\right)^3 \tilde{E} \ . \tag{1.25}$$

Fluctuations of mass less than M_{J} are stable against gravitational collapse, while those of greater mass are unstable.

Besides the Jeans length the particle horizon $d_{\mathrm{h}} \sim \ell_{\mathrm{H}}$ is important in the description of cosmological perturbations. Let us call perturbations with wave length greater than d_{h} superhorizon perturbations and those with wave length smaller than d_{h} subhorizon perturbations. The superhorizon perturbations cannot grow due to the interplay between pressure and gravitational attraction, but they can grow due to geometrical effects of general relativity. We will discuss these effects in chapter four. Subhorizon perturbations are influenced by local processes. This is the region where the Jeans analysis is reasonable (weak gravitational fields and nonrelativistic velocities).

In the relativistic analysis the nonvanishing density contrast produces a deviation from the background metric, a metric perturbation

$$g_{\mu\nu} := \tilde{g}_{\mu\nu} + \delta g_{\mu\nu} \ ,$$

via the Einstein equations (1.9). On superhorizon scales there are two kinds of perturbations:

- Curvature (or adiabatic or isentropic) fluctuations are perturbations in the curvature on superhorizon scales.
- Isocurvature (or isothermal) fluctuations are perturbations in the local equation of state. On superhorizon scales they produce no perturbations in the curvature.

After horizon crossing isocurvature perturbations will turn into true curvature perturbations as well. In this work we will deal only with curvature fluctuations.

To understand the superhorizon perturbation general relativity is necessary. A rough picture can be obtained from a comparison of a $\kappa = 0$ and a $\kappa = 1$ FLRW model. The corresponding Friedmann equations read:

$$\begin{aligned} H^2 &= \frac{16\pi G}{n(n-1)} E - \frac{1}{S^2} \\ \tilde{H}^2 &= \frac{16\pi G}{n(n-1)} \tilde{E} \ . \end{aligned}$$

Comparing them when their expansion rate is equal leads to

$$\delta = \frac{E - \tilde{E}}{\tilde{E}} \sim \frac{1}{S^2 \tilde{E}} \ . \qquad (1.26)$$

If the density contrast is small, the scale factors are similar. With (1.15)

$$\delta \sim S^{n(1+w)-2} \qquad (1.27)$$

follows. For the RD and MD epoch the exponent is positive, we therefore expect a growth of the density contrast at superhorizon scales.

Assume a universe consisting of baryons and photons only [4]. In the RD epoch the initial fluctuations oscillate with constant amplitude on subhorizon scales. A local overdensity of mass points embedded in a RD universe cannot grow (Mészáros effect) [17]. When the model universe becomes MD, perturbations larger than ℓ_{J} can grow. After the decoupling of the baryons from the photons, the baryon Jeans wave length is much smaller than the horizon size. Some of the baryon overdensities will grow until $\delta \sim 1$. At this point nonlinear effects will become important. Additional effects as free streaming and directional dispersion will damp small scale fluctuations. They will be discussed later on.

The generic nature of the first generation of gravitationally bounded systems can be estimated by the analysis by Zel'dovich [18]. It applies to curvature perturbations that collapse during the MD epoch. The analysis shows that matter most likely forms an ellipsoid (without axial symmetry) from initially spherical distributions and that the shortest axis of this ellipsoidal overdensity will collapse first. This results in a sheetlike structure, the Zel'dovich pancake.

1.3 Primordial fluctuations

The Jeans analysis showed that gravity can act as an amplifier of density fluctuations, but the origin of the primordial fluctuations remains unknown.

Candidates to produce these fluctuations are the inflationary theories and theories of topological defects, like cosmic strings or textures.

The spectrum of the density fluctuations

$$\delta(t,\mathbf{k}) := \int d\mathbf{x} e^{-\imath \mathbf{k}\mathbf{x}} \delta(t,\mathbf{x})$$

at some time t, together with the appropriate initial conditions of all other variables in the Einstein equations, specifies the evolution of $\delta(t,\mathbf{x})$. Within the Newtonian approximation it is useful not to specify the spectrum at a fixed cosmic time, but to specify it for each mode $\mathbf{k}$ at horizon crossing, i.e. $t_h := S(t_h)\ell/2 = S(t_h)\pi/|\mathbf{k}|$. Otherwise a part of the perturbations would be superhorizon, the rest subhorizon. For the latter their detailed evolution after horizon crossing would be necessary to specify the spectrum. A scale-invariant spectrum

$$\delta_h(\mathbf{k}) := \delta(t_h,\mathbf{k}) = Ak^{\alpha}$$

was proposed. Harrison and Zel'dovich [19] suggested that $\alpha = 0$ and $A = 10^{-4}$ are the preferred values for those scales that are involved in the process of galaxy formation. δ_h can easily be related to the spectrum at a fixed epoch $t < t_{\mathrm{eq}}$ for superhorizon perturbations. From (1.27) $\delta_h(\mathbf{k}) = S^{n-1}(t_h)\delta(t,\mathbf{k})/S^{n-1}(t)$. Therefore

$$\delta(t_{\mathrm{initial}},\mathbf{k}) \sim k^{nx} \sim \ell^{-nx} \sim N^{-x}$$

with $x = \alpha/n + 2/n$. N is the number of particles in a volume ℓ^n. From thermal fluctuations we would expect $x = 1/2$ yielding $\alpha = (n-4)/2$ at horizon crossing, which would make galaxy formation impossible in three spatial dimensions [4].

All inflationary models predict a Harrison-Zel'dovich like spectrum ($x \sim 2/n$). The fluctuations are quantum fluctuations in the metric tensor, which are frozen in by the rapid expansion of space-time.

Topological defects are created during first order phase transitions. At the boundaries of the various bubbles a large amount of energy is stored. This gives rise to ripples in space-time. These defects of space-time may be four (textures), three (domain walls), two (cosmic strings), or one (monopoles) dimensional objects in space-time, depending on the group structure of the vacuum after the phase transition. Domain walls and monopoles are unrealistic, because they would dominate the mass of the universe leading to $\Omega \gg 1$.

Chapter 2

Linear perturbations

For small fluctuations a linearization of the general relativistic equations is useful. The theory of linear perturbations in a FLRW model dates back to Lifshitz' work in 1946 [20]. The metric perturbations and the corresponding perturbed energy-momentum tensor are decomposed into scalar, vector, and tensor parts according to their behaviour under spatial coordinate transformations. In linear theory these parts evolve independently. Any tensor $t^\mu{}_\nu$ is divided into a background part $\tilde{t}^\mu{}_\nu$ and a perturbation $\delta t^\mu{}_\nu := t^\mu{}_\nu - \tilde{t}^\mu{}_\nu$. The background is given by a FLRW model, as described in Chapter 1. The evolution of the metric and the matter perturbations is governed by the Einstein equation

$$\delta G^\mu{}_\nu = -8\pi G \delta T^\mu{}_\nu \ . \tag{2.1}$$

Unless stated otherwise, we use conformal coordinates (1.5).

2.1 Gauge dependence

The mapping of points x^μ on the physical manifold to points $\tilde{x}^\mu$ on the background is not unique. Therefore, unphysical (gauge) modes arise in the solutions. To give an example, it is possible to gauge the density contrast (1.19) to zero everywhere. This can be done by selecting a particular family of spacelike hypersurfaces of the physical manifold. An extensive discussion on the geometrical picture of cosmological perturbations can be found in [21].

Does this mean that the Jeans analysis from Chapter 1 is meaningless? It does not, because, implicitly, we fixed the frame to that of a comoving observer.

The relativistic treatment of linear perturbations was first done by Lifshitz [20], who introduced the synchronous gauge. It fixes the non-spatial components of the metric perturbations to zero. Because there is a residual gauge freedom in the synchronous gauge, a lot of confusion is found in the literature (the analysis in [20] is correct and almost complete for perfect fluid models, though). A discussion of several gauge dependent aspects within this gauge is presented in [22].

The longitudinal gauge (for the scalar metric perturbations) together with the vector gauge (for the vector metric perturbations) was first used by Stewart [23]. The advantage of this gauge is that there is no residual gauge freedom and that the Newtonian limit is well defined (in contrast to the synchronous gauge). A comparison of these gauges is given in [24].

There are also some other gauges. One example is the de Donder gauge [25]. The authors of [25] claim that in the de Donder gauge the "physical interpretation of results is obvious" (in contrast to the synchronous gauge), and from their analysis of the density contrast in the de Donder gauge they conclude "Gauge solutions should therefore not be taken as unphysical". It is obvious that this misleaded conclusions are caused by gauge artefacts. This is one example of a wrong result due to the use of a 'better' gauge.

The gauge modes can be avoided by using Bardeen's [26] gauge-invariant variables for the metric and matter components. We will use this formalism in order to avoid problems with residual gauge modes. In addition, the equations of motion for the metric potentials (see below) are the same as in the longitudinal gauge [27]. From the field theoretic point of view a gauge-invariant description seems to be more natural, i.e. the effective action is gauge-invariant for fixed background gauge.

Let us state, without proof, two general lemmata from [28] which are relevant for the construction and the understanding of gauge-invariant quantities. Note that by 'gauge invariance' we do not mean the coordinate invariance (diffeomorphisms) of general relativity, but the invariance under the change of the identification of points on the physical and the background manifold.

Lemma 1: The change of a linear perturbation δQ on $\mathcal{M}$, the physical space-time, under the change of the mapping of points from the background space-time $\tilde{\mathcal{M}}$ to $\mathcal{M}$ is given by

$$\Delta\delta Q := \delta Q' - \delta Q = \mathcal{L}_\xi \tilde{Q} \ ,$$

where the prime denotes the new identification and $\mathcal{L}_\xi$ is the Lie derivative defined by the vector field $\xi(x) = x' - x$.

Lemma 2: The linear perturbation δQ is identification gauge invariant, if and only if one of the following holds:

(i) $\tilde{Q}$ vanishes,

(ii) $\tilde{Q}$ is a constant scalar,

(iii) $\tilde{Q}$ is a constant linear combination of products of Kronecker deltas.

From the second lemma it is clear that the components of the Weyl tensor define gauge-invariant quantities, because the Weyl tensor vanishes for all FLRW models. In flat space-time the Ricci tensor may be used to define gauge-invariant quantities.

A better geometrical understanding of Bardeen's variables has been obtained by the group of Ellis [21]. Their analysis relies on a fluid description of the universe and is not restricted to linear perturbations. In contrast to Bardeen's work all equations are formulated for the fluid variables. It was shown that Bardeen's metric potentials are related to spatial gradients of components of the Weyl tensor.

Besides the splitting into scalar, vector, and tensor components the spatial dependence has been separated from the time evolution by the decomposition into spherical harmonics by Lifshitz [20]. The approach of Bardeen followed this tradition. In the linear regime the various modes decouple, and a set of ordinary differential equations remains.

A formulation of gauge-invariant linear perturbations which does not decouple the spatial dependence was given in [29]. In the formulation of Ellis and coworkers the harmonic analysis is omitted, too. As their formalism applies to nonlinear perturbations as well, the harmonic modes would not decouple any more.

Under what circumstances is the theory of linear perturbations valid? We mentioned that the fluctuations should be small — how can we asign a definite meaning to that statement? By means of gauge transformations we may blow up any gauge mode to arbitrary size. Therefore it is sufficient to demand that all gauge-invariant variables should be small, i.e. their absolut value should be much smaller than 1. Moreover, using a hydrodynamic model for the matter content of the universe — the basic quantity being the flow of the fluid u^μ — we assume that the space-velocity

$$\mathbf{v} := \frac{\mathbf{u}}{u^0}$$

is nonrelativistic. Even if matter is dominated by relativistic particles, this is a good approximation, because $\mathbf{v}$ is the mean velocity of particles.

For useful reviews of gauge-invariant cosmological perturbation theory see, e.g. Refs. [30], [27], [31], and [32].

2.2 Bardeen's variables

As already explained above, the perturbed tensors are divided into scalar, vector and tensor parts:

$$\begin{array}{rcl} \delta g_{\mu\nu} & = & \delta g^S_{\mu\nu} + \delta g^V_{\mu\nu} + \delta g^T_{\mu\nu} \ , \\ \delta T^\mu{}_\nu & = & \delta T^{S\mu}{}_\nu + \delta T^{V\mu}{}_\nu + \delta T^{T\mu}{}_\nu \ . \end{array} \tag{2.2}$$

Both tensors have $(n+2)(n+1)/2$ independent components, four of which belong to the scalar, $2n-2$ to the vector and $n(n-1)/2-1$ to the tensor part (the latter correspond to the polarizations of a gravitational wave).

In a spatially homogeneous and isotropic universe all scalars, vectors and tensors may be decomposed into spherical harmonics. This is useful to separate the time evolution from the spatial dependence. All spherical harmonics are solutions of the Helmholtz equation:

$$(\triangle + k^2) Q^{(a)}_{i_1,\ldots,i_a} = 0 \ ,$$

where $\triangle := \nabla_i \nabla_j \gamma^{ij}$, and γ_{ij} is the spatial background metric without the cosmic scale factor. ∇_i is the covariant derivative with respect to γ_{ij}. The scale of the perturbation is set by its wave number k. $a = 0, 1, 2$ stands for scalar, vector, and tensor harmonics. A vector can be defined from the scalar harmonics by

$$Q^{(0)}_i := -\frac{1}{k} \nabla_i Q^{(0)}$$

and a traceless, symmetric tensor by

$$Q^{(0)}_{ij} := \frac{1}{k^2} \left(\nabla_i \nabla_j - \frac{1}{n} \gamma_{ij} \triangle \right) Q^{(0)} \ .$$

From the vector harmonics a traceless, transverse, and symmetric tensor is given by

$$Q^{(0)}_{ij} := -\frac{1}{k} \nabla_{(i} Q^{(1)}_{j)} \ .$$

With this harmonics any symmetric tensor can be decomposed into its scalar, vector and tensor part. This is done for each individual mode proportional to $Q^{(a)}$ of Eqs. (2.2) as follows $[\{\mu, \nu\} = \{(0,i),(0,j)\}]$:

$$\delta g^S_{\mu\nu} = S^2 \begin{pmatrix} -2AQ^{(0)} & -B^{(0)} Q^{(0)}_j \\ -B^{(0)} Q^{(0)}_i & 2\left[\gamma_{ij} H_L Q^{(0)} + H^{(0)}_T Q^{(0)}_{ij}\right] \end{pmatrix} , \tag{2.3}$$

$$\delta g^V_{\mu\nu} = S^2 \begin{pmatrix} 0 & -B^{(1)} Q^{(1)}_j \\ -B^{(1)} Q^{(1)}_i & 2H^{(1)}_T Q^{(1)}_{ij} \end{pmatrix} , \tag{2.4}$$

$$\delta g^T_{\mu\nu} = S^2 \begin{pmatrix} 0 & 0 \\ 0 & 2H^{(2)}_T Q^{(2)}_{ij} \end{pmatrix} \tag{2.5}$$

and

$$\begin{aligned}
\delta T^{S\mu}{}_{\nu} &= \begin{pmatrix} -\tilde{E}\delta Q^{(0)} & (\tilde{E}+\tilde{P})\left(v^{(0)}-B^{(0)}\right)Q_j^{(0)} \\ -(\tilde{E}+\tilde{P})v^{(0)}Q^{(0)i} & \tilde{P}\left(\delta^i_j\pi_L Q^{(0)}+\pi_T^{(0)}Q_j^{(0)i}\right) \end{pmatrix}, \quad (2.6)\\
\delta T^{V\mu}{}_{\nu} &= \begin{pmatrix} 0 & (\tilde{E}+\tilde{P})\left(v^{(1)}-B^{(1)}\right)Q_j^{(1)} \\ -(\tilde{E}+\tilde{P})v^{(1)}Q^{(1)i} & \tilde{P}\pi_T^{(1)}Q_j^{(1)i} \end{pmatrix}, \quad (2.7)\\
\delta T^{T\mu}{}_{\nu} &= \begin{pmatrix} 0 & 0 \\ 0 & \tilde{P}\pi_T^{(2)}Q_j^{(2)i} \end{pmatrix}. \quad (2.8)
\end{aligned}$$

The metric components $A(\tau,k)$, $B^{(a)}(\tau,k)$, $H_L(\tau,k)$, $H_T^{(a)}(\tau,k)$ and the matter variables $\delta(\tau,k)$, $v^{(a)}(\tau,k)$, $\pi_L(\tau,k)$, $\pi_T^{(a)}(\tau,k)$ with $a=\{0,1\}$ transform non-trivially under gauge transformations, i.e., coordinate transformations of the perturbed manifold while keeping the background fixed. Only the tensor components ($a=2$) are gauge-invariant by themselves. The gauge transformations for scalar modes are

$$\begin{aligned}
\bar{\tau} &= \tau + T(\tau,k)Q^{(0)}\,,\\
\bar{x}^i &= x^i + L^{(0)}(\tau,k)Q^{(0)i}\,,
\end{aligned} \tag{2.9}$$

and

$$\bar{x}^i = x^i + L^{(1)}(\tau,k)Q^{(1)i} \tag{2.10}$$

for the vector perturbations. Note, these are restricted gauge transformations in the sense that they have to respect the foliation of space-time.

From (2.9) and (2.10) follows that only two scalar "potentials" and one vector "potential" of the metric perturbations are gauge-invariant. A set of such metric potentials is given by

$$\begin{aligned}
\Phi &:= 2\left[H_L + \tfrac{1}{n}H_T^{(0)} + \tfrac{1}{k}\tfrac{S'}{S}(B^{(0)} - \tfrac{1}{k}H_T'^{(0)})\right]\,,\\
\Pi &:= -\left[A + (n-2)\left(H_L + \tfrac{1}{n}H_T^{(0)}\right) + \tfrac{1}{k}(B^{(0)} - \tfrac{1}{k}H_T'^{(0)})'\right.\\
&\quad \left. + \tfrac{n-1}{k}\tfrac{S'}{S}(B^{(0)} - \tfrac{1}{k}H_T'^{(0)})\right]
\end{aligned} \tag{2.11}$$

for the scalar part and by

$$\Psi := B^{(1)} - \frac{1}{k}H_T'^{(1)} \tag{2.12}$$

for the vector perturbations. Φ and Π are transformed into the variables used by Bardeen [26] by

$$\begin{aligned}
\Phi_H &= \frac{1}{2}\Phi\\
\Phi_A &= -\Pi - \frac{n-2}{2}\Phi\,.
\end{aligned}$$

In the same manner gauge-invariant matter variables can be defined. For the scalar perturbations we introduce

$$
\begin{array}{rcl}
\eta & := & \pi_L - \frac{c_s^2}{w}\delta \\
v_s^{(0)} & := & v^{(0)} - \frac{1}{k} H_T^{\prime(0)} \\
\epsilon_m & := & \delta + n(1+w)\frac{1}{k}\frac{S'}{S}\left(v^{(0)} - B^{(0)}\right) \\
\epsilon_g & := & \epsilon_m - n(1+w)\frac{1}{k}\frac{S'}{S} v_s^{(0)} \ .
\end{array} \tag{2.13}
$$

η is called the entropy perturbation, although it may not coincide with the perturbation in the true physical entropy. $v_s^{(0)}$ is the amplitude of the matter velocity and is related to the shear σ by $\sigma = v_s^{(0)} k/S$ [26]. ϵ_m is the density contrast on a spacelike hypersurface which represents the local rest-frame of matter everywhere, whereas ϵ_g is the density perturbation on a hypersurface whose normal vector has no shear. The anisotropic pressure $\pi_T^{(0)}$ is gauge-invariant by itself.

For vector perturbations the invariant matter variables are

$$
v_s^{(1)} := v^{(1)} - \frac{1}{k} H_T^{\prime(1)} =: v_c + \Psi \ , \tag{2.14}
$$

where $v_s^{(1)}$ can be understood as in the scalar case and v_c is the velocity relative to the normal to the constant-time hypersurface. $v_c k/S$ is the intrinsic angular velocity (vorticity) [26]. The anisotropic pressure $\pi_T^{(1)}$ is gauge-invariant as above. For tensor perturbations the only physical variables are given by the metric potential $H_T^{(2)} =: H$ and the anisotropic pressure $\pi_T^{(2)}$, both already gauge-invariant. (Here we follow the conventions of Ref. [26], which differ from the definitions of Ψ and H in Ref. [45] by a factor of 2.)

From the Einstein equations (2.1) relations between the metric potentials Φ, Π, Ψ, and H and the matter variables $\eta, \epsilon_m, \epsilon_g, \pi_T^{(a)}, v_s^{(a)}$, and v_c follow. The details are given in Ref. [26]. For the scalar components

$$
(k^2 - n\kappa)\Phi = \frac{16\pi G S^2 \tilde{E}}{n-1}\epsilon_m \tag{2.15}
$$

$$
k^2 \Pi = 8\pi G S^2 \tilde{P} \pi_T^{(0)} \ , \tag{2.16}
$$

which shows the reason for our choice of the metric potentials: Φ is a potential for the density perturbation and Π the potential for the anisotropic pressure perturbation. Eq. (2.15) is the Poisson equation used in the Jeans analysis (chapter 1) with $\Phi = -2\phi$, $S = 1$, and $\tilde{E}\epsilon_m = E$. Another set of equations is useful:

$$\begin{aligned}&(n-1)\left\{\tfrac{n}{2}\Phi''+n(n-1)\tfrac{S'}{S}\Phi'+\tfrac{1}{2}\left[2n(n-2)\left(\tfrac{S'}{S}\right)'\right.\right.\\&\left.+n(n-1)(n-2)\left(\tfrac{S'}{S}\right)^2+k^2-n(n-1)\kappa\right]\Phi+n\tfrac{S'}{S}\Pi'\\&\left.+\left[2n\left(\tfrac{S'}{S}\right)'+n(n-1)\left(\tfrac{S'}{S}\right)^2-k^2\right]\Pi\right\}=-8\pi GS^2\tilde{E}\left[nw\eta+(nc_{\mathrm{s}}^2-1)\epsilon_g\right]\end{aligned} \tag{2.17}$$

$$\begin{aligned}&(n-1)\left\{\tfrac{n}{2}\tfrac{S'}{S}\Phi'+\tfrac{1}{2}\left[n(n-2)\left(\tfrac{S'}{S}\right)^2+k^2-n\kappa\right]\Phi+\right.\\&\left.n\left(\tfrac{S'}{S}\right)^2\Pi\right\}=8\pi GS^2\tilde{E}\epsilon_g\ .\end{aligned} \tag{2.18}$$

Covariant conservation of the perturbed energy-momentum tensor implies

$$\frac{1}{k}(v_s'^{(0)}+\frac{S'}{S}v_s^{(0)})=\frac{c_{\mathrm{s}}^2}{w+1}\epsilon_m+\frac{w}{w+1}\eta-\frac{(n-1)w}{n(w+1)}(1-\frac{n\kappa}{k^2})\pi_T^{(0)}-\frac{n-2}{2}\Phi-\Pi. \tag{2.19}$$

For vector perturbations the Einstein equations read

$$\left[k^2-(n-1)\kappa\right]\Psi=16\pi G(\tilde{E}+\tilde{P})S^2v_c\ , \tag{2.20}$$

and conservation of the energy-momentum tensor yields

$$v_c'+(1-nc_{\mathrm{s}}^2)\frac{S'}{S}v_c=-\frac{k^2-(n-1)\kappa}{2k}\frac{w}{1+w}\pi_T^{(1)}. \tag{2.21}$$

Tensor perturbations fulfill

$$H''+(n-1)\frac{S'}{S}H'+(k^2+2\kappa)H=8\pi G\tilde{P}S^2\pi_T^{(2)}\ . \tag{2.22}$$

Without further information about the matter perturbations these equations are not closed. The simplest way to find equations for the matter variables is to assume a macroscopic equation of state. A natural example is a perfect fluid, according to the behaviour of the background. In a more fundamental approach microphysical information should be incorporated.

2.3 Perfect fluid perturbations

We restrict the discussion of solutions to the flat FLRW models, i.e. $\kappa=0$. It is useful to rescale the conformal time by the wave number k,

$$x:=k\tau\ .$$

Thus, every differentiation is multiplied by k, and in the following we keep the prime to denote the differentiation with respect to x. All modes k enter the horizon at $x = \pi$, because

$$\frac{x}{\pi} = \frac{2}{\ell}\tau = \frac{2}{\ell_{\text{phys}}} d_{\text{h}}(\tau) ,$$

where ℓ is the comoving wave length corresponding to the comoving wave number k and $\ell_{\text{phys}} = S(\tau)\ell$ is the physical wave length.

In the case of a perfect fluid the anisotropic pressure vanishes ($\pi_T^{(a)} \equiv 0$ for all a). Additionally, we assume adiabatic (isentropic) perturbations, i.e. $\eta = 0$. Eq. (2.16) implies $\Pi \equiv 0$.

2.3.1 Radiation dominated model

For the RD model (Einstein-de Sitter) $w = c_{\text{s}}^2 = 1/n$. Thus, Eq. (2.17) reads:

$$\Phi'' + \frac{4}{x}\Phi' + \frac{1}{n}\Phi = 0 .$$

The solution is given by a spherical Bessel function for regular behaviour at $x = 0$ and a spherical Neumann function for singular behaviour in the origin:

$$\Phi = \frac{1}{x}\left(c^{(0)} j_1(\frac{x}{\sqrt{n}}) + d^{(0)} y_1(\frac{x}{\sqrt{n}}) \right) ,$$

where $c^{(0)}$ and $d^{(0)}$ are constants. The regular solution approaches a constant for small x (superhorizon scales), which leads to a growing $\epsilon_m \sim x^2$ because of Eq. (2.15). $x^2 \sim S^{n-1}$, which equals the result of the estimate (1.26). Figure 2.1 shows the singular and regular solutions for ϵ_m.

Vector perturbations in a perfect fluid have constant v_c from (2.21), which is a consequence of the Helmholtz-Kelvin circulation theorem [18]. Regular behaviour of Ψ at $x = 0$, however, implies $v_c = 0$, for otherwise Ψ would be proportional to $1/x^2$. The tensor perturbations are freely propagating gravity waves; the solution of (2.22) is given by

$$H = c^{(2)} j_0(x) + d^{(2)} y_0(x) ,$$

which can be regular or singular as $x \to 0$. The regular solution is plotted in Fig. 4.14. Their amplitude decays ($\sim x^{-1} \sim S^{-\frac{n-1}{2}}$) for large x in accordance with energy conservation [18]. (The energy of a gravitational wave is proportional to the square of the ratio of amplitude and physical wave length.) The behaviour of vector and tensor modes is independent of the dimension n. Only the phase velocity of the acoustic sound waves of the density contrast depends on n.

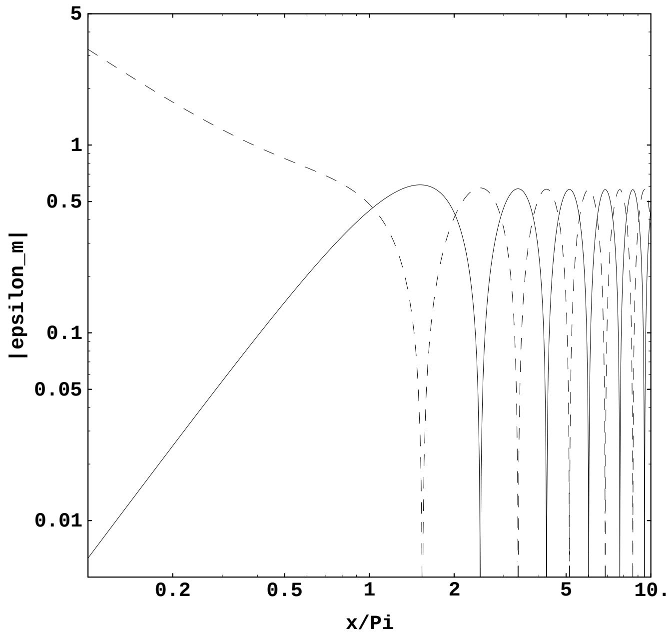

Figure 2.1: The full line shows the regular, the dashed line the singular solution for ϵ_m.

2.3.2 Matter dominated model

The MD model (dust) is characterized by $w = c_s^2 = 0$. From the equations (2.17) and (2.18)

$$\Phi'' = -\frac{4n-6}{n-2}\frac{1}{x}\Phi'$$

follows. The solutions are

$$\Phi = c^{(0)} + d^{(0)} x^{-\frac{3n-4}{n-2}} \ .$$

Therefore the growing solution for small x reads $\epsilon_m \sim x^2$. All modes may grow, because the sound velocity vanishes, i.e. there is no pressure, which could act against gravitational attraction, at all.

Singular vector perturbations follow from

$$v_c \sim x^{\frac{2}{2-n}} \ ,$$

they read

$$\Psi = d^{(1)} x^{\frac{2(n-1)}{2-n}} \ .$$

As above there are no regular solutions.

Tensor perturbations

$$H = x^{-\frac{n}{2(n-2)}} \left(c^{(2)} J_{\frac{n}{2(n-2)}}(x) + d^{(2)} Y_{\frac{n}{2(n-2)}}(x) \right)$$

decay like $x^{-\frac{n-1}{n-2}} \sim S^{-\frac{n-1}{2}}$ due to energy conservation.

If we allow pressure in the perturbations, i.e. $c_{\rm s} \neq 0$, equations (2.17) and (2.18) yield

$$x^2\Phi'' + \frac{4n-6+2nc_{\rm s}^2}{n-2}x\Phi' + \left(x^2 + \frac{4n}{n-2}\right)c_{\rm s}^2\Phi = 0 \ .$$

With $\Phi \sim x^{-2}\epsilon_{\rm m}$ we obtain

$$x^2\epsilon_{\rm m}'' + \frac{2(1+nc_{\rm s}^2)}{n-2}x\epsilon_{\rm m}' + \left(x^2c_{\rm s}^2 - \frac{2n}{n-2}\right)\epsilon_{\rm m} = 0 \ . \qquad (2.23)$$

The coefficient of $\epsilon_{\rm m}$ vanishes at the Jeans wave number

$$k_{\rm J} = \frac{x_{\rm J}}{\tau} = \sqrt{\frac{2n}{(n-2)c_{\rm s}^2}}\frac{1}{\tau} \sim c_{\rm s}^{-1}S^{-\frac{n-2}{2}} \ .$$

This confirms the validity of Jeans' result. The solutions to equation (2.23) are given by spherical Bessel functions.

The regular component of the vector prturbations is vanishing also for $c_{\rm s} \neq 0$, and the gravitational waves do not depend on $c_{\rm s}$ at all.

2.4 Perfect fluid plus relativistic plasma

The universe contains various forms of matter as radiation and baryons, which may be described by a perfect fluid. But there are also particles for which this is not a good description. An example is a collisionless, massless gas, e.g. neutrinos after their decoupling below the electroweak scale. Another example are background gravitons left over from the epoch of quantum gravity. In both examples all other matter may be described by a perfect fluid during a certain epoch, while collisions keep it close to thermal equilibrium.

Once a species of thermalized massless particles decouples the rest of matter, it keeps the thermal distribution as long as the background model provides a conformal time-like Killing vector. This is the case for the FLRW models. Thus, only the temperature of the distribution changes with S^{-1}. An example is the observed Planck spectrum of the decoupled photons forming the CBR (Fig. 1.2).

To model such systems we derive the equations for cosmological perturbations evolving in a mixture of a relativistic plasma and a perfect fluid. We assume that the plasma and the fluid interact only through gravitational forces, thus

$$T^{\mu}{}_{\nu} = T_{\rm rp}{}^{\mu}{}_{\nu} + T_{\rm pf}{}^{\mu}{}_{\nu} \ . \qquad (2.24)$$

To describe the radiation dominated epoch of the universe we assume that the components of the background perfect-fluid energy-momentum tensor $\tilde{T}_{\rm pf}{}^{\mu}{}_{\nu}$ and the relativistic plasma components obey the same equation of state, i.e. $\tilde{E}_{\rm pf,rp} = n\tilde{P}_{\rm pf,rp}$. For both perturbed energy-momentum tensors, $\delta T_{\rm rp}{}^{\mu}{}_{\nu}$ and $\delta T_{\rm pf}{}^{\mu}{}_{\nu}$, gauge-invariant matter variables are defined as in this chapter. We define the ratio of the plasma background energy-density to the total background energy-density to be

$$\alpha := \frac{\tilde{E}_{\rm rp}}{\tilde{E}_{\rm rp} + \tilde{E}_{\rm pf}} \; . \tag{2.25}$$

In order to gain a closed set of gauge-invariant equations we only allow adiabatic (isentropic) perturbations, i.e. $\eta = \alpha\eta_{\rm rp} + (1-\alpha)\eta_{\rm pf} = 0$. Entropy perturbations would arise, e.g., from phase transitions [27], which lie beyond the scope of this work.

The extension of Bardeen's [26] gauge-invariant formalism to a multi-fluid universe was given in Refs. [30, 33]. In connection with a collisionless gas this was done in Ref. [40]. Since we only deal with two components fulfilling the same background equation of state, the more general formalism of these references is not necessary here. The gauge-invariant equations are derived from (2.1) applying (2.24).

2.4.1 Collisionless damping

To understand the subhorizon behaviour of perturbations in a collisionless gas of particles damping processes are important. Massless particles are damped due to *directional dispersion.* Let us consider a simple model for this process. The distribution F of the collisionless gas satisfies the Vlasov equation

$$F' + \mathbf{v}\cdot\nabla F = 0 \; ;$$

after a Fourier transformation of the spatial components

$$F_k(\tau) = F_k(0)e^{\imath k v \tau \mu} \qquad \text{with } \mu := \frac{\mathbf{kv}}{kv} \; .$$

A density perturbation is a superposition of such waves. Because the particles are massless, they move with the speed of light ($c = 1$).

$$\begin{aligned}
\delta_k(\tau) \;&\sim\; \int_0^\infty dv v^{n-1}\delta(v-1)\int_{-1}^1 d\mu(1-\mu^2)^{\frac{n-3}{2}}e^{\imath v k\tau\mu} \\
&\sim\; (k\tau)^{-\frac{n-2}{2}}\int_0^\infty dv v^{\frac{n}{2}}\delta(v-1)J_{\frac{n-2}{2}}(vk\tau) \qquad (2.26)\\
&\sim\; x^{-\frac{n-2}{2}}J_{\frac{n-2}{2}}(x) \qquad (x := k\tau) \; . \qquad (2.27)
\end{aligned}$$

This means that density perturbations are damped at large x as $x^{-\frac{n-1}{2}}$. There is no damping in one spatial dimension, because left and right moving particles move with the same speed and thus preserve the over- and underdensities.

Massive particles are damped by *free streaming*. The thermal velocity dispersion leads to additional damping resulting in an exponential decay. Inserting a Maxwell-Boltzmann distribution (we now deal with nonrelativistic velocities)

$$y^{\frac{n}{2}} e^{-\frac{y}{2} v^2} \quad \text{with } y := \frac{m}{T}$$

instead of the delta function into (2.26) leads to

$$\delta_k(\tau) \sim e^{-\frac{x^2}{2y}} \ .$$

Gravitational attraction between the particles with mass m has not been taken into account in this estimate. It becomes important at $T \sim m$, gravitational interactions will amplify perturbations below that temperature. Therefore the free streaming scale is defined as $\ell_{\mathrm{fs-phys}} = d_h(T = m) \sim (g_* G T^{n+1})^{-\frac{1}{2}} \sim (g_* m_{\mathrm{Planck}}^{-2} m^{n+1})^{-\frac{1}{2}}$, the first scale that can grow after entering the horizon.

Chapter 3

Thermalized matter

The Einstein equation describes the evolution of the metric perturbations for given matter perturbations. The covariant conservation of the perturbed energy-momentum tensor results from the Bianchi identity. This does not fix $\delta T^{\mu}{}_{\nu}$ completely; additional input is needed. The simplest possibility is to assume that both the perturbed and the unperturbed medium satisfy a simple macroscopic equation of state, as has been done at the end of the last chapter.

More complicated forms of matter in the early universe require, of course, a microscopic description. Such a description was first developed by Peebles and Yu [34] on the basis of kinetic theory [35]. There the Boltzmann equation in seven dimensional phase space $(\tau, \mathbf{x}, \mathbf{p})$, with an ansatz for the collision term, is used. $\mathbf{x}$ denotes the spatial coordinate and $\mathbf{p}$ the spatial momentum. The timelike component of the momentum is not independent, since the particles are on the mass-shell $p^0 = \sqrt{p^2 + m^2}$ $(p = |\mathbf{p}|)$. The Boltzmann equation together with Eq. (2.1) has then usually to be solved numerically. A lot of work has been accomplished within this framework [23, 30, 36, 37, 38, 39, 40].

A different approach has recently been formulated by Kraemmer and Rebhan [41]. In a completely field-theoretical framework the matter perturbation $\delta T^{\mu}{}_{\nu}$ is determined by the (thermal) graviton self-energy [42], evaluated on the given background. In contrast to kinetic theory this framework is fully quantum theoretical from the beginning, and might turn out to be an alternative to the still to be formulated quantum kinetic theory [43]. This approach was used to incorporate collisionless, massless matter [41, 44], possibly mixed with a perfect fluid component [45, 46, 47, 48], which can be described perturbatively by the high-temperature limit of the underlying field theory. Classical kinetic theory applied to the quanta of the field theory was shown to coincide with the high-temperature limit of thermal field theory

[47].

In the next section we will discuss the leading order (1-loop contribution) for arbitrary spatial dimension n.

To go beyond collisionless matter a weakly self-interacting scalar field has been investigated — a scalar theory with a $\lambda\varphi^4$ potential in three spatial dimensions [49, 50]. This is the subject of the second section of this chapter.

Apart from some notable exceptions [51, 52, 32] all results given in the literature within kinetic theory have been derived by choosing a specific gauge. As was shown in [47], this dependence on the gauge may be circumvented by completing the program lined out by Kasai and Tomita [40]. We will discuss this program in the last section of this chapter.

3.1 The thermal graviton self-energy

A manifestly gauge-invariant approach is provided by thermal field theory. For a system containing gravity as well as matter at a physical temperature T below the Planck scale ($T \ll m_{PL}$) the effective action (i.e., including all radiative contributions) $\Gamma[g]$ can be split up in a part describing classical gravity, the Einstein-Hilbert action S^G itself, and an effective action $\Gamma[g]^M$ induced by the thermal matter with classical action S^M,

$$\Gamma|_{T \ll m_{\text{Planck}}} = S^G + \Gamma^M \ . \tag{3.1}$$

This is automatically gauge-invariant provided any gauge fields are subject to background-covariant gauge conditions.

Γ^M does not depend on curvature effects in the leading-order temperature contribution. In the radiation dominated regime the Ricci tensor is proportional to GT^{n+1}. Thus for temperatures below the Planck scale ($T \ll m_{\text{Planck}}$) curvature effects are lower order in temperature, i.e. $\ll T^{n-1}$.

The energy-momentum tensor is given by

$$T^{\mu\nu}(x) := \frac{2}{\sqrt{-g}} \frac{\delta \Gamma^M}{\delta g_{\mu\nu}} \ , \tag{3.2}$$

and self-consistent perturbations thereof have to satisfy

$$\delta T^\mu{}_\nu(x) = \int_{x'} \frac{\delta T^\mu{}_\nu(x)}{\delta g_{\rho\sigma}(x')} \delta g_{\rho\sigma}(x') \ . \tag{3.3}$$

This relates the perturbed matter variables to the thermal graviton self-energy, which is defined by

$$\Pi^{\mu\nu\rho\sigma}(x, x') := \frac{1}{2} \frac{\delta(\sqrt{-g} T^{\mu\nu}(x))}{\delta g_{\rho\sigma}(x')} \ . \tag{3.4}$$

A perturbative expansion in Feynman diagrams is appropriate for weakly interacting matter. Higher loop orders due to internal graviton propagators are suppressed by powers of $GT^2 \ll 1$ for $T \ll m_{PL}$. A high-temperature expansion of Γ^M in the sense of $k_{\rm phys} \ll T$ is appropriate for the study of cosmological perturbations, because the external scale is set by the Hubble horizon $d_h = 2/(n-1)H^{-1} \sim (g_*(T)GT^{n+1})^{-1/2}$, which is $\gg T^{-1}$ for temperatures well below the Planck scale.

First attempts to calculate the thermal gravity self-energy have been undertaken in Refs. [53]. A complete calculation of the leading high-temperature contribution was first given by Rebhan in Ref. [42]. For collisionless matter only one-loop diagrams without internal graviton lines need to be computed. Similar issues have been studied in Refs. [54]. Recently, de Almeida et al. [55] have computed the next-to-leading order contributions for radiation and bosonic matter in the massive, but still collisionless case.

By calculating the graviton self-energy from thermal field theory on the cosmological background one can obtain the r.h.s. of the Einstein equations (2.1) from (3.3) using the definition (3.4). In the kinetic theory approach the Boltzmann-Einstein system of equations has to be solved simultaneously. This can be done analytically for collisionless, massless matter, but in general only numerical solutions can be obtained. In the thermal field theory approach the corresponding problem is to calculate the graviton self-energy on a curved background space-time. An explicit reference to perturbations of distribution functions is completely obviated, which might turn out to be useful when more than the classical limit is of interest. A complete evaluation of the thermal graviton self-energy in curved space is certainly a formidable task. However, restricting our attention to massless matter again, one can take advantage of the fact that the high-temperature limit of the effective action possesses, in addition to diffeomorphism invariance, an invariance under conformal transformations, which is expressed by the Ward identity [41, 45]

$$\Pi^{\alpha\beta\gamma}{}_{\gamma} = -\frac{1}{2}\sqrt{-g}T^{\alpha\beta} \ .$$

In the following we will restrict the discussion to the $\kappa = 0$ models, we will return to more general models in the last chapter. Since the Einstein-de Sitter model is conformally flat, the graviton self-energy, which is a non-local differential operator in space-time, can be simply calculated by evaluating $\Pi_{\alpha\beta\gamma\delta}$ on flat space-time and transferring it to the curved space by multiplication with cosmic scale factors S. This calculation was done in Refs. [42, 45].

In flat space-time we may choose plane waves for the harmonic analysis, i.e. $Q^{(0)} = \exp(-\imath\mathbf{kx})$. The graviton self-energy $\Pi_{\alpha\beta\gamma\delta}$ is related to the

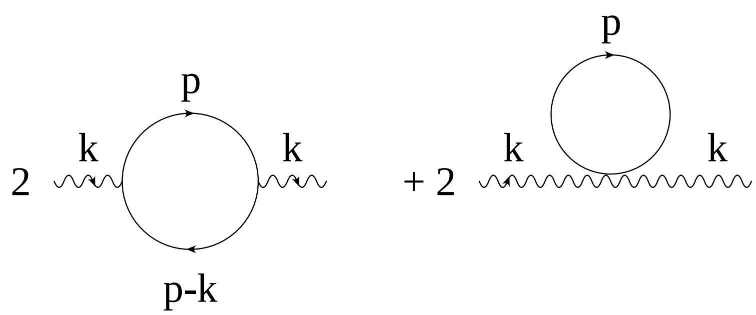

Figure 3.1: 1-loop contributions to the graviton self-energy.

Fourier transformed self-energy in flat space-time $\bar{\Pi}^{\alpha\beta\gamma\delta}$ by

$$\Pi^{\mu\nu\rho\sigma}(x,x')\big|_{g=S^2\eta} = S^{-2}(\tau)\int \frac{d^{n+1}K}{(2\pi)^{n+1}} e^{\imath K(x-x')}\, \bar{\Pi}^{\mu\nu\rho\sigma}(k)\Big|_{\eta} S^{-2}(\tau') \ . \quad (3.5)$$

In the high-temperature limit its tensorial structure turns out to be the same for any field theory and is given by

$$\bar{\Pi}^{\mu\nu\rho\sigma}\Big|_{g=\eta} = g_* \left[\frac{1}{2} I^{\mu\nu\rho\sigma} - \frac{1}{2}\left(\delta^{\mu}_{\alpha}\delta^{(\rho}_{\beta}\eta^{\sigma)\nu} + \delta^{\nu}_{\alpha}\delta^{(\rho}_{\beta}\eta^{\sigma)\mu}\right)\eta_{\gamma\delta} I^{\alpha\beta\gamma\delta}\right] \ , \quad (3.6)$$

which follows — in a straightforward calculation — from the Feynman rules of the imaginary time formulation (see e.g. [13]) of thermal field theory. The corresponding diagrams are shown in Fig. 3.1. The totally symmetric quantity $I^{\alpha\beta\gamma\delta}$ is given by

$$I^{\alpha\beta\gamma\delta}(k) = T \sum_{j=\frac{p_0}{2\pi\imath T}} \int \frac{d^n\mathbf{p}}{(2\pi)^3} \frac{p^\alpha p^\beta p^\gamma p^\delta}{p^2(p-k)^2} \ . \quad (3.7)$$

Sum and integral are conveniently performed with the help of the so-called Dzyaloshinski algorithm [56, 13]. Its values are tabulated in the appendix B. The integrals are polynomials in k_0/k times

$$F\left(\frac{1}{2}, 1; \frac{n}{2}; \left(\frac{k_0}{k}\right)^{-2}\right) \ ,$$

a hypergeometric function which is related to associated Legendre functions of the second kind:

$$F(\frac{1}{2}, 1; \frac{n}{2}; z^{-2}) = \imath \exp(\imath\pi\frac{n}{2})\Gamma(\frac{n}{2}) 2^{\frac{n-1}{2}} \pi^{-\frac{1}{2}} z (z^2-1)^{\frac{n-3}{4}} Q^{-\frac{n-3}{2}}_{\frac{n-3}{2}}(z) \ .$$

For $n = 3$

$$Q_0(\frac{k_0}{k}) = \frac{1}{2}\ln\left(\frac{k_0+k}{k_0-k}\right)$$

is the zeroth Legendre function of second kind.

Like all other quantities the graviton self-energy is expanded into plane waves. Therefore only the Fourier transformation of k_0 into τ in (3.5) has to be performed. The integrals involved are

$$\begin{aligned}\lim_{\gamma\to 0^+}\frac{1}{2\pi}\int_{-\infty+\imath\gamma}^{\infty+\imath\gamma} d\omega e^{-\imath\omega x}\left[(\omega^2-1)^l F(\frac{1}{2},1;\frac{n}{2};\omega^{-2}) - q_l(\omega^2)\right] = \\ (-1)^l\frac{\Gamma(\frac{n}{2})\Gamma(\frac{n-1+2l}{2})}{\Gamma(\frac{n-1}{2})}\Theta(x)\frac{d}{dx}\left[\left(\frac{2}{x}\right)^{\frac{n-2+2l}{2}} J_{\frac{n-2+2l}{2}}(x)\right]\ ,\end{aligned} \tag{3.8}$$

where $\omega = k_0/k$ and retarded boundary conditions are imposed. The polynoms

$$q_l(\omega^2) = \sum_{m=0}^{l}(-1)^{l-m}\binom{l}{m}\sum_{j=0}^{m}\frac{B(\frac{1}{2}+m-j,\frac{n-1}{2})}{B(\frac{1}{2},\frac{n-1}{2})}\omega^{2j}$$

of degree $2l$ guarantee the asymptotic $1/\omega$ behaviour of the kernel without the exponential.

In Eq. (3.3) this leads to convolution integrals of the form

$$\sum_l \alpha_l\int^{\infty} dx'\Theta(x-x')\left(\frac{2}{x-x'}\right)^{\frac{n-2+2l}{2}} J_{\frac{n-2+2l}{2}}(x-x')\{\Phi,\Pi,\Psi,H\}'(x').$$

There has to be a finite non-negative integration bound x_0, because $\tau \geq 0$. On the other hand, the functional derivative in equation (3.3) is usually defined without restriction. For that reason we have to put in the initial conditions for x_0 by hand. We do this by the replacement of the metric potentials by

$$\{\Phi,\Pi,\Psi,H\}'(x) \to \{\Phi,\Pi,\Psi,H\}'(x)\Theta(x-x_0) + \sum_{l=0}^{\infty}\gamma_l^{(a)}\delta^{(l)}(x-x_0)\ . \tag{3.9}$$

The infinite sum provides the initial conditions for a formally infinite-order differential equation, which is obtained differentiating the convolution integral above (see [45]). The infinite sum yields derivatives of Bessel functions, which can be rewritten into pure Bessel functions. For odd spatial dimensions these may be written as spherical Bessel functions.

3.1.1 Scalar perturbations

To arrive at the expressions for the matter perturbations in thermal field theory we have to relate them to the graviton self-energy through Eq. (3.3). The matter variables on the r.h.s. of Eqs. (2.17) and (2.18) read:

$$\eta = 0$$

and

$$\begin{aligned}\epsilon_g = \frac{n+1}{2}\Big[&(n-2)\Phi + 2\Pi - \\ &\Gamma(\frac{n}{2})\int_{x_0}^{x} dx'\left(\frac{2}{x-x'}\right)^{\frac{n-2}{2}} J_{\frac{n-2}{2}}(x-x')\left((n-1)\Phi + 2\Pi\right)'(x') - \\ &\Gamma(\frac{n}{2})\sum_{l=0}^{\infty}\gamma_l^{(0)}\Big(\left(\frac{2}{x-x_0}\right)^{\frac{n-2}{2}} J_{\frac{n-2}{2}}(x-x_0)\Big)^{(l)}\Big]\,.\end{aligned} \tag{3.10}$$

The other matter variables read:

$$\begin{aligned}v_{\mathrm{s}}^{(0)} = -\Gamma(\frac{n}{2}+1)\Big[&\int_{x_0}^{x} dx'\left(\frac{2}{x-x'}\right)^{\frac{n-2}{2}} J_{\frac{n}{2}}(x-x')\left((n-1)\Phi + 2\Pi\right)'(x') + \\ &\sum_{l=0}^{\infty}\gamma_l^{(0)}\Big(\left(\frac{2}{x-x_0}\right)^{\frac{n-2}{2}} J_{\frac{n}{2}}(x-x_0)\Big)^{(l)}\Big]\,,\end{aligned} \tag{3.11}$$

$$\begin{aligned}\pi_{\mathrm{T}}^{(0)} = -(n+1)\Gamma(\frac{n}{2}+1)\Big[&\int_{x_0}^{x} dx'\left(\frac{2}{x-x'}\right)^{\frac{n-2}{2}} J_{\frac{n+2}{2}}(x-x')\times \\ &\qquad\left((n-1)\Phi + 2\Pi\right)'(x') + \\ &\sum_{l=0}^{\infty}\gamma_l^{(0)}\Big(\left(\frac{2}{x-x_0}\right)^{\frac{n-2}{2}} J_{\frac{n+2}{2}}(x-x_0)\Big)^{(l)}\Big]\,,\end{aligned} \tag{3.12}$$

and ϵ_{m} is given by Eq. (2.13).

3.1.2 Vector perturbations

In a similar manner we obtain for vector perturbations

$$\begin{aligned}v_c = -\Psi + \Gamma(\frac{n}{2}+1)\Big[&\int_{x_0}^{x} dx'\left(\frac{2}{x-x'}\right)^{\frac{n}{2}} J_{\frac{n}{2}}(x-x')\Psi'(x') + \\ &\sum_{l=0}^{\infty}\gamma_l^{(1)}\Big(\left(\frac{2}{x-x_0}\right)^{\frac{n}{2}} J_{\frac{n}{2}}(x-x_0)\Big)^{(l)}\Big]\,.\end{aligned} \tag{3.13}$$

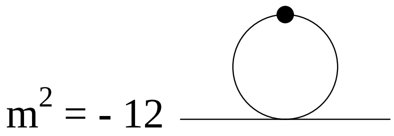

Figure 3.2: Definition of the thermally induced mass. The dot indicates that the propagator in the loop is a massive one.

3.1.3 Tensor perturbations

In this case

$$\pi_T^{(2)} = -(n+1)\Gamma(\frac{n}{2}+1)\Big[\int_{x_0}^{x} dx' \left(\frac{2}{x-x'}\right)^{\frac{n+2}{2}} J_{\frac{n+2}{2}}(x-x')H'(x') + \sum_{l=0}^{\infty}\gamma_l^{(2)}\left(\left(\frac{2}{x-x_0}\right)^{\frac{n+2}{2}} J_{\frac{n+2}{2}}(x-x_0)\right)^{(l)}\Big] . \tag{3.14}$$

3.2 Collisional matter (n=3)

All particles interact in some way with other particles or with themselves. The simplest example is a self-interacting scalar particle with quartic coupling $\lambda\varphi^4$. This gives rise to a renormalizable quantum field theory in three spatial dimensions. We therefore restrict our analysis to $n = 3$. Besides the minimal coupling, the general covariance allows for an interaction term $R\varphi^2$. Because $R \sim (GT^4) \ll T^2$, this is a subleading contribution which we ignore. The coupling constant λ is dimensionless, and therefore it does not introduce a new scale, preserving the conformal symmetry in the high temperature limit. The result in Einstein-de Sitter space-time is again obtained by a conformal transformation from flat space-time.

Recently, a model with massive, self-interacting scalar fields has been suggested to provide the dark matter [57], but it has been shown that this model can be ruled out by several constraints from observations [58].

The thermal self-energy of a scalar field theory [12] defines the thermal mass (Fig. 3.2). It is clear from the figure that this mass is proportional to $\sqrt{\lambda}T$. The dot on the internal line indicates that this propagator is assumed to have the same mass m. Neglecting logarithms, evaluation of the diagram in Fig. 3.2 yields

$$m^2 = \lambda T^2 - \frac{3\lambda}{2}Tm + \lambda O\left(m^2 \ln(\frac{m}{T})\right) . \tag{3.15}$$

A naive calculation of higher loops (using massless propagators) yields infrared divergent results. This is due to the breakdown of the series expansion

Figure 3.3: The resummed vertex with one external graviton. Vertices with more external gravitons are resummed in the same way.

in powers of λ for thermal field theory. The perturbation series has to be resummed according to the scheme of Braaten and Pisarski [59]. There are two scales for the momenta, the hard scale T and the soft scale $\sqrt{\lambda}T$. At the tree level there is no need for resummation, because there is only the hard scale. As soon as we include tadpole diagrams as in Fig 3.2, the soft scale appears. The internal line of such a tadpole contains a contribution with a hard internal momentum, yielding an amplitude of order $\lambda T^2/K^2$, with K being the external momentum. Therefore it is called a hard thermal loop. For hard external momenta, the amplitude contributes at the one loop level, but for a soft external momentum this amplitude gives a contribution comparable to the tree level. To yield a consistent expansion in the coupling constant all hard thermal loops have to be resummed. For scalar theory there is only the tadpole in Fig. 3.2. It gives rise to the mass resummation. A simple way to do that is to include the thermal mass in the Lagrange density and subtract it again as a counterterm. Now all diagrams involve massive propagators. The contributions from the counterterm cancels the hard thermal loops. In the scheme of Braaten and Pisarski this task is performed by subtracting the hard thermal contribution only. The situation is more complicated when gauge fields (Yang-Mills or gravitation) are included. Then also additional hard thermal vertices show up.

On the r.h.s. of Fig. 3.3 two one loop diagrams contributing to the effective vertex of two scalar and one graviton line are shown. These are hard thermal loops, which are included in a resummed vertex. We indicate a resummed vertex by a full box. Again this resummation gives rise to counterterms in the action (the hard thermal vertices alone). The perturbation series is organized in terms of resummed vertices and (massive) propagators. The counterterms cancel all hard thermal loops.

To demonstrate the resummation we calculate the energy-momentum tensor up to order $\lambda^{\frac{3}{2}}$. The energy-momentum tensor is the effective graviton one-point function. The Feynman diagrams at the resummed 2-loop level are shown in Fig. 3.4. All propagators are massive with mass m defined in (3.15). The first three diagrams include the one and two loop diagrams of the unresummed theory. The last two diagrams include the mass counterterm (cross) and the vertex counterterm (circle-cross). Using the definition

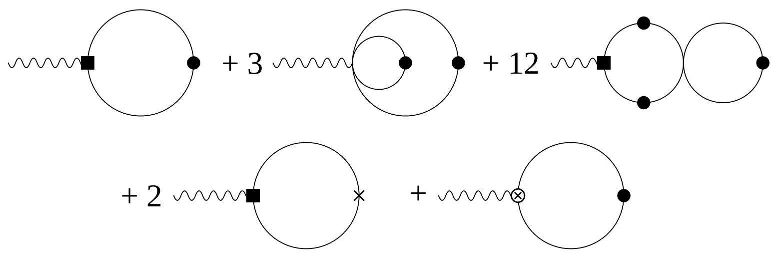

Figure 3.4: Resummed diagrams contributing to the energy momentum tensor at the two loop level. Using the definition of the thermal mass and the resummed vertex, the third and fourth diagrams cancel and the fifth diagram cancels, the box in the first diagram. The crosses denote counterterms.

of the mass in Fig. 3.2 the second diagram is canceled by the fourth graph. The resummed vertex appears linearly only, therefore the hard thermal loops cancel with the counter-vertex, and the remaining graphs yield:

$$T^{\mu\nu} = \Sigma_1 \left(\frac{1}{2}\eta^{\mu\nu}P^2 - P^\mu P^\nu\right) - 3\lambda\eta^{\mu\nu}\Sigma_1^2 \,. \tag{3.16}$$

The abbreviation Σ_i is defined in appendix B and denotes the thermal sum and momentum integration as well as the massive propagator(s) of the internal line(s). Evaluating this integral by the methods of appendix B the energy-momentum tensor corresponds to a traceless perfect fluid energy-momentum tensor with energy density

$$\tilde{E} = \frac{\pi^2 T^4}{30}\left[1 - \frac{15}{8}\frac{\lambda}{\pi^2} + \frac{15}{2}\left(\frac{\lambda}{\pi^2}\right)^{\frac{3}{2}} + O\left(\lambda^2\ln(\lambda)\right)\right] \,. \tag{3.17}$$

The conformal transformation introduces the dependence on the cosmic scale factor S^{-4}. The hard thermal loops are due to thermal fluctuations only; quantum effects do not enter [59].

In the same way the graviton self-energy is obtained. After the resummation and cancellation of hard thermal loops the diagrams of Fig. 3.4 remain. These are only the graphs contributing up to $\lambda^{\frac{3}{2}}$. All propagators are massive, but the vertices are the bare ones. The three loop contributions are the consequence of the resummed vertices. The algebra now reads:

$$\begin{aligned}
\Pi^{\alpha\beta\gamma\delta} \;&=\; 2\Sigma_2\left(\frac{1}{4}\eta^{\alpha\beta}(PQ) - \frac{1}{2}P^{(\alpha}Q^{\beta)}\right)\left(\frac{1}{4}\eta^{\gamma\delta}(PQ) - \frac{1}{2}P^{(\gamma}Q^{\delta)}\right) \\
&\quad + \Sigma_1\Big[\left(\frac{1}{8}\eta^{\alpha\beta}\eta^{\gamma\delta} - \frac{1}{4}\eta^{\alpha(\gamma}\eta^{\delta)\beta}\right)P^2 + \\
&\quad\quad \frac{1}{2}(\eta^{\alpha(\gamma}P^{\delta)}P^\beta + \eta^{\delta(\gamma}P^{\delta)}P^\alpha) - \frac{1}{4}(\eta^{\alpha\beta}P^\gamma P^\delta + \eta^{\gamma\delta}P^\alpha P^\beta)\Big]
\end{aligned}$$

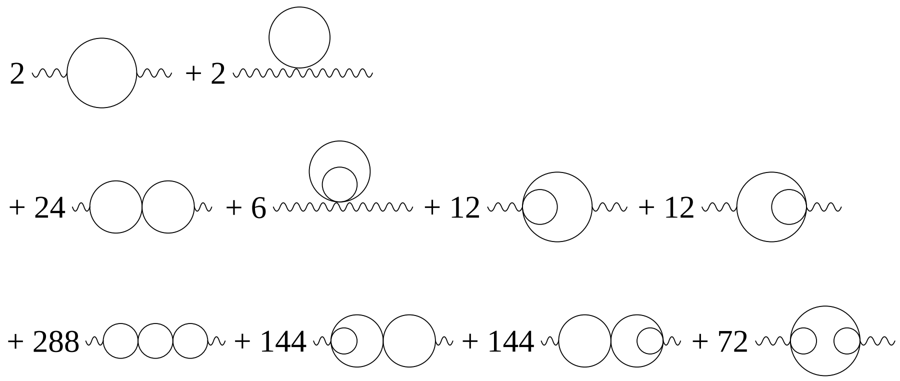

Figure 3.5: The graviton self-energy up to $\lambda^{\frac{3}{2}}$. All propagators are massive.

$$
\begin{aligned}
&-6\lambda\Sigma_2(\frac{1}{2}\eta^{\alpha\beta}(PQ)-P^{(\alpha}Q^{\beta)})\Sigma_2(\frac{1}{2}\eta^{\gamma\delta}(PQ)-P^{(\gamma}Q^{\delta)})\\
&-3\lambda(\frac{1}{4}\eta^{\alpha\beta}\eta^{\gamma\delta}-\frac{1}{2}\eta^{\alpha(\gamma}\eta^{\delta)\beta})\Sigma_1^2\\
&-3\lambda\left[\eta^{\alpha\beta}\Sigma_1\Sigma_2(\frac{1}{2}\eta^{\gamma\delta}(PQ)-P^{(\gamma}Q^{\delta)})+(\{\alpha\beta\}\leftrightarrow\{\gamma\delta\})\right]\\
&+72\lambda^2\Sigma_2\Sigma_2(\frac{1}{2}\eta^{\alpha\beta}(PQ)-P^{(\alpha}Q^{\beta)})\Sigma_2(\frac{1}{2}\eta^{\gamma\delta}(PQ)-P^{(\gamma}Q^{\delta)})\\
&+36\lambda^2\Sigma_2\left[\eta^{\alpha\beta}\Sigma_1\Sigma_2(\frac{1}{2}\eta^{\gamma\delta}(PQ)-P^{(\gamma}Q^{\delta)})+(\{\alpha\beta\}\leftrightarrow\{\gamma\delta\})\right]\\
&+18\lambda^2\eta^{\alpha\beta}\eta^{\gamma\delta}\Sigma_1^2\Sigma_2 \qquad (3.18)
\end{aligned}
$$

The internal momentuma are P and $Q = P - K$, where K is the external momentum. Equation (3.18) satisfies the diffeomorphism Ward identity, and together with the integrals of appendix B (which are evaluated in the high temperature limit) the conformal Ward identity is satisfied, too.

Due to the existence of the thermal mass there are three kinematic regions: In region I the external momentum $K_\mu = (k_0, \mathbf{k})$ is space-like, i.e. $\omega^2 < 1$ (remember $k_0/k =: \omega$). In this region plasmon modes are damped, the self-energy has an imaginary part (Landau damping). Above the light-cone the modes can propagate. At energies $\omega^2 k^2 > 4m^2 + k^2$ the production of a pair of quasi-particles with mass m is possible. This is region III. It also yields an imaginary part, which corresponds to the decay of a virtual graviton into a pair of quasi-scalars. In between there is region II, i.e. $k^2 < \omega^2 k^2 < 4m^2 + k^2$, where (3.18) is real.

Because λ may take large values compared to GT^2, which is the order parameter of internal graviton lines and curvature effects, $k \ll m$ in the high temperature limit. Therefore we can ignore region III. All possible contractions with the metric, the external momentum, and the fluid velocity u_μ (it picks the direction of the heat bath) of the integrals in (3.18) are tabulated in appendix B.2. They are calculated in region II in the limit $k \ll m$ with $m = m(\sqrt{\lambda})$ substituted. The values in region I are obtained by analytic continuation in ω. The integrals have been calculated by a *Mathematica* program written by H. Nachbagauer and have been checked by calculating the imaginary part and analytic continuation as described in [60]. More details are given in appendix B.2. The next step is the Fourier transformation of the self-energy as in (3.5).

3.2.1 Scalar perturbations

Let us restrict our attention to ϵ_g. The other matter variables do not introduce additional integrals. The contribution in order λ^0 can be read off (3.10) by setting $n = 3$. Let us denote the kernel of the integral in (3.10) by

$$K_0^{(0)}(x) = \Theta(x) j_0(x) \; . \tag{3.19}$$

We have included the prefactor into its definition, such that $K_0^{(0)}(0_+) = 1$. The lower index indicates the order λ^0. At the next order

$$\begin{aligned} K_1^{(0)}(x) &= \frac{5\lambda\imath}{16\pi^2} \int_{-\infty+\imath\varepsilon}^{\infty+\imath\varepsilon} \frac{d\omega}{2\pi} \left(\omega^2 \ln^2 \frac{\omega+1}{\omega-1} - \ln \frac{\omega+1}{\omega-1} - \frac{2\omega}{\omega^2-1} \right) \\ &= \frac{5\lambda}{8\pi^2} \left(2\kappa' - j_0 - \cos\right)(x)\Theta(x) \; , \end{aligned} \tag{3.20}$$

where have defined

$$\begin{aligned} \kappa(x) &:= \frac{1}{x} \left[\sin(x)\mathrm{Si}(2x) + \cos(x) \left(\mathrm{Ci}(2x) - \gamma - \ln(2x) \right) \right] \\ &= 2 \sum_{m=0}^{\infty} \frac{(-1)^m x^{2m+1}}{(2m+2)!} \sum_{j=0}^{m} \frac{1}{2j+1} \; , \end{aligned} \tag{3.21}$$

with Si and Ci being the sine and cosine integral. In contrast to $K_0^{(0)}$ the asymptotic behaviour is now dominated by the cosine term. The $\kappa'(x)$ decays like $\ln(x)/x$ for large x. The order $\lambda^{\frac{3}{2}}$ contribution is given by

$$\begin{aligned} K_{\frac{3}{2}}^{(0)}(x) &= \frac{15\imath}{8} \left(\frac{\lambda}{\pi^2} \right)^{\frac{3}{2}} \int_{-\infty+\imath\varepsilon}^{\infty+\imath\varepsilon} \frac{d\omega}{2\pi} \left[\frac{1}{3(\omega^2-1)^{\frac{3}{2}}} + \frac{\omega}{\omega^2-1} + \frac{2}{\sqrt{\omega^2-1}} \right. \\ & +\omega - \sqrt{\omega^2-1} + \left(\sqrt{\omega^2-1} - \omega \right) \omega \ln \frac{\omega+1}{\omega-1} - \frac{\omega}{\sqrt{\omega^2-1}} \ln \frac{\omega+1}{\omega-1} \\ & \left. +(\omega^2-1)\frac{\omega}{4} \ln^2 \frac{\omega+1}{\omega-1} - \sqrt{\omega^2-1}\frac{\omega^2}{4} \ln^2 \frac{\omega+1}{\omega-1} \right] \end{aligned}$$

$$
\begin{aligned}
&= \frac{15}{8}\left(\frac{\lambda}{\pi^2}\right)^{\frac{3}{2}}\left(\cos + \frac{x}{3}J_{-1} + 2J_0 + \frac{1}{x}J_1 + \frac{4}{3}j_2 - \frac{2}{3}j_0\right. \\
&\left. -4\nu'' - 2\nu - \kappa' - \kappa'' - \frac{1}{6}\xi\right)\Theta(x)\ . \qquad (3.22)
\end{aligned}
$$

Here we have introduced the functions

$$
\begin{aligned}
\nu(x) &:= \int_{-1}^{1}\frac{d\omega}{2\pi}\cos(\omega x)\frac{\omega}{\sqrt{1-\omega^2}}\ln\frac{1+\omega}{1-\omega} \\
&= \sum_{m=0}^{\infty}\frac{(-1)^m x^2 m}{(2m)!}\sum_{l=0}^{m}\frac{\Gamma(l+\frac{1}{2})}{\Gamma(\frac{1}{2})l!(1+2m-2l)} \qquad (3.23) \\
\xi(x) &:= -12\int_{-1}^{1}\frac{d\omega}{2\pi}\cos(\omega x)\sqrt{1-\omega^2}\left(\frac{\omega}{2}\ln\frac{1+\omega}{1-\omega}\right)^2 - \frac{3\pi^2}{2}\left(\frac{J_1}{x}\right)'' \\
&= \sum_{m=0}^{\infty}\frac{(-1)^m x^2 m}{(2m)!}\frac{\Gamma(\frac{1}{2})\Gamma(m+\frac{3}{2})}{\Gamma(m+3)}\times \\
&\quad \left(-1 + \sum_{l=0}^{m}\frac{\Gamma(l+1)}{\Gamma(l+\frac{3}{2})}\sum_{j=0}^{l}\frac{\Gamma(j+\frac{1}{2})}{j!(j-m+\frac{3}{2})}\right)\ . \qquad (3.24)
\end{aligned}
$$

In the asymptotic region the xJ_{-1} grows like $x^{\frac{1}{2}}$. The new functions $\xi(x)$ and $\nu(x)$ decay faster than $\kappa'(x)$.

3.2.2 Vector perturbations

The λ^0 contribution may be obtained from (3.13). The kernel of the integral in (3.13) is

$$K_0^{(1)}(x) = \Theta(x)\frac{j_2(x)}{x}\ . \qquad (3.25)$$

In the higher orders of λ we obtain:

$$
\begin{aligned}
K_1^{(1)}(x) &= -\Theta(x)\frac{5\lambda}{8\pi^2}j_2'(x) \qquad (3.26) \\
K_{\frac{3}{2}}^{(1)}(x) &= -\Theta(x)\left(\frac{\lambda}{\pi^2}\right)^{\frac{3}{2}}\left(\frac{5}{8}J_0' + \frac{3}{2}j_3 - \frac{3}{8}j_1\right)(x)\ . \qquad (3.27)
\end{aligned}
$$

Asymptotically the λ^0, λ^1, and $\lambda^{\frac{3}{2}}$ contributions decay as x^{-2}, x^{-1}, and $x^{-\frac{1}{2}}$.

3.2.3 Tensor perturbations

The kernel of the integral in (3.14) is

$$K_0^{(2)}(x) = \Theta(x)\frac{j_2(x)}{x^2}\ . \qquad (3.28)$$

At higher orders of λ we obtain:

$$K_1^{(2)}(x) = -\Theta(x)\frac{15\lambda}{\pi^2}\frac{j_2'(x)}{x} \quad (3.29)$$

$$K_{\frac{3}{2}}^{(2)}(x) = -\Theta(x)15\left(\frac{\lambda}{\pi^2}\right)^{\frac{3}{2}}\frac{1}{x}\left(J_1 + 3j_1 + \frac{j_2}{2x}\right)(x) . \quad (3.30)$$

3.3 The Boltzmann equation (n=3)

The framework for kinetic theory within general relativity was set up long ago, see, *e.g.*, Refs. [35, 61]; a recent book on this subject is Ref. [62]. In the context of cosmological perturbations kinetic theory was firstly used by Peebles and Yu [34]. They discussed the coupled Boltzmann and Einstein equations for photons interacting with electrons via Thomson scattering. For collisionless, massless neutrinos Stewart [23] derived the full set of Einstein-Vlasov equations. An extensive investigation of density perturbations with massive and massless neutrinos, radiation and other matter was performed numerically by Bond and Szalay [39].

Kinetic theory is applicable for particles whose de Broglie wavelength is smaller than their mean free path. For collisionless matter this is certainly the case. Moreover, the de Broglie wavelength $2\pi/p$ has to be smaller than the Hubble horizon $d_h = 2/(n-1)H^{-1} \sim (g_*(T)GT^{n+1})^{-1/2}$, i.e. with

$$p^{-1} \sim T^{-1} \ll m_{\text{Planck}}T^{-2} \quad (3.31)$$

the temperature T has to be below the Planck scale [62].

In this section we shall concentrate on the case of collisionless, massless matter in three spatial dimensions. The massless case is somewhat exceptional in that it is rigorously consistent with a thermal equilibrium situation. A thermal equilibrium in an expanding universe can only be obtained in the case of massless particles, since the FLRW models provide a conformal timelike Killing-vector only [35], or in the nonrelativistic limit.

In setting up the kinetic approach to cosmological perturbations we follow the paper by Kasai and Tomita [40]. They use gauge-invariant distribution functions, split up into scalar, vector and tensor modes. Other authors are usually working in a specific gauge [23, 36, 37, 38, 39, 24]. An infinite set of gauge-invariant equations for the fluid variables describing density perturbations has been obtained in Ref. [52]. The authors of Ref. [40] use kinetic theory within the tetrad description of general relativity [61]. The tetrad is defined by $g_{\mu\nu} = e^a_\mu e^b_\nu \eta_{ab}$. It spans an orthonormal basis in the tangent space.

The phase space of an ensemble of particles is described by the four space-time coordinates x^μ and the momentum components of the particles

$p^\mu := dx^\mu/ds$, s being an affine parameter. Since the particles' energy is on the mass-shell $p^0 = |\mathbf{p}| =: p$ (for $m = 0$), the dimension of the phase space is seven. An invariant volume of momentum 3-space is given by $dp^1 dp^2 dp^3/p =: d^3p/p$, where the indices refer to the tetrad basis. The distribution function $F(\tau, \mathbf{x}, \mathbf{p})$ satisfies the Boltzmann equation

$$L(F) := \left(p^\mu \frac{\partial}{\partial x^\mu} - \Gamma^\mu_{\nu\rho} p^\nu p^\rho \frac{\partial}{\partial p^\mu} \right) F(\tau, \mathbf{x}, \mathbf{p}) = C[F] \; . \tag{3.32}$$

The collision term C is a functional of F and is usually put in by hand. It is identically zero for collisionless matter. $\Gamma^\mu_{\nu\rho}$ denotes the usual Christoffel symbol.

The energy-momentum tensor is defined by

$$T^\mu{}_\nu := \int \frac{d^3p}{p} p^\mu p_\nu F \; . \tag{3.33}$$

In the collisionless case covariant conservation of $T^\mu{}_\nu$ follows from the Vlasov equation $L(F) = 0$. The perturbations of the energy-momentum tensor are given by

$$\delta T^\mu{}_\nu = \int \frac{d^3p}{p} \left(\tilde{p}^\mu \tilde{p}_\nu \delta F + (\delta p^\mu \tilde{p}_\nu + \tilde{p}^\mu \delta p_\nu) \tilde{F} \right) \; . \tag{3.34}$$

The perturbations of the particle momenta δp^μ are calculated with help of the inverse tetrad, which reads

$$e^\mu_a = \frac{1}{S} \left(\delta^\mu_a - \frac{1}{2} \delta g^\mu{}_a \right)$$

in linear theory. $\delta p^\mu = \delta e^\mu_a p^a$ relates δp^μ to the metric perturbations. In (3.34) the perturbed distribution function is $\delta F = F - \tilde{F}$, where $\tilde{F} = \tilde{F}(Sp)$ is the background distribution function. In thermal equilibrium the latter is a Bose-Einstein or a Fermi-Dirac distribution depending on $S(\tau)p$, the energy of the particles in comoving coordinates, only. Thus,

$$\tilde{F} = \frac{1}{e^{\beta S p} \pm 1} \; ,$$

with $\beta S(\tau)$ being the inverse temperature.

The decomposition into scalar, vector and tensor perturbations in the plane wave expansion is given by

$$\delta F(\tau, \mathbf{x}, \mathbf{p}) = \sum_{\mathbf{k}} \left(f^{(0)} + f^{(1)} \frac{\mathbf{p} \cdot \mathbf{w}}{p} + f^{(2)} \frac{\mathbf{p}^T \cdot \mathbf{t} \cdot \mathbf{p}}{p^2} \right) e^{i\mathbf{k}\mathbf{x}} \; . \tag{3.35}$$

$\mathbf{w}$ is a transverse vector and t a transverse-traceless symmetric tensor.

With an isotropic background distribution the $f^{(a)}$ depend on τ, the absolute values k and p, and on the cosine $\mu := \mathbf{k}\cdot\mathbf{p}/kp$. For a given mode with wave vector $\mathbf{k}$ we write $f^{(a)} = f^{(a)}(x,p,\mu)$. Like the matter variables introduced in Eq. (2.2) the distribution function is not invariant under the gauge transformations (2.2).

3.3.1 Scalar perturbations

For scalar perturbations a gauge-invariant distribution function is given by

$$I^{(0)}(x,p,\mu) := f^{(0)} + p\frac{\partial\tilde{F}}{\partial p}\left(\frac{1}{x}(B^{(0)} - H_T'^{(0)}) + \imath\mu(\frac{1}{2}B^{(0)} - H_T'^{(0)})\right) \ , \quad (3.36)$$

or by

$$J(x,p,\mu) := I^{(0)} - \frac{p}{2}\frac{\partial\tilde{F}}{\partial p}\Phi \ . \quad (3.37)$$

According to the expansion theorem for Legendre functions

$$I^{(0)}(x,p,\mu) = \sum_{n=0}^{\infty} a_n^{(0)}(x,p)\imath^n P_n(\mu) \quad (3.38)$$

for every $I^{(0)}(\mu) \in L^2[-1,1]$. The utility of (3.38) becomes apparent by calculating the gauge invariant matter variables $\epsilon_g, v_s^{(0)}$ and $\pi_T^{(0)}$ from (2.13) and (3.34) (a more detailed derivation is given in [40]):

$$\epsilon_g = \frac{4\pi}{\tilde{E}}\int_0^\infty dp\, p^3 a_0^{(0)}(x,p) \quad (3.39)$$

$$v_s^{(0)} = -\frac{\pi}{\tilde{E}}\int_0^\infty dp\, p^3 a_1^{(0)}(x,p) \quad (3.40)$$

$$\pi_T^{(0)} = \frac{12\pi}{5\tilde{E}}\int_0^\infty dp\, p^3 a_2^{(0)}(x,p) \ . \quad (3.41)$$

Here the orthogonality of the Legendre polynomials has been used. ϵ_m follows from ϵ_g and $v_s^{(0)}$. η vanishes, since $p^\mu p_\mu = 0$ in (3.34), and $\delta(p^\mu p_\mu) = 0$ as well. Inserting J into (3.32) for scalar perturbations leads to the equation

$$J' - \frac{1}{x}p^a\frac{\partial J}{\partial p^a} + \imath\mu J = -\imath\mu p\frac{\partial\tilde{F}}{\partial p}(\Phi + \Pi) \ , \quad (3.42)$$

where a takes the values $1,2,3$ and refers to the tetrad basis. Its solution is

$$J(x,p,\mu) = e^{-\imath\mu(x-x_0)}J(x_0,p,\mu) - \imath\mu p\frac{\partial\tilde{F}}{\partial p}\int_{x_0}^{x} dx'\,(\Phi + \Pi)(x')e^{-\imath\mu(x-x')} \ . \quad (3.43)$$

$$\epsilon_g = \frac{1}{\tilde{E}} \int \frac{d^3p}{p} p^2 J(x,p,\mu) - 2\Phi$$

and

$$\frac{1}{\tilde{E}} \int_0^\infty dp\, p^4 \frac{\partial \tilde{F}}{\partial p} = -\frac{1}{\pi}$$

result in

$$\epsilon_{\rm g} = 2\Phi + 4\Pi - 4\int_{x_0}^{x} dx' j_0(x-x')\,(\Phi+\Pi)'\,(x') + 4\sum_{n=0}^{\infty} \beta_n^{(0)} j_n(x-x_0)\ . \quad (3.44)$$

The spherical Bessel functions $j_n(x-x_0)$ are the Fourier transforms of the Legendre polynomials in Eq. (3.38). The last term on the r.h.s. determines the initial conditions. The coefficients $\beta_n^{(0)}$ are defined by

$$\begin{array}{lcl} \beta_0^{(0)} & := & \frac{\pi}{\tilde{E}} \int_0^\infty dp\, p^3 a_0^{(0)}(x_0,p) - \Pi(x_0) - \frac{1}{2}\Phi(x_0)\ , \\ \beta_n^{(0)} & := & \frac{\pi}{\tilde{E}} \int_0^\infty dp\, p^3 a_n^{(0)}(x_0,p)\ , \qquad n \geq 1\ . \end{array} \quad (3.45)$$

Equation (3.44) is the same as (3.10) in the field theoretic approach, except that the initial conditions are parametrized differently. The coefficients $\gamma_n^{(0)}$ appearing in Eq. (3.10) can be related to the $\beta_n^{(0)}$ through the formula

$$j_n' = \frac{1}{2n+1}\left(n j_{n-1} - (n+1) j_{n+1}\right) \quad (3.46)$$

by a linear transformation which is non-singular and of upper-triangular form (albeit infinite-dimensional). If $\beta_n^{(0)} = 0$ for all $n \geq 3$, which is a frequently adopted simplifying assumption in the kinetic approach (the so-called 14-moment approximation, see, e.g., Ref. [63]), this relationship is given by

$$\begin{array}{lcl} \gamma_0^{(0)} & = & -\beta_0^{(0)} - \frac{1}{2}\beta_2^{(0)}, \\ \gamma_1^{(0)} & = & \beta_1^{(0)}, \\ \gamma_2^{(0)} & = & -\frac{3}{2}\beta_2^{(0)}. \end{array} \quad (3.47)$$

3.3.2 Vector perturbations

Here we use the gauge-invariant distribution function

$$I^{(1)}(x,p,\mu) := f^{(1)} + \frac{p}{2}\frac{\partial \tilde{F}}{\partial p} B^{(1)} \quad (3.48)$$

and expand it, as above, into Legendre polynomials in μ:

$$I^{(1)}(x,p,\mu) = \sum_{n=0}^{\infty} a_n^{(1)}(x,p) \imath^n P_n(\mu)\ . \quad (3.49)$$

In terms of the coefficients $a_n^{(1)}$, the matter variables are

$$v_c = \frac{\pi}{\tilde{E}} \int_0^\infty dp\, p^3 \left(a_0^{(1)}(x,p) + \frac{1}{5} a_2^{(1)}(x,p) \right) \ , \tag{3.50}$$

$$\pi_T^{(1)} = -\frac{24\pi}{5\tilde{E}} \int_0^\infty dp\, p^3 \left(\frac{1}{3} a_1^{(1)}(x,p) + \frac{1}{7} a_3^{(1)}(x,p) \right) \ . \tag{3.51}$$

For vector perturbations Eq. (3.32) reads:

$$I'^{(1)} - \frac{1}{x} p^a \frac{\partial I^{(1)}}{\partial p^a} + \imath \mu I^{(1)} = \imath \mu p \frac{\partial \tilde{F}}{p} \Psi \ . \tag{3.52}$$

Its solution is:

$$I^{(1)}(x,p,\mu) = e^{-\imath\mu(x-x_0)} I^{(1)}(x_0,p,\mu) + \imath \mu p \frac{\partial \tilde{F}}{\partial p} \int_{x_0}^{x} dx' \Psi(x') e^{-\imath\mu(x-x')} \ . \tag{3.53}$$

With this solution v_c reads:

$$v_c = -3 \int_{x_0}^{x} dx' \frac{j_2(x-x')}{x-x'} \Psi(x') + \frac{3}{2} \sum_{n=0}^{\infty} \beta_n^{(1)} \left(j_n(x-x_0) + j_n''(x-x_0) \right) \ . \tag{3.54}$$

The initial conditions are given by the coefficients

$$\beta_n^{(1)} = \frac{\pi}{\tilde{E}} \int_0^\infty dp\, p^3 a_n^{(1)}(x_0,p) \ . \tag{3.55}$$

Relating the coefficients $\beta_n^{(1)}$ to the $\gamma_n^{(1)}$, which parametrize the initial conditions in Eq. (3.13), the result of the kinetic approach equals that of the field theoretic calculation. Because of $j_0 + j_0'' = \frac{2}{3}(j_0 + j_2)$ the relationship between the $\gamma^{(1)}$ and the $\beta^{(1)}$ is, apart from an over-all sign, the same as in the scalar case. Hence, we have

$$\begin{aligned} \gamma_0^{(1)} &= \beta_0^{(1)} + \frac{1}{2}\beta_2^{(1)}, \\ \gamma_1^{(1)} &= -\beta_1^{(1)}, \\ \gamma_2^{(1)} &= \frac{3}{2}\beta_2^{(1)}. \end{aligned} \tag{3.56}$$

3.3.3 Tensor perturbations

For tensor perturbations the distribution function $f^{(2)}$ is gauge-invariant itself. With its expansion into Legendre polynomials

$$f^{(2)}(x,p,\mu) = \sum_{n=0}^{\infty} a_n^{(2)}(x,p) \imath^n P_n(\mu) \tag{3.57}$$

the anisotropic pressure reads:

$$\pi_T^{(2)} = \frac{24\pi}{15\tilde{E}} \int_0^\infty dp\, p^3 \left(a_0^{(2)}(x,p) + \frac{2}{7} a_2^{(2)}(x,p) + \frac{1}{21} a_4^{(2)}(x,p) \right) . \qquad (3.58)$$

The Vlasov equation for the tensor perturbations reads:

$$f'^{(2)} - \frac{1}{x} p^a \frac{\partial f^{(2)}}{\partial p^a} + \imath \mu f^{(2)} = p \frac{\partial \tilde{F}}{\partial p} H' . \qquad (3.59)$$

It is solved by

$$f^{(2)}(x,p,\mu) = e^{-\imath\mu(x-x_0)} f^{(2)}(x_0,p,\mu) + p \frac{\partial \tilde{F}}{\partial p} \int_{x_0}^x dx' H'(x') e^{-\imath\mu(x-x')} . \quad (3.60)$$

For the anisotropic pressure this yields

$$\begin{aligned} \pi_T^{(2)} &= -24 \int_{x_0}^x dx' \frac{j_2(x-x')}{(x-x')^2} H'(x') \\ &+ 3 \sum_{n=0}^\infty \beta_n^{(2)} \left(j_n(x-x_0) + 2 j_n''(x-x_0) + j_n^{(IV)}(x-x_0) \right) . \end{aligned} \qquad (3.61)$$

The coefficients encoding the initial conditions are

$$\beta_n^{(2)} = \frac{\pi}{\tilde{E}} \int_0^\infty dp\, p^3 a_n^{(2)}(x_0,p) , \qquad (3.62)$$

which is again Eq. (3.14). Because of $j_0 + 2j_0'' + j_0^{(IV)} = 8(\frac{1}{15}j_0 + \frac{2}{21}j_2 + \frac{1}{35}j_4)$ the first three coefficients $\gamma_n^{(2)}$ and $\beta_n^{(2)}$ are related to each other by

$$\begin{aligned} \gamma_0^{(2)} &= -\beta_0^{(2)} - \frac{1}{2}\beta_2^{(2)}, \\ \gamma_1^{(2)} &= \beta_1^{(2)}, \\ \gamma_2^{(2)} &= -\frac{3}{2}\beta_2^{(2)}, \end{aligned} \qquad (3.63)$$

if all higher coefficients are zero, exactly as in the scalar case.

Summarizing, the kinetic theory approach in the gauge invariant formulation of Ref. [40] and the thermal-field-theory approach in the high temperature limit lead to the same matter perturbations in a Einstein-de Sitter universe filled with collisionless, massless particles. There is a difference, however, in the way how the initial conditions are introduced, which may seem somewhat arbitrary in the field theoretical approach. In fact, the initial condition terms in Eqs. (3.44), (3.54), and (3.61) are completely arbitrary functions due to the Neumann expansion theorem. We could therefore just have added the inhomogeneous terms by hand at the end of the field theoretic calculation, but as we have seen there is still a close relation to the initial moments of the initial distribution function of the kinetic approach.

Chapter 4

Cosmological perturbations with ultrarelativistic plasmas

In this chapter we study the evolution of cosmological perturbations in the radiation dominated epoch in the presence of a collisionless or weakly interacting ultrarelativistic plasma. Photons, electrons and baryons may be described by a perfect fluid before decoupling of the photons, as was discussed in section 2.3.1. But it turns out that these particles alone can not account for the observed large-scale structure. Some dark matter (DM) is needed. For a discussion we refer to the standard textbooks, e.g. [3]. Hot dark matter (HDM) particles are still relativistic when the cosmologically relevant scales (say $1h^{-1}$ Mpc – $3h^{-1}$ Gpc) cross into the horizon (the scale of $1h^{-1}$ Mpc crosses close to equilibration time, where the temperature is several eV), whereas particles that are nonrelativistic at that time are called cold dark matter (CDM). The most prominent candidates for HDM are massive neutrinos with a mass of several eV. After the weak phase transition the neutrinos are decoupled, whereas the other particles remain in thermal equilibrium.

We investigate the effects of collisionless matter in addition to a perfect fluid component in the next section. The second section of this chapter deals with dimension dependent features of ultrarelativistic plasmas, the last section is devoted to weakly self-interacting plasmas.

The equations of motion for the scalar, vector and tensor metric potentials follow from (2.15) – (2.22) together with the expressions for the gauge invariant matter variables from chapter 3 and the considerations of section 2.4. We consider isentropic perturbations only ($\eta = 0$). The closed system of integro-differential equations for the scalar perturbations reads:

$$\Phi(x) = \Phi_{\rm pf}(x) + \Phi_{\rm rp}(x) \tag{4.1}$$

$$
\begin{aligned}
x^2\Phi_{\mathrm{rp}}(x) &= \frac{2n(n+1)}{(n-1)^2}\alpha\left[2\Pi(x)+(n-2)\Phi(x)-\right. \\
&\quad \left.\int^x dx' K^{(0)}_{\epsilon_m}(x-x')\left(2\Pi+(n-1)\Phi\right)'(x')\right] \qquad (4.2) \\
x^2\Pi &= -\frac{(n+1)n}{n-1}\alpha\int^x dx' K^{(0)}_{\pi_T}(x-x')\times \\
&\quad \left(2\Pi+(n-1)\Phi\right)'(x') \qquad (4.3) \\
\Phi''+\frac{4}{x}\Phi'+\frac{1}{n}\Phi &= -\frac{4}{(n-1)x}\Pi'+\frac{2}{n}\Pi \qquad (4.4)
\end{aligned}
$$

For $\alpha = 1$ we use

$$
\begin{aligned}
&x^2\left[\frac{2}{(n-1)x}\Phi'+\left(\frac{1}{n}+\frac{4(n-2)}{(n-1)^2x^2}\right)\Phi+\frac{8}{(n-1)^2x^2}\Pi\right]= \\
&\frac{2(n+1)}{(n-1)^2}\left[2\Pi(x)+(n-2)\Phi(x)-\right. \\
&\left.\int^x dx' K^{(0)}_{\epsilon_g}(x-x')\left(2\Pi+(n-1)\Phi\right)'(x')\right] \qquad (4.5)
\end{aligned}
$$

together with (4.4). The vector equation reads:

$$
x^2\Psi = \frac{4(n+1)}{n-1}\left[(1-\alpha)v_{\mathrm{c\ pf}}-\alpha n\int^x dx' K^{(1)}_{v_c}(x-x')\Psi(x')\right], \qquad (4.6)
$$

where $v_{\mathrm{c\ pf}}$ is constant. The tensor perturbations satisfy

$$
x^2\left(H''+\frac{2}{x}H'+H\right) = -\alpha\frac{4n(n+1)}{n-1}\int^x dx' K^{(2)}_{\pi_T}(x-x')H'(x'). \qquad (4.7)
$$

The kernels $K^{(a)}_i$ can be read off the expressions for the matter variables in chapter 3. The initial conditions are omitted here. They follow from the replacement (3.9).

The above integro-differential equations cannot, in general, be solved by, say, a power series ansatz around x_0. Various methods have been employed to solve them approximately: direct numerical integration [36, 39, 51]; approximation by a finite sum of spherical Bessel functions [23] or by a finite system of ordinary differential equations [52].

However, for $x_0 \to 0$, which is usually the most interesting point to define initial conditions anyway, a generalized power series ansatz can be solved recursively. Exact regular solutions were found in this way in Refs. [41, 45], where it turned out that the power series involved had infinite radius of convergence and converged faster than trigonometric functions do. In the following, this will be generalized to include singular solutions as well as the most general initial data at $x_0 = 0$. Some of the more unwieldy details are relegated to the Appendix C.

If $F(x)$ represents one of the metric potentials Φ, Π, Ψ, H, the general solution with $x_0 = 0$ turns out to be of the form

$$F(x) = C_1 F_{\mathrm{reg}}(x) + C_2 x^{\sigma} F_{\mathrm{sing}}(x) \tag{4.8}$$

with

$$F_{\mathrm{reg,sing}}(x) = \sum_{l=0}^{\infty} c_l^{\mathrm{reg,sing}} \frac{x^l}{l!} \tag{4.9}$$

and C_1, C_2 being arbitrary constants. This form is a consequence from demanding that the coefficients $\gamma_l^{(a)}$ remain finite as $x_0 \to 0$.

When inserted into the integro-differential equations (4.1 – 4.7) this leads to solvable recursion relations for the coefficients c_l such that $c_l = c_l(c_0, \ldots, c_{l-1}; \alpha, n, \{\gamma\})$, because the power series representation of the kernels

$$K_i^{(a)}(x - x') = \sum_{m=0}^{\infty} K_i^{(a)}(m)(x - x')^{2m+k} \tag{4.10}$$

leads to integrals

$$\int_0^x dx'(x - x')^m x'^{\nu} = \frac{m!}{(1+\nu)\cdots(1+m+\nu)} x^{1+m+\nu}, \tag{4.11}$$

where m is a natural number and ν arbitrary.

Solving these recursion relations it turns out that the coefficients $\gamma_l^{(a)}$ (or, equivalently, $\beta_l^{(a)}$) in Eqs. (4.1 – 4.7) either have to be all zero, which also puts F_{reg} to zero, H_{reg} is the exception, or have to satisfy certain constraints dictated by the values $F_{\mathrm{reg}}(0)$. In each case a singular part in Eq. (4.8) exists that can be superimposed on the regular solutions by choosing $C_2 \neq 0$. With $x_0 = 0$ only the regular part depends on the initial data. The presence of singular perturbations means that the initial singularity is no longer approximately one of the FLRW type, but is essentially anisotropic. Linear perturbation theory then applies only for those values of x where F has become sufficiently small.

It turns out that the singular behaviour for $x \to 0$ is given by

$$\sigma_{\pm}^{(a)} = -\frac{5}{2} + a \pm \sqrt{\frac{(n+2)(n-1) - 16\alpha(n+1)}{4(n+2)(n-1)}} \tag{4.12}$$

with $a = 0, 1, 2$ for $(a) = S, V, T$. If the fraction α of energy density contained in collisionless matter exceeds $\alpha_{\mathrm{crit.}} = \frac{5}{32}$ for $n = 3$ and $\alpha_{\mathrm{crit.}} = \frac{(n+2)(n-1)}{16(n+1)}$ for general n, σ becomes complex, leading to an essential singularity at $x = 0$ with F oscillating like $\cos([\mathrm{Im}\sigma] \ln x)$. This asymptotic behaviour has been previously found by Zakharov [37] and examined further by Vishniac [38].[1] As explained by the latter, the essentially singular oscillatory behaviour for $x \to 0$ arises, because the momentum flux carried by the collisionless particles preferentially depends on the expansion of the universe in their direction of travel, and not on the net expansion of the volume, which leads to an excessive feedback for $\alpha > \alpha_{\mathrm{crit.}}$. Thus, in this case the initial singularity can be of a mixmaster type [14]. It has been shown by Lukash et al. [15] that collisionless matter provides an efficient means to disperse the initially strong anisotropy of such models; the singular parts of our solutions (4.8) could therefore correspond to the later stage of such a scenario where the linear regime has already been reached.

4.1 Collisionless matter mixed with a perfect fluid

Let us restrict the discussion to $n = 3$ in this section. Because the interpretation of the initial conditions is simpler in the kinetic approach than in the field theoretic approach, let us specify the initial conditions in terms of $\beta_l^{(a)}$'s.

4.1.1 Scalar perturbations

Regular solutions for scalar perturbations, where $\Phi(x)$ and $\Pi(x)$ stay finite for $x \to 0$, are only possible, when the coefficients $\beta_n^{(0)}$ in Eqs. (4.2) and (4.3) satisfy certain constraints. Evaluation of these equations and their first derivatives at $x = x_0 = 0$ yields restrictions on the initial matter distribution, i.e.

$$\beta_1^{(0)} = \beta_2^{(0)} = \beta_3^{(0)} = 0 \ , \tag{4.13}$$

and relations between the initial values of the metric potentials

$$\Phi(0) + 2\Pi(0) = -4\beta_0^{(0)} \tag{4.14}$$

and

$$2\Phi'(0) = -\Pi'(0) \ . \tag{4.15}$$

[1] The result of Eq. (4.12) agrees with the asymptotic behaviour found in Ref. [37] for scalar, vector, and tensor perturbations, but not with Ref. [38], where the vector case was reported to have a different critical value $\alpha_{\mathrm{crit.}}$.

The restrictions on $\beta_0^{(0)}$, $\beta_1^{(0)}$, and $\beta_2^{(0)}$ can be understood from the Einstein equations written in the form of Eqs. (2.16) and (2.18) together with covariant conservation of the energy-momentum tensor, Eq. (2.19), by inserting the definitions in Eqs. (3.39) – (3.41) and (3.45); the vanishing of $\beta_3^{(0)}$ is a consequence of demanding regularity of Π in Eq. (4.3).

The explicit recursion relations defining $\Phi_{\rm rp}, \Phi_{\rm pf}$, and Π follow from the Eqs. (4.1) – (4.4). They are listed in the first part of appendix C. The recursion relations uniquely determine the regular parts of all potentials for a given set of $\beta_l^{(0)}$'s, respecting Eq. (4.13) (or equivalently a set of $\gamma_l^{(0)}$'s, satisfying more involved conditions). The singular solutions do not depend on the inhomogeneous terms. Thus, they can be added to any regular solution. Singular solutions for the metric potentials with poles of first or second order are forbidden for $x_0 = 0$, since in this case the integral (4.11) is divergent for all negative integers ν. For finite x_0, however, such solutions exist. (An example can be found in Ref. [38], Eq. (40b).)

In Fig. 4.1, regular solutions for ϵ_m, which coincides with the energy-density contrast δ on comoving hypersurfaces, are given in the purely collisionless case for three different initial data: one, where only $\beta_0^{(0)}$ is non-vanishing, a second, where the first four coefficients have been put to zero, and a more generic one. All of them grow according to a power-law on superhorizon scales, where the second (dashed-line) solution exemplifies that an arbitrarily high power can be achieved by appropriately contrived initial data; on sub-horizon scales all solutions undergo damped oscillations, whose amplitude falls off like $1/x$ eventually. The exact matching of the allowed asymptotic behaviour is, however, seen to strongly depend on the form of the initial data. The asymptotic regimes themselves are determined by rather different physical situations. On superhorizon scales, $x \ll 1$, everything can be viewed as being determined by the global geometry set up in accordance with the inital matter distribution. For $x \gg 1$, microphysics becomes important, and there the damped oscillations can be understood as the dispersion of density contrast carried by the collisionless particles through directional dispersion [39]. The intermediate growth of the amplitude of the dotted solution in Fig. 4.1 after its 5th maximum is due to a nonzero $\beta_{20}^{(0)}$. This demonstrates that higher momenta in the initial distribution function may have considerable effects even at subhorizon scales. [2]

In Fig. 4.2 a particular regular solution is shown in the two-component case with equal energy density in the perfect-fluid and in the collisionless component. In order that the collisionless component can be smoothly matched

[2] The sometimes used 14-moment approximation [52] therefore potentially misses important details in the evolution of cosmological perturbations.

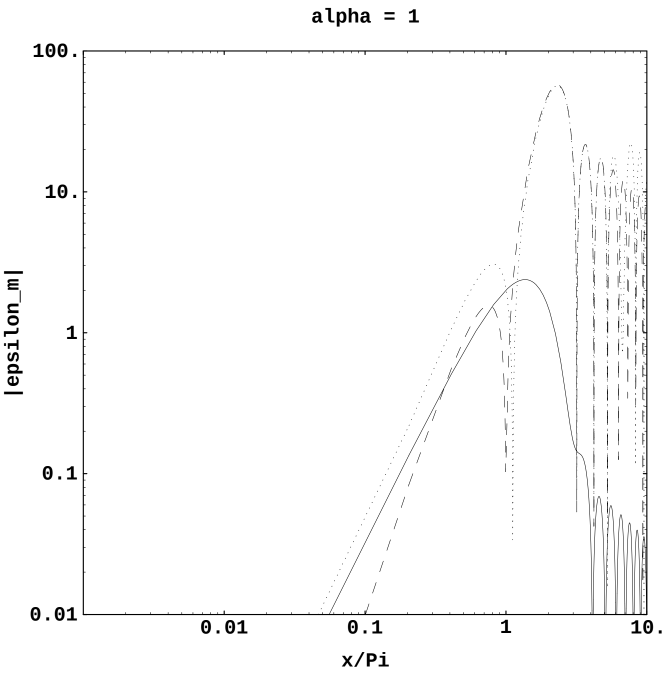

Figure 4.1: Regular density perturbations on comoving hypersurfaces in the purely collisionless case ($\alpha = 0$). The full line shows a regular solution for $|\epsilon_{\rm m}|$ with $\beta_0^{(0)} = -5/28$ and all other $\beta_n^{(0)}$'s vanishing. The dashed line represents a solution with $\beta_5^{(0)} = -1309/20$ nonvanishing only. For the dotted line $\beta_0^{(0)}$ takes the above value, and $\beta_5^{(0)} = -10$, $\beta_{20}^{(0)} = 60$.

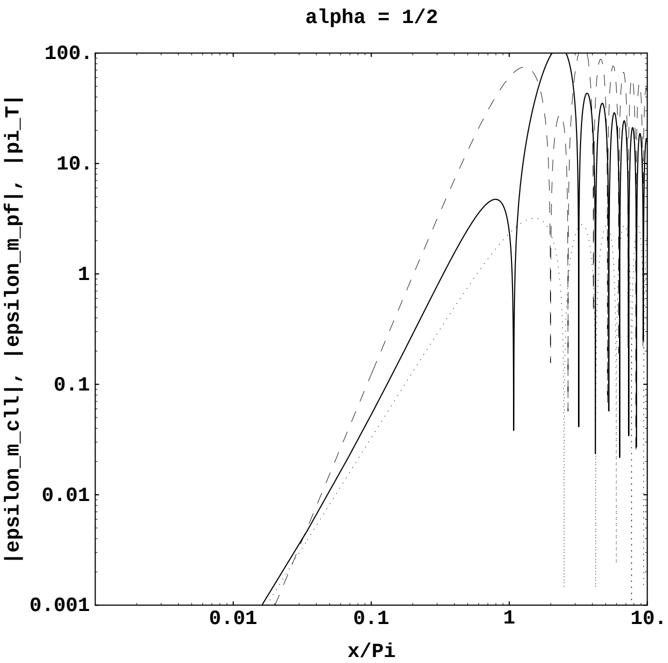

Figure 4.2: Regular scalar perturbations in a two-component universe ($\alpha = 1/2$). The various lines show regular solutions for $|\epsilon_{\mathrm{m\ rp}}|$ (full line), $|\epsilon_{\mathrm{m\ pf}}|$ (dotted line), and $|\pi_T^{(0)}|$ (dashed line). The initial conditions are specified by $\beta_0^{(0)} = -1/4, \beta_5^{(0)} = -1309/20$, and $\beta_4^{(0)} = 7/8$.

to a perfect-fluid behaviour for $x \to 0$, the initial data have been chosen so that $\Pi(0) = 0$, which makes $\Phi_{\mathrm{pf}}(0) = \Phi_{\mathrm{rp}}(0)$. After horizon-crossing the energy-density contrast that remains in the perfect-fluid component is seen to be undamped and to have a smaller phase velocity, namely $c/\sqrt{3}$, in contrast to c in the strongly damped collisionless component. The ratio of $\epsilon_{\mathrm{m\ rp}}$ to $\epsilon_{\mathrm{m\ pf}}$ at horizon crossing strongly depends on the initial data chosen. In Fig. 4.2 the collisionless component dominates over the perfect-fluid component up to fairly large values of x; the solutions presented in Refs. [46] show opposite behaviour[3], due to having chosen $\beta_5^{(0)} \neq 0$ in the case of Fig. 4.2.

In Figs. 4.3–4.5 singular solutions are displayed with $\beta_n^{(0)} = 0$ for all n. These do not have perturbed initial matter distribution at $x_0 = 0$, which underlines their geometrical nature. In Fig. 4.3 the energy-density contrast δ and the anisotropic pressure π_T is plotted for the purely collisionless case $\alpha = 1$. Now there are also oscillations on superhorizon scales as discussed above, which go over to damped oscillations with phase velocity equal to c on subhorizon scales, showing the same asymptotic behaviour there as the

[3]The author of Ref. [51] claims that $\pi_T^{(0)} < \epsilon_m$ in general, which is seen to hold true for certain initial conditions only.

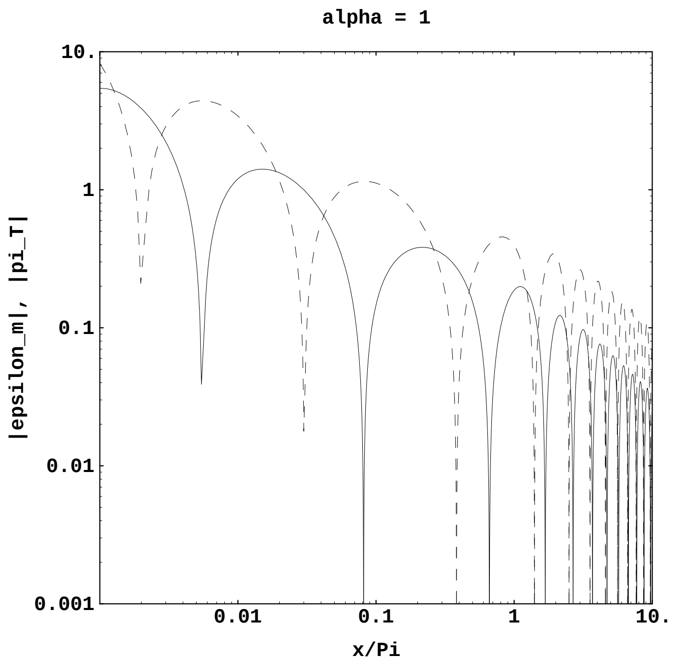

Figure 4.3: Singular solutions for $|\epsilon_{\rm m}|$ (full line) and $|\pi_T^{(0)}|$ (dashed line) for $\alpha = 1$ (purely collisionless case). Superhorizon oscillations show up for $x/\pi < 1$. Note the logarithmic scale in x — the solutions are essentially singular as $x \to 0$. The second solution corresponding to $\sigma_-^{(0)}$ in Eq. (4.12), which is not plotted, differs essentially by a phase.

regular solutions. In Fig. 4.4 the singular solutions are plotted for $\alpha = 5/32$, where the perfect-fluid component is just strong enough to eliminate the superhorizon oscillations. For smaller values of α there a two essentially different solutions with different degree of singularity. For $\alpha = 1/10$ they are rendered in Fig. 4.5. In the two-component cases of Figs. 4.4 and 4.5 the perfect-fluid component turns out to have a regular limit for $x \to 0$, growing until horizon crossing, after which they again turn into undamped acoustic waves with phase velocity $c/\sqrt{3}$.

4.1.2 Vector perturbations

The requirement of regularity yields the conditions

$$\frac{\alpha}{\alpha - 1}\left(\beta_0^{(1)} + \frac{1}{5}\beta_2^{(1)}\right) = v_{\rm c\ pf} \tag{4.16}$$

and

$$\beta_1^{(1)} = -\frac{3}{7}\beta_3^{(1)} \tag{4.17}$$

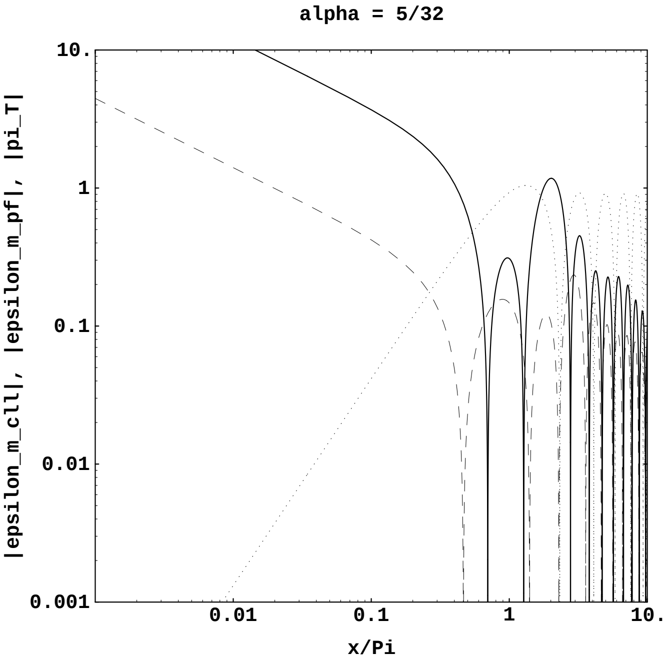

Figure 4.4: Singular scalar perturbations for the critical value of $\alpha = 5/32$. $|\epsilon_{\mathrm{m\ rp}}|$ (full line), $|\epsilon_{\mathrm{m\ pf}}|$ (dotted line), and $|\pi_T^{(0)}|$ (dashed line) are plotted.

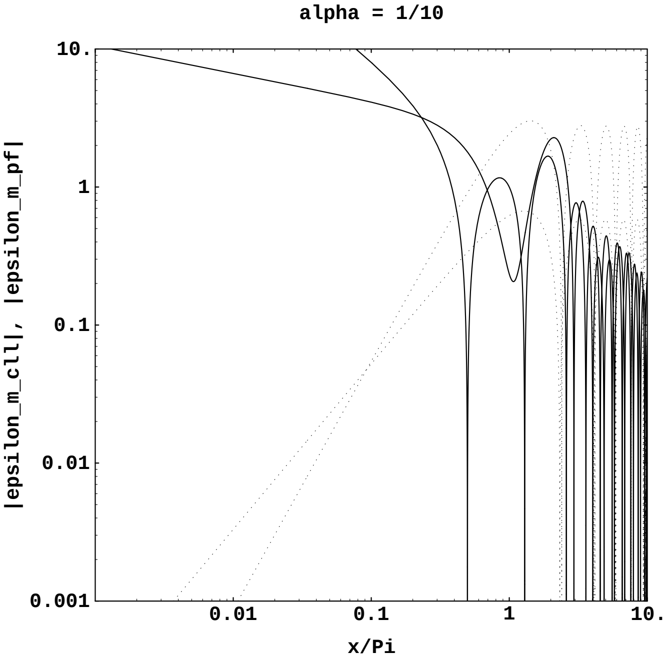

Figure 4.5: Singular scalar perturbations in the subcritical case ($\alpha < 5/32$). The two different modes ($\sigma_{\pm}^{(0)}$) are shown by the full lines for $|\epsilon_{\mathrm{m\ rp}}|$ and by the dotted ones for $|\epsilon_{\mathrm{m\ pf}}|$. They have different power-law behaviour on superhorizon scales.

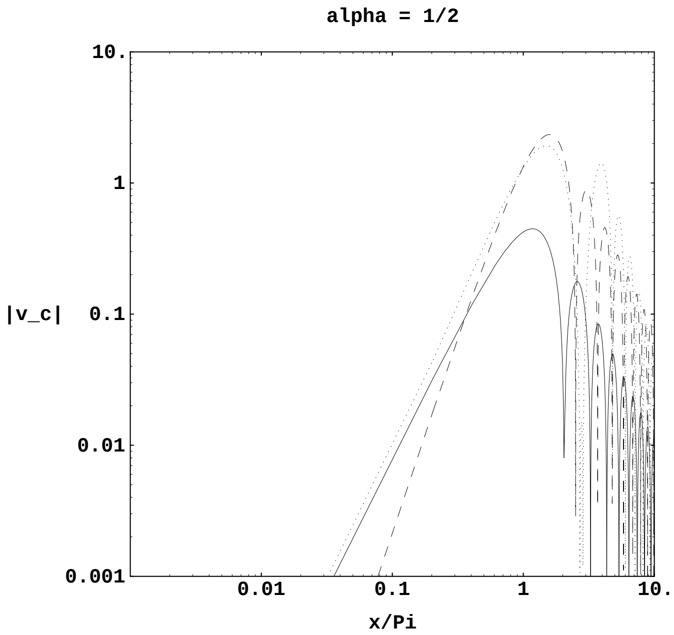

Figure 4.6: Regular vector perturbations with $v_{c\ \mathrm{pf}} = 0$. The solutions for $|v_c|$ are given with $\beta_0^{(1)} = -21/16$ being nonzero only (full line), $\beta_1^{(1)} = -1197/80$ nonzero only (dashed line), and $\beta_0^{(1)} = -21/16, \beta_1^{(1)} = -10$ and $\beta_{10}^{(1)} = 20$ for the dotted line.

for the vector perturbations. These conditions follow from Eq. (4.6) and its first derivative at $x = x_0 = 0$. The singular solutions may be added as in the scalar case.

For the perfect-fluid case $\alpha = 0$ there are no regular solutions as mentioned at the end of chapter 2. However, with collisionless matter, vorticity can be generated on super-horizon scales, which after horizon-crossing dies out through directional dispersion. This is shown for various initial data in Fig. 4.6 for $\alpha = 1/2$. The growth in $v \sim x^2$ at superhorizon scales is brought about by $\Psi(x)$ approaching a constant for $x \to 0$. A more rapid growth arises when Ψ itself goes like a positive power of x, which is the case for $\beta_0^{(1)} = 0$ and nonvanishing higher coefficients. One such example is shown by the dashed line in Fig. 4.6. In all these cases there is a genuine production of vorticity, which in the perfect-fluid case is forbidden by the Helmholtz-Kelvin circulation theorem [64].

With different initial matter distributions it is also possible to arrange a nonvanishing initial vorticity in the perfect-fluid component, which is compensated by an equal amount with opposite sign in the collisionless component on superhorizon scales. A net vorticity then survives on subhorizon

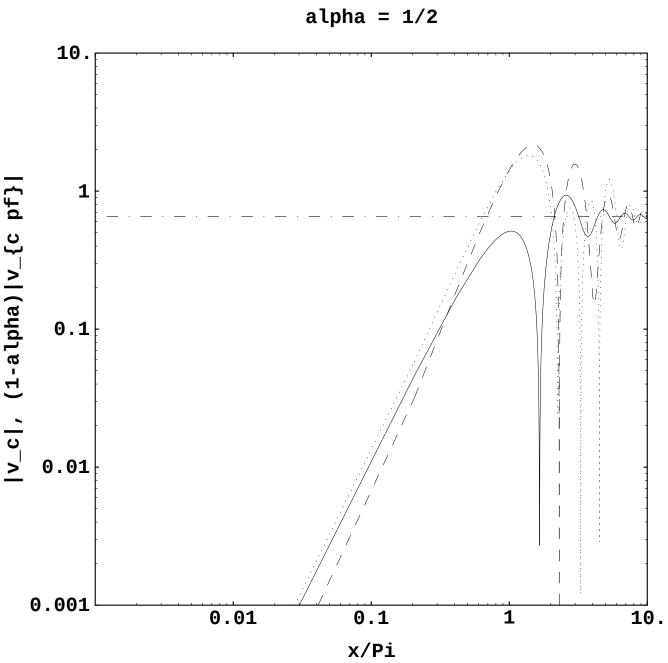

Figure 4.7: Regular vector perturbations with non-vanishing vorticity in the perfect-fluid component. The contribution of $v_{c\ \rm pf} = -21/16$ to $|v_c|$ is plotted dashed-dotted. The other lines show various solutions for $|v_c|$ using the same initial conditions as in Fig. 4.6 except for $\beta_2^{(1)}$, which is determined by Eq. (4.16).

scales after the dispersion of the collisionless part. In Fig. 4.7 such solutions are plotted for several initial conditions. This interesting possibility has been studied extensively in Refs. [45, 46], to which we refer the reader for more details. Here we just mention that the vorticity in the perfect-fluid component, which with collisionless matter being present can be reconciled with an initial FLRW-type singularity, gives rise to magnetic fields during the transition to the matter-dominated area, and the limits set by the anisotropy of the cosmic microwave background are such that astrophysically interesting amounts of primordial magnetic fields seem possible [46].

In Fig. 4.8 we display the singular vector solutions for $\alpha = 1$, $5/32$, and $1/10$. For $\alpha > 5/32$ there are superhorizon oscillations again, which cease at $\alpha = 5/32$, and for smaller α two different power-law asymptotics occur. While $v \to 0$ for $x \to 0$, the metric potential Ψ, in fact, diverges. Hence, these solutions do not correspond to a Friedmann-type initial singularity, but are essentially anisotropic.

On sub-horizon scales, where the mechanism of directional dispersion becomes operative, both the regular and the singular solutions decay like

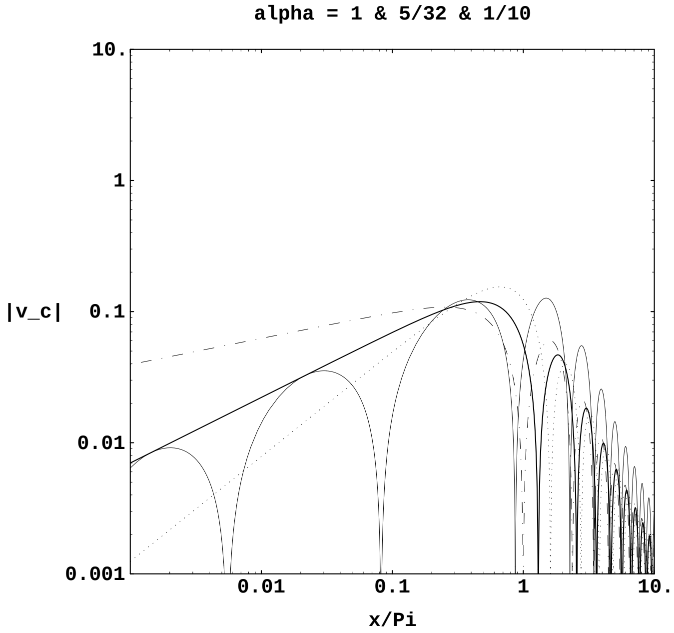

Figure 4.8: Singular vector perturbations in terms of $|v_c|$. The different lines correspond to different values of α and to different modes. The solutions with, e.g., $\alpha = 1$ (thin full line) show superhorizon oszillations, whereas solutions for $\alpha_{\mathrm{crit.}}$ (thick full line) and below, e.g. $\alpha = 1/10$ (dashed-dotted and dotted), do not. The latter two lines correspond to the two different modes from Eq. (4.12). In the supercritical case both modes differ by their phase only.

$1/x^2$ for large x.

4.1.3 Tensor perturbations

A necessary condition for the regular solutions is obtained from Eq. (4.7) at $x = x_0 = 0$, i.e.

$$\beta_0^{(2)} + \frac{2}{7}\beta_2^{(2)} + \frac{1}{21}\beta_4^{(2)} = 0 \ . \qquad (4.18)$$

In contrast to vector and scalar perturbations the initial value $H(0)$ is not fixed by the initial matter distribution. This corresponds to the existence of gravitational waves. Both polarisations evolve with the same $H(x)$, since there is no preferred direction. Again the singular solutions can be added to the regular ones.

In Fig. 4.9 various regular solutions for the metric potential H are given. The ones that start out as constants at superhorizon scales are similar to the ones already found in the perfect-fluid case (see above), the only difference being the amplitude dropping more strongly at horizon-crossing. On subhorizon scales these solutions become gravitational waves and their decay $\sim 1/x$ is determined by the expansion, exactly as in the perfect-fluid case. A novel type of solution is obtained, however, by putting $\beta_0^{(2)} = 0$. As shown by the dashed curve, this gives a growing solution on superhorizon scales.

Finally, in Fig. 4.10 we also exhibit the singular solutions for H for the same set of parameters as in Fig. 4.8. Again the spectacular behaviour is restricted to superhorizon scales, upon horizon crossing these solutions again describe ordinary, albeit primordial, gravitational waves.

4.2 Dimension dependent effects

We already studied the dependence on the spatial dimension of perfect fluid perturbations in section 2.3. Only the isentropic speed of sound is dimension dependent, i.e. $c_{\rm s} = n^{-\frac{1}{2}}$. The energy density of the background changes according to (1.17). This simple picture changes, when more collisional matter is added. The singular solutions show again oscillations on superhorizon scales for $\alpha > \alpha_{\rm crit.}(n)$. But $\alpha_{\rm crit.}(n)$ is monotonically increasing with n (4.12). It exceeds unity at $n = 17$. For dimensions $n \geq 17$ no superhorizon oscillations can occur. In just two spatial dimensions $\alpha_{\rm crit.}$ vanishes and all singular solutions show superhorizon oscillations.

On subhorizon scales the damping effects are most important. We already discussed the mechanism of directional dispersion in section 2.4.1. To study

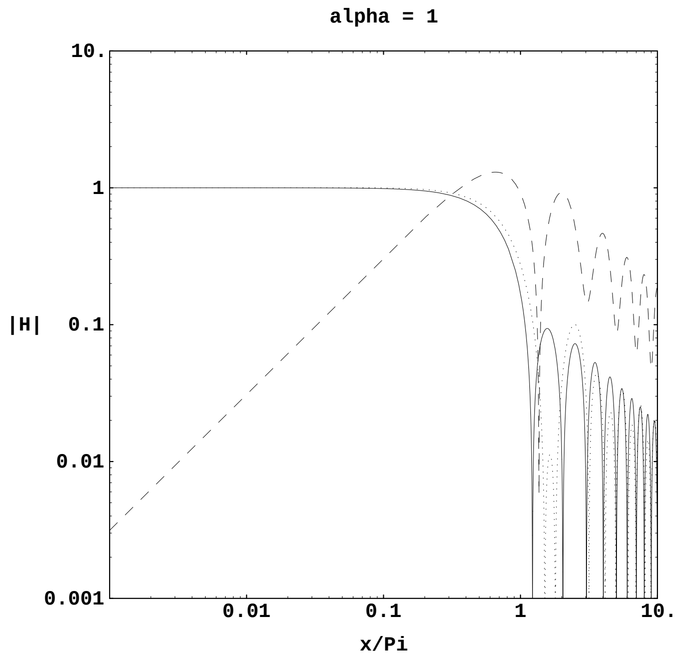

Figure 4.9: Regular tensor perturbations. The solutions, representing gravitational waves for $x \gg 1$, are normalized to $H(0) = 1$, except for the dashed line ($H(0) = 0, \beta_1^{(2)} = 63/2$). The full line shows the solution with all $\beta_n^{(2)}$'s vanishing. Again the dotted line represents a more general case with $\beta_1^{(2)} = 1, \beta_4^{(2)} = 5, \beta_6^{(2)} = -10$, and $\beta_7^{(2)} = 20$ nonzero.

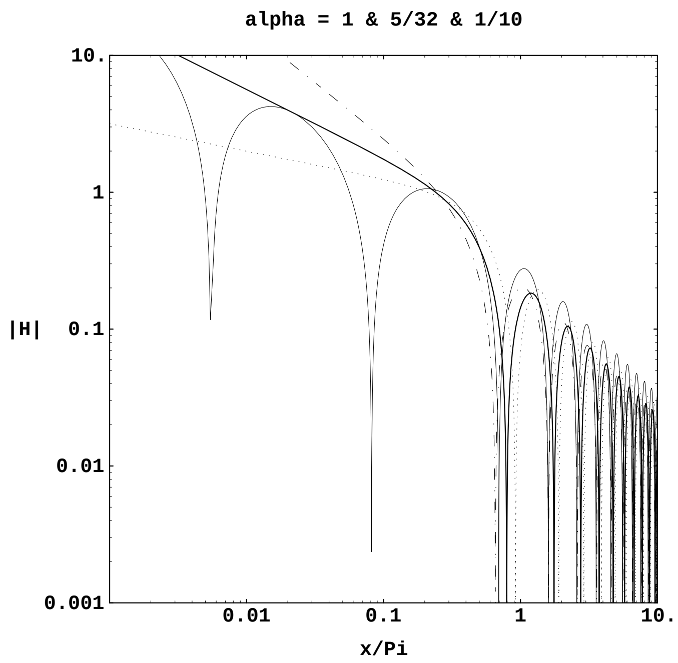

Figure 4.10: Singular tensor perturbations. $|H|$ is plotted for the same values of α as for the vector perturbations of Fig. 4.8.

these effects let us neglect the perfect fluid perturbations, i.e. $\alpha = 1$, and let us stick to the regular solutions.

4.2.1 Scalar perturbations

In Fig. 4.11 the density contrast $|\epsilon_{\mathrm{m}}|$ is plotted for $n = 3, 4$, and 7. The simplest initial conditions are used ($\gamma_0^{(0)} =$ const. and all other $\gamma_n^{(0)}$ vanish). The normalization of the solutions is arbitrary. The perturbations are damped ($\sim x^{-(n-1)/2}$) indeed, as predicted by the simple consideration in section 2.4.1. Note that the asymptotic behaviour of the solutions is determined by the asymptotic behaviour of the kernel in (4.5). The phase velocity is the speed of light for all dimensions. A new feature is the tiny shift of the maximum of the perturbation to later times, i.e. in higher dimensions perturbations start to "feel" the horizon at a later time.

4.2.2 Vector perturbations

The vorticity perturbations for $n = 3, 4$, and 7 are shown in Fig. 4.12. Again the simplest initial conditions with $\gamma_0^{(1)} = (n+2)^{-1}\gamma_2^{(1)}$ have been chosen. All other $\gamma_n^{(1)}$ vanish. The normalization is again arbitrary. These perturbations are damped due to directional dispersion, too, but stronger than the scalar

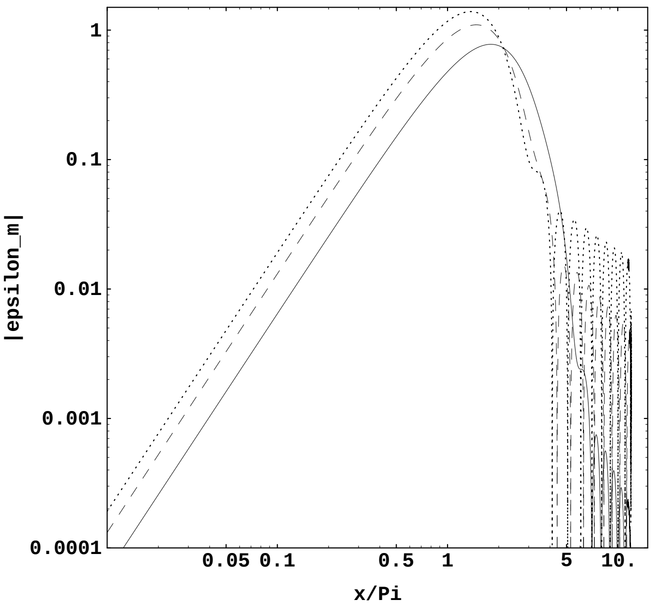

Figure 4.11: Scalar perturbations in three (dotted), four (dashed), and eight (full line) spatial dimensions. On subhorizon scales the damping is faster in higher dimensions.

perturbations ($\sim x^{-(n+1)/2}$) in agreement with the asymptotic behaviour of the kernel in (4.6). The maximum of the perturbation is shifted as for the scalar perturbations.

4.2.3 Tensor perturbations

The situation for tensor perturbations is different. There is no directional dispersion of gravity waves. All damping is due to the conservation of the energy of the gravity wave. This is shown in Fig. 4.13. We normalize initially the amplitude to unity. The decay of the solutions in $n = 3, 4$, and 7 spatial dimensions is proportional to x^{-1}. The asymptotic behaviour is not determined by the kernel of (4.7), but by the second order differential operator on the r.h.s. The amplitude inside the horizon depends on the number of spatial dimensions. It is bigger for a higher number of dimensions. For a big number of spatial dimensions it converges to the solution of a perfect fluid (Fig. 4.14).

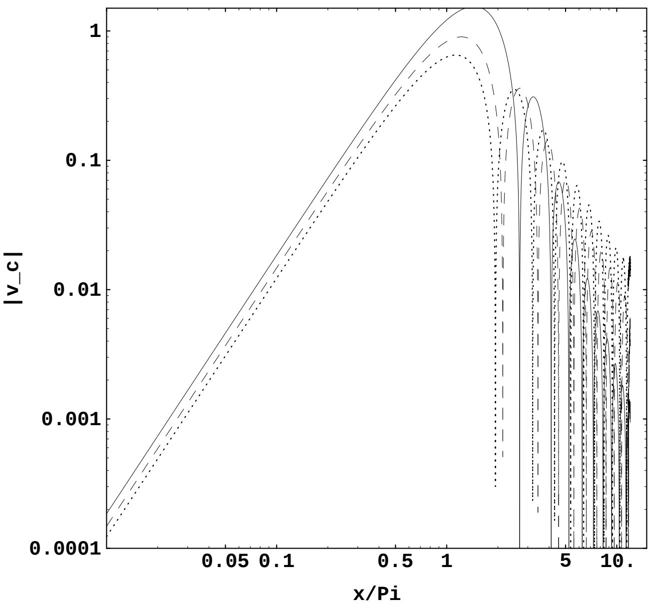

Figure 4.12: Vector perturbations in various spatial dimensions (as in Fig. 4.11).

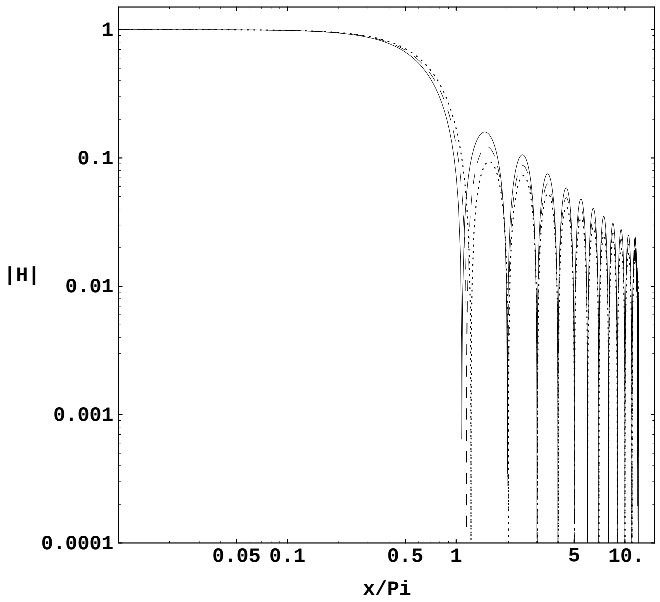

Figure 4.13: Tensor perturbations as in Fig. 4.11 and 4.12, but now the damping on subhorizon scales does not depend on the number of spatial dimensions.

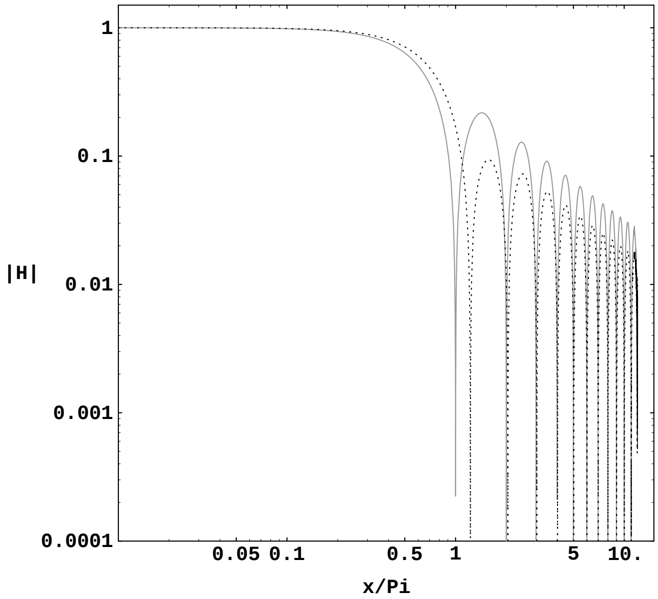

Figure 4.14: Comparison of tensor perturbations in a perfect fluid (fine dotted line) and a collisionless gas in three spatial dimensions (dotted line).

4.3 Weakly self-interacting matter

Let us discuss the modifications due to collisions in the plasma. In section 3.3 we obtained the contributions to the kernels of the integro-differential equations in order λ and $\lambda^{\frac{3}{2}}$.

Restricting the discussion to scalar perturbations with $n = 3$ and $\alpha = 1$, the effects of weak self-interactions might be relevant for HDM particles in the early universe. With the explict result for $K_1^{(0)}$ (3.20) and $K_{\frac{3}{2}}^{(0)}$ (3.22), which have a well-behaved power series representation, the same methods as in the preceding sections can be used to solve the coupled equations (4.4) and (4.5). Since $(K_1^{(0)} + K_{\frac{3}{2}}^{(0)})(x) \propto x^4 + O(x^6)$, $K^{(0)} = K_0^{(0)} + K_1^{(0)} + K_{\frac{3}{2}}^{(0)}$ still satisfies

$$K^{(0)}(0_+) = 1, \qquad K^{(0)}(0_+) + 3K^{(0)\prime\prime}(0_+) = 0 \ , \tag{4.19}$$

as did $K_0^{(0)}$. Therefore the conditions (4.13) on the initial data are left unchanged.

The behaviour of the singular solutions is modified by the weak self-

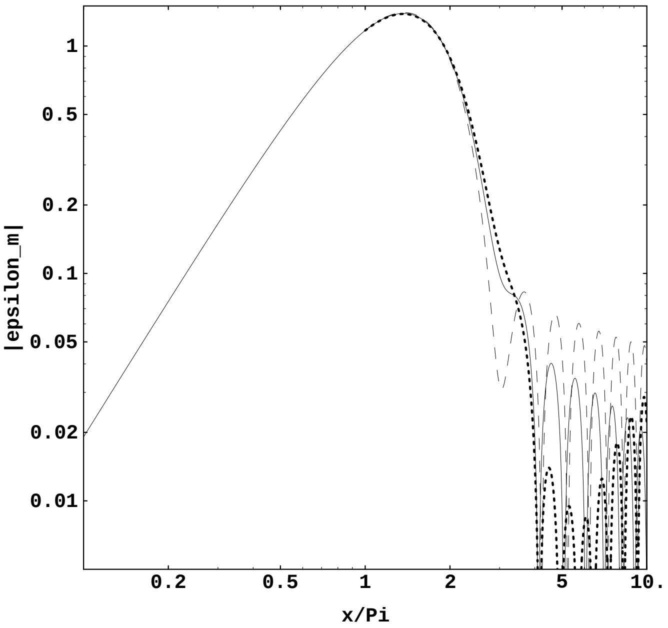

Figure 4.15: Collisional perturbations at the order λ $(=1)$ (dashed line) and order $\lambda^{\frac{3}{2}}$ (dotted line) are compared with collisionless perturbations (solid line). It is obvious that the order $\lambda^{\frac{3}{2}}$ contribution can not be neglected for such a big λ.

interactions, to wit,

$$\Phi, \Pi \sim x^{-5/2} \cos[\sqrt{\frac{27}{20} - \frac{2\lambda}{\pi^2} + \frac{21\lambda^{\frac{3}{2}}}{2\pi^3}} \ln(x)] \ , \tag{4.20}$$

up to a constant shift of phase.

With an ansatz like in sections 4.1 and 4.2 we obtain power series representations for the metric perturbations. For the particular initial condition determined by $\gamma_l = 0$, $l \geq 1$, with $\lambda = 1$ the solution for ϵ_m is shown in Fig. 4.15 by the dotted line up to $\lambda^{\frac{3}{2}}$. The contribution from the collisionless kernel $K_0^{(0)}$ is shown by the full line, whereas the contribution of the kernel up to order λ is plotted dashed. On superhorizon scales, $x \ll 1$, the solutions are dominated by the constant modes in Φ and Π. The amount of anisotropic pressure associated with a given density contrast is determined by $|\Pi/\Phi|$. With

$$\frac{\Pi(0)}{\Phi(0)} = \frac{-32805\lambda^{\frac{9}{2}} + 131220\lambda^4\pi - 262440\lambda^{\frac{7}{2}}\pi^2 + 324000\lambda^3\pi^3 -}{2\left(32805\lambda^{\frac{9}{2}} - 131220\lambda^4\pi + 262440\lambda^{\frac{7}{2}}\pi^2 - 324000\lambda^3\pi^3 +\right.} \tag{4.21}$$

$$
\frac{-267840\lambda^{\frac{5}{2}}\pi^4 + 149760\lambda^2\pi^5 - 53760\lambda^{\frac{3}{2}}\pi^6 + 10240\lambda\pi^7 - 8192\pi^9}{+267840\lambda^{\frac{5}{2}}\pi^4 - 149760\lambda^2\pi^5 + 53760\lambda^{\frac{3}{2}}\pi^6 - 10240\lambda\pi^7 + 28672\pi^9\Big)}
$$

$$
\sim \quad -\frac{1}{7}\left[1 - \frac{25\lambda}{28\pi^2} + \frac{75}{16}\left(\frac{\lambda}{\pi^2}\right)^{\frac{3}{2}} \mp O(\lambda^2)\right]
$$

it is seen to be reduced when λ increases form zero to a value of about 1/2. This is in agreement with intuitive expectation, since the collision-dominated case of a perfect fluid has $\Pi \equiv 0$. For larger values of λ the ratio (4.21) is decreasing again. There higher order terms are no longer neglegible.

For large $x \gg 1$, the asymptotic behaviour of the density contrast $\epsilon_{\rm m}(x)$ is proportional to the one of $K^{(0)}(x)$. In the collisionless case $K^{(0)}(x) = K_0^{(0)}(x) \sim \sin(x)/x$, whereas in the other extreme case of a perfect fluid $\epsilon_{\rm m} \sim \sin(x/\sqrt{3})$. With weak self-interactions the asymptotic behaviour is modified towards weaker damping at order λ (see Fig. 4.15 and 4.16), which ceases completely for sufficiently large x, where $K(x) \sim \lambda \cos(x)$. However, in this case the correction $K_1^{(0)}$ is overtaking the lowest order term $K_0^{(0)}$, which signals a possible breakdown of perturbation theory.

The convergence of perturbation theory gets worse including the order $\lambda^{\frac{3}{2}}$. For sufficiently large x we obtain $K^{(0)}(x) \sim \sqrt{x}\cos(x)$, which corresponds to anti-damping and clearly indicates the breakdown of perturbation theory (see dotted line in Fig. 4.15). The extremely strong damping between $x/\pi = 3$ and $x/\pi = 6$ in Fig. 4.15 is not reliable, either. It is clear that perturbation theory is not valid at $\lambda = 1$. In Fig. 4.16 ϵ_m is plotted for $\lambda = 1/10$. Again, for small $x/\pi > 1$ the solution including the order $\lambda^{\frac{3}{2}}$ is damped more strongly than the collisionless solution.

On subhorizon scales the convergence of the perturbation theory can be improved by ordering the kernel in powers of m/T instead of $\sqrt{\lambda}$. Using (3.15) the result reads,

$$
K^{(0)} = K_0^{(0)} + \frac{5m^2}{8\pi^2T^2}\widetilde{K}_1^{(0)} + \frac{15m^3}{8\pi^3T^3}\left(\widetilde{K}_1^{(0)} + \widetilde{K}_{\frac{3}{2}}^{(0)}\right) , \qquad (4.22)
$$

where the tilde indicates that the factors in front of the parenthesis in (3.20) and (3.22) are omitted. In the last term the cosines of (3.20) and (3.22) cancel. The asymptotic behaviour is still dominated by $xJ_{-1}(x)$, but on intermediate scales $x/\pi \sim 1$ the cosine cancelation improves the convergence considerably.

Inspecting the analytic structure that gives rise to the different asymptotic behaviour of $K^{(0)}(x)$, one finds that the discontinuity in the integrand of Eq. (3.20) and (3.22) is singular on the light-cone $\omega = \pm 1$. There are logarithmically singular terms which are responsible for $\kappa'(x) \sim \sin(x)\ln(x)/x$,

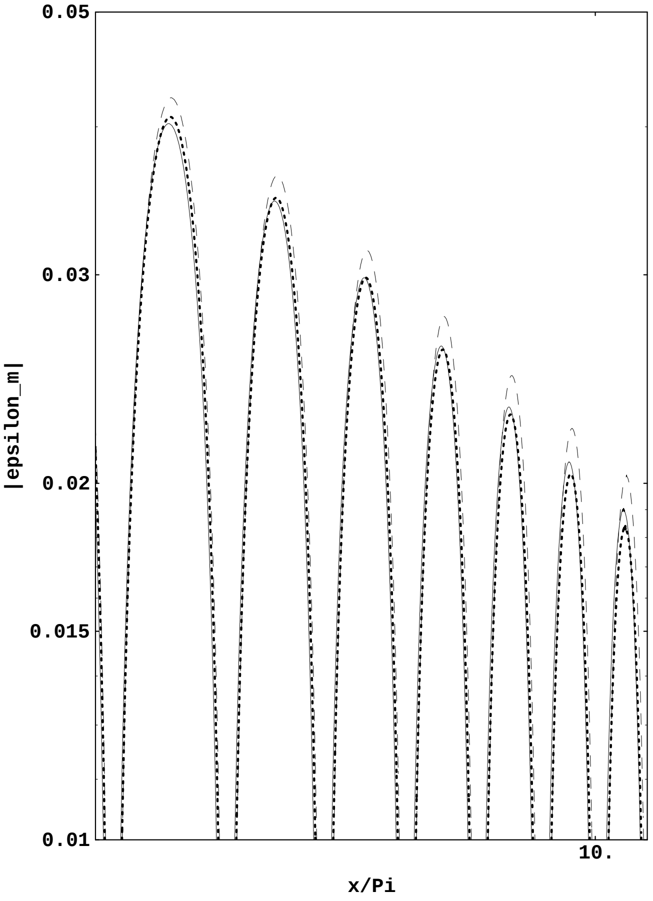

Figure 4.16: As Fig. 4.15, but for $\lambda = 1/10$.

$\nu(x)$ and $\xi(x)$ (κ' dominates over $\nu(x)$ and $\xi(x)$ for large x), the roots leading to the integer Bessel functions, and there are even poles at $\omega = \pm 1$, which contribute to the term involving the $\cos(x)$. However, the scalar particles, whose rest masses are negligible at sufficiently high temperature, acquire thermal masses m. A resummation of these should remove the singularities at $\omega = \pm 1$ which are associated with the masslessness of the scalar particles, but this did not happen in our calculation, because the high temperature expansion is in conflict with the scale set by the distance to the light cone. The limits $T/k \to \infty$ and $\omega \to \pm 1$ do not commute due to the divergencies at the light-cone [60].

Let us calculate the integrals involved in the one-loop diagrams more carefully to obtain the correct behaviour near the light-cone. The resummation of mass insertions replaces the leading-order result $K_0^{(0)}(x) = j_0(x)\theta(x)$ by

$$K_0^{\text{res.}}(x) = -\theta(x) \int_{-1}^{1} d\omega e^{-i\omega x} \times \int_{m/\sqrt{1-\omega^2}}^{\infty} dp\, p^4 \frac{d}{dp}\left(\frac{1}{\exp(p/T)-1}\right) \Big/ \left(\frac{8\pi^4 T^4}{15}\right) \tag{4.23}$$

up to terms whose amplitude is down by factors of λ. With a non-zero $m = \sqrt{\lambda} T$ the integrand is now seen to vanish at $\omega = \pm 1$, whereas before it was a constant; in fact, it vanishes together with all its derivatives, but rapidly recovers the bare one-loop value away from the light-cone. This is a negligible effect for small x, but the large x behaviour is dominated by the (non-analytic) integration region $|\omega| \approx 1$.

Eq. (4.23) can be evaluated by a Mellin transform [65], which yields

$$K_0^{\text{res.}}(x) = \theta(x)\frac{\sqrt{\pi}}{2}\frac{15}{8\pi^4} \times \sum_{k=0}^{\infty} \lambda^{k/2} \frac{(-1)^{1+k}(k-4)\zeta(k-3)}{(2\pi)^{k-4}\Gamma(1+k/2)} \left(\frac{2}{x}\right)^{\frac{1-k}{2}} J_{\frac{1-k}{2}}(x) \tag{4.24}$$

in the term concerning $k = 4$ one has to substitute $(k-4)\zeta(k-3) \to 1$. For small x,

$$K_0^{\text{res.}}(x) = \theta(x)\left(j_0(x) - \frac{5\lambda}{8\pi^2}\cos(x) + \frac{5\lambda^{\frac{3}{2}}}{8\pi^3} x J_{-1}(x)\right) + O(\lambda^2) \tag{4.25}$$

is a good approximation; for $x \gg 1$, on the other hand, the complete function $K_0^{\text{res.}}(x)$ turns out to decay slightly faster than $j_0(x)$, oscillating with a reduced phase velocity

$$v = 1 - \frac{5\lambda}{8\pi^2} + O(\lambda^{3/2}). \tag{4.26}$$

Restricting to the order λ contributions, a first approximation for a fully resummed calculation has therefore to change

$$K_0^{(0)}(x) \propto j_0(x) \to j_0((1-\frac{5\lambda}{8\pi^2})x),$$

which reduces

$$K_1^{(0)}(x) \to \frac{5\lambda}{4\pi^2}(\kappa' - j_0)(x)\theta(x)$$

up to higher orders in λ. However, the latter of the relations in Eq. (4.19) is now violated at the higher order $O(\lambda^2)$, which drastically restricts the solvability of the perturbation equations, resulting in a need for further modifications. It is a natural solution to change the phase velocity in $K_1^{(0)}$ by the same amount as in $K_0^{(0)}$ and to adjust the prefactor in $K_1^{(0)}$ appropriately. This leads in a unique manner to the remarkably simple result

$$K^{\text{res.}}(x) = \left(j_0 + \frac{1-v^2}{v^2}(\kappa' - j_0)\right)(vx)\,\theta(x). \tag{4.27}$$

Up to and including order λ, this is the same as $K_0^{(0)} + K_1^{(0)}$. But now the asymptotic behaviour of $\epsilon_{\rm m}(x)$ for large x, which is linked to $K^{(0)}(x)$, is about $\kappa'(vx) \sim \sin(vx)\ln(x)/x$. Thus, there is still strong damping of subhorizon-scale oscillations, which is only logarithmically weaker than in the collisionless case. Moreover, the phase velocity v is now smaller than 1, as one may expect from the comparison with the strongly collisional case of a perfect radiation fluid, where (undamped) acoustic waves oscillate with $v = 1/\sqrt{3}$. In Fig. 4.17 the effects of the above resummation are shown for $x/\pi > 1$. Note that only for the leading order in λ the whole kernel can be rewritten in terms of the phase velocity v. At higher orders the explicit λ (or m/T) dependence of the kernel cannot be avoided.

Similar issues also arise also in the case of vector (rotational) as well as tensor perturbations (primordial gravitational waves). For small x weak self-interactions mainly affect the singular solutions, and the same shift of frequency of the superhorizon oscillation occurs as in Eq. (4.20); for large x vector and tensor perturbations differ from the scalar case in such a way that their asymptotic behaviour is not changed that much. Sticking to leading order in λ, subhorizon-scale vector perturbations still have vorticity decaying $\sim \sin(x)/x$, and resummation only changes the phase velocity; tensor perturbations are stable against the kind of resummation performed above, and have the same asymptotic behaviour as the collisionless ones, which already equals the perfect fluid behaviour.

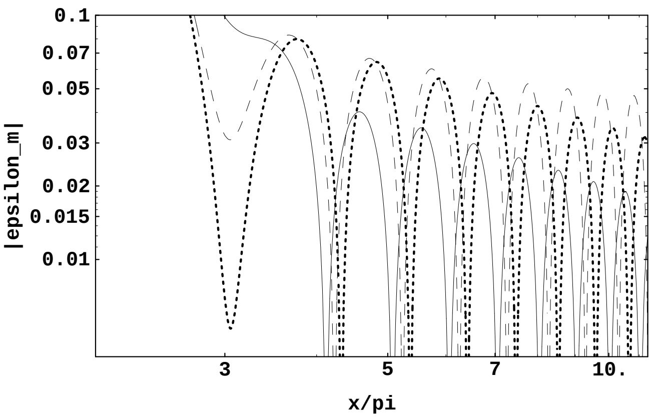

Figure 4.17: The solid line and the dashed line are the same as in Fig. 4.15, the dotted line shows the solution with the resummed kernel at order λ ($\lambda = 1$).

Chapter 5

Conclusion and outlook

We have presented a detailed analytical study of cosmological perturbations of an Einstein-de Sitter universe filled with a relativistic plasma of massless particles and a perfect radiation fluid in terms of the gauge-invariant variables of Bardeen. A closed set of equations for the latter has been derived within the approach based on thermal field theory on a curved background (Sec. 2). The response of matter under metric perturbations is determined by the thermal graviton two-point function, its leading terms in a high-temperature expansion describe ultrarelativistic collisionless matter at the one loop level (Sec. 3.1). Higher loops introduce collisional matter. As a toy model, we have studied a minimally coupled scalar field (Sec. 3.2). For collisionless matter we have found complete equivalence with classical kinetic theory (Sec. 3.3), if the latter is recast in terms of gauge invariant quantities along the lines of Ref. [40]. A conceptual advantage of the thermal-field-theory approach appears to be its purely geometrical character — no explicit recourse to the generally gauge-variant distribution functions of kinetic theory is required.

In extension of the work of Refs. [41, 45] we have given the general solutions of the linear perturbation equations in terms of generalized power series expansions (Sec. 4), the asymptotic behaviour of which has been obtained previously in Ref. [37]. In a strictly FLRW setting only the regular solutions are admitted, but the general solutions are required to match earlier, inflationary epochs, where the initial perturbations may have been generated quantum-mechanically [66].

With special emphasis on the role of the initial data (Sec. 4.1) we have also presented a selection of explicit results for regular and singular solutions for scalar, vector, and tensor cosmological perturbations. Typically, the regular solutions exhibit growth on superhorizon scales $\sim x^l$, with l a characteristic integer, which can be increased by special choices of the initial data. The singular solutions have a small-x behaviour dictated only by the ratio α, which gives the ratio between the energy-density in collisionless matter and the total one. For $\alpha > 5/32$ there is an essential singularity for $x \to 0$, giving rise to superhorizon oscillations, whereas for $\alpha \leq 5/32$ all perturbations have a (singular) power-law behaviour for small x. After horizon-crossing all types of perturbations that are carried by collisionless matter decay. In the scalar and vector case this is due to directional dispersion, whereas tensor perturbations only decrease according to the expansion of the FRLW universe. We have found that the transition between superhorizon and subhorizon regimes rather strongly depends on the initial data. While previous investigations have always considered the simplest cases only, our results indicate that the effective matching of the asymptotic regimes can vary considerably by allowing more complicated initial matter distributions.

In section 4.2 the dependence on the number of spatial dimensions was investigated. We found that superhorizon oscillations in the singular solutions can occur for $n < 17$ only. On subhorizon scales the amount of damping due to directional dispersion depends on the dimension n for scalar and vector perturbations. The behaviour of tensor perturbations after horizon crossing is determined by energy conservation and does not depend on the dimension of space.

The effects found from collisions (Sec. 4.3) are a change in the phase velocity and a weaker damping at subhorizon scales. The amplitude of anisotropic pressure is diminished in comparison to the collisionless case. In the limit of strongly interacting particles the perturbations should behave like a perfect fluid, i.e. constant amplitude of the density perturbation, no anisotropic pressure and phase velocity $1/\sqrt{3}$. The phase velocity of the singular solutions at superhorizon scales changes due to the collisions.

It is clear that our study of effects of ultrarelativistic plasmas has not been exhaustive. For collisional matter the resummation of perturbation theory has to be improved in order to obtain the correct asymptotic behaviour of cosmological perturbations. Probably, this is out of the scope of perturbation theory. It might be of help to understand the relation between thermal field theory and the Boltzmann equation with a non-vanishing collision term.

To understand the evolution of cosmological perturbations for HDM within the thermal field theory approach, massive particles should be included. This means to calculate the next-to-leading order contributions to the graviton self-energy, i.e. m^2T^2, k^2T^2. At temperatures $T \sim m$ and below these terms start to dominate. In flat space-time these contributions were calculated in [55]. This introduces a critical scale for massive, collisionless particles. The perturbations exceeding this critical scale — the collisionless Jeans length (see e.g. [11]) — grow (e.g. [39]). Perturbations below that scale are damped by free streaming (see section 2.4.1). The additional scale set by m breaks the conformal symmetry of the high temperature limit non-locally. Therefore a method to calculate the graviton self-energy directly in curved space-time has to be developed.

Up to now we have restricted our attention to $\kappa = 0$ FLRW models, especially the Einstein-de Sitter model. It would be interesting to extend the thermal field theory approach to $\kappa = \pm 1$. The spatial curvature introduces an additional scale

$$\ell_{\rm curv} = S|\kappa|^{-\frac{1}{2}} = H^{-1}|\Omega - 1|^{-\frac{1}{2}} \ .$$

For $\kappa = +1$ only discrete values of k are allowed. Another modification may result from the addition of a small cosmological constant. This again introduces a new scale $\Lambda^{-\frac{1}{2}}$. In both cases we might expect that the conformal invariance of the effective action holds, because $T \gg \ell_{\rm curv}^{-1}$ and $\Lambda^{\frac{1}{2}}$. But these scales are comparable with the scale of cosmological perturbations k. Therefore the solutions will depend on k explicitly. For $\kappa = 0$ they depend on the conformally invariant variable x only.

In the introduction we mentioned Kaluza-Klein cosmologies as a motivation to study higher dimensional cosmological models. The theory of cosmological perturbations within these models and within anisotropic models in three spatial dimensions [67] is much more complicated. Evolution of scalar, vector, and tensor perturbations is no longer independent. The gravitational perturbations can act as a source for the scalar ones. The question of a gauge-invariant description of the perturbations is not settled, either. There is no set of useful gauge-invariant variables for general anisotropic models. The Biancchi I universes and their higher dimensional analoga seem to be the exception [68].

In the FLRW models such a mixing of scalar, vector, and tensor perturbations will occur at the next order ('quadratic' perturbations). This will come into play when the linear perturbations are of order unity (in our figures that was the case, but our normalization was arbitrary!), or when the linear contribution is suppressed, as it happens for anisotropic pressure and vector perturbations in a perfect fluid universe. A study of these will involve the graviton three-point effective vertex, which has already been calculated in flat space-time by Taylor and Frenkel (third citation in [54]).

Appendix A

Notations

Below a list of the most important symbols of the text is given.

c	speed of light
c_{s}	speed of sound (1.21)
d_{h}	distance to the horizon (1.6)
g_*	number of thermal degrees of freedom
$g_{\mu\nu}$	metric tensor
h	cf. H_0
k_{B}	Boltzmann constant
ℓ_{H}	Hubble length
ℓ_{J}	Jeans wave length
ℓ_{Planck}	Planck length
m_{Planck}	Planck mass
n	dimension of space
u_μ	fluid velocity
v_{c}	amplitude of matter velocity related to vorticity
$v_{\mathrm{s}}^{(a)}$	amplitude of matter velocity related to shear
w	ratio of background pressure and energy density
z	redshift
E	energy density
G	gravitational constant
$G^{\mu\nu}$	Einstein tensor [below (1.9)]
H	expansion rate *or*
H	metric potential for tensor perturbations
H_0	todays value of H — Hubble constant (1.1)
P	pressure
S	cosmic scale factor
T	temperature
$T^{\mu\nu}$	energy momentum tensor (1.10)

δ	density contrast (1.19)
ε	cf. (1.17)
ϵ_m	gauge-invariant density contrast in the rest frame of matter
ϵ_g	gauge-invariant density contrast on Newtonian slicing
η	entropy perturbation
$\eta_{\mu\nu}$	Minkowski metric tensor
κ	cf. (1.3)
$\pi_T^{(a)}$	anisotropic pressure
ϕ	Newtonian gravity potential
Π	scalar metric potential
Φ	scalar metric potential
Ψ	vector metric potential
Ω	cf. (1.14)
Ω_0	todays value of Ω

We use the following sets of coordinates:

t, r, θ_i	RW coordinates (1.3)
t, χ, θ_i	comoving coordinates (1.4)
τ, χ, θ_i	conformal coordinates (1.5)
T, R, θ_i	conformal-flat coordinates (1.8)

The surface element of a $n-1$ dimensional Euclidian sphere in (1.3) reads:

$$d\Omega_{n-1} = \prod_{i=1}^{n-1} \sin^{n-1-i}\theta_i d\theta_i$$

The surface itself is:

$$\Omega_{n-1} = \int d\Omega_{n-1} = \frac{2\pi^{\frac{n}{2}}}{\Gamma(\frac{n}{2})}$$

The definition of the curvature tensor is

$$R^{\mu}_{\nu\alpha\beta} = \Gamma^{\mu}_{\nu\beta,\alpha} - \Gamma^{\mu}_{\nu\alpha,\beta} + \Gamma^{\mu}_{\rho\alpha}\Gamma^{\rho}_{\nu\beta} - \Gamma^{\mu}_{\rho\beta}\Gamma^{\rho}_{\nu\alpha} \ ,$$

with the Christoffel symbol

$$\Gamma^{\alpha}_{\beta\gamma} = \frac{1}{2} g^{\alpha\mu}\left(g_{\mu\beta,\gamma} + g_{\mu\gamma,\beta} - g_{\beta\gamma,\mu}\right) \ .$$

The Ricci tensor and scalar read:

$$R_{\alpha\beta} = R^{\gamma}_{\alpha\gamma\beta} \quad \text{and } R = R^{\alpha}_{\alpha} \ .$$

Greek indices denote space-time tensor components and run from 0 to n. Latin indices from the middle of the alphabet denote space indices and run from 1 to n. The latin indices from the beginning of the alphabet denote indices corresponding to the tangent space of the space-time manifold.

The gravitational action reads:

$$S^G = \int d^{n+1}x \frac{\sqrt{-g}}{16\pi G} R$$

We neglect Gauss-Bonnet terms in higher dimensions. A cosmological constant can be taken care of by the energy-momentum tensor. The matter action reads for a scalar field:

$$S^M_\varphi = -\int d^{n+1}x \sqrt{-g} \frac{1}{2}(\partial_\mu \varphi \partial^\mu \varphi + m^2) \ .$$

In three spatial dimensions minimal coupling yields the interaction term

$$-\int d^4x \sqrt{-g} \lambda \varphi^4 \ .$$

The total action is $S^{\text{all}} = S^G + S^M$.

Appendix B

Integrals

B.1 Collisionless matter

Below we list all possible contractions of $I^{\alpha\beta\gamma\delta}$ in the high temperature limit ($\omega := \frac{k_0}{k}$):

$$
\begin{aligned}
I^{0000} &= \varepsilon(n)T^{n+1}\left(\frac{n-2}{2} - \frac{n+1}{2}F(\frac{1}{2},1;\frac{n}{2};\omega^{-2})\right) && \text{(B.1)}\\
I^{\nu\ \mu}_{\ \nu\ \mu} &= 0 && \text{(B.2)}\\
I^{00\mu}{}_{\mu} &= \varepsilon(n)T^{n+1} && \text{(B.3)}\\
I^{\alpha0\mu}{}_{\mu}K_\alpha &= \varepsilon(n)T^{n+1}\omega k && \text{(B.4)}\\
I^{\alpha000}K_\alpha &= -\varepsilon(n)T^{n+1}\frac{3}{2}\omega k && \text{(B.5)}\\
I^{\alpha\beta\mu}{}_{\mu}K_\alpha K_\beta &= \varepsilon(n)T^{n+1}\left(\omega^2+\frac{1}{n}\right)k^2 && \text{(B.6)}\\
I^{\alpha\beta00}K_\alpha K_\beta &= -\varepsilon(n)T^{n+1}\frac{1}{2}\left(3\omega^2-1\right)k^2 && \text{(B.7)}\\
I^{\alpha\beta\gamma0}K_\alpha K_\beta K_\gamma &= -\varepsilon(n)T^{n+1}\omega\left(\frac{3}{2}\omega^2-\frac{2n-1}{2n}\right)k^3 && \text{(B.8)}\\
I^{\alpha\beta\gamma\delta}K_\alpha K_\beta K_\gamma K_\delta &= \varepsilon(n)T^{n+1}\frac{1}{2}\left(1-\omega^2\right)\left(3\omega^2+\frac{3}{n}\right)k^4 && \text{(B.9)}
\end{aligned}
$$

These integrals have been calculated using the so-called Dzyaloshinski algorithm as described in [56].

B.2 Collisional matter

We introduce the operators

$$\Sigma_1 := T\sum_{p^0}\int\frac{dp^3}{(2\pi)^3}\Delta(P)\cdot \tag{B.10}$$

$$\Sigma_2 := T\sum_{p^0}\int\frac{dp^3}{(2\pi)^3}\Delta(P)\Delta(Q)\cdot\ , \tag{B.11}$$

with $Q := P - K$, K being the external momentum. The dot indicates the insertion of a function of the momenta P and Q. $\Delta(P)$ denotes the propagator in momentum space with the thermal mass m

$$\Delta(P) = \frac{-1}{P^2+m^2}\ . \tag{B.12}$$

The integrals have been evaluated in region II ($1 < \omega^2 < 4m^2/k^2 + 1$) in the limit $k \ll m$.

$$\frac{m}{T} = \lambda^{\frac{1}{2}} - \frac{3}{2}\frac{\lambda}{\pi^2} + \frac{9}{8}\left(\frac{\lambda}{\pi^2}\right)^{\frac{3}{2}}$$

has been substituted. The calculation was performed by a *Mathematica* program written by H. Nachbagauer. The procedure is the following:

(i) The program makes a partial fraction decomposition in p^0 of the kernel that has to be integrated.

(ii) With help of the formulas

$$T\sum_{p^0}\frac{1}{p^0-x} = -\mathrm{sign}(x)\left(\frac{1}{2}+n(|x|)\right)$$

$$T\sum_{p^0}\frac{1}{(p^0-x)^2} = -n'(|x|) \qquad |x|>0$$

the thermal sum is calculated. The first of the above formulas is not convegent as it is written, but it occurs only in combinations where the divergent part cancels and the above formula remains. Only terms contributing in the high temperature limit are kept. $n(|x|)$ denotes the Einstein-Bose distribution function.

(iii) In all integrals with $n(\sqrt{q^2+m^2})$ the variables q and p are interchanged.

(iv) The $\mathbf{p}$ integration is split up into a integration over the cosine $z := \mathbf{pk}/pk$ and k. The integration over z is performed after a partial fraction decomposition in p.

(v) The last step is the integration of p, which is reduced to a couple of integrals solved by hand and incorporated into the program.

The program was checked by calculating the imaginary parts of some of the integrals with the methods described in [60]. The real part can be obtained by analytic continuation or using the Cauchy theorem in the specific form (sometimes called the Kramers-Kronig relation):

$$\Re f(\omega) = \frac{1}{\pi}\mathsf{P}\int_{-\infty}^{\infty} d\omega' \frac{\Im f(\omega')}{\omega' - \omega}$$

Retarded boundary conditions are assumed for $f(z)$, i.e. $f(z) \to 0$ as $|z| \to \infty$ and $0 \le \arg(z) \le \pi$. The integral is defined by the principal value prescription.

The $\lambda^0 T^4$ contributions coincide with the results in B.1 for $n = 3$.

$$\Sigma_1 = \frac{T^2}{12}\left(-1 + 3\left(\frac{\lambda}{\pi^2}\right)^{\frac{1}{2}} - \frac{9\lambda}{2\pi^2} + \frac{27}{8}\left(\frac{\lambda}{\pi^2}\right)^{\frac{3}{2}}\right) \tag{B.13}$$

$$\Sigma_2 = \lambda^{-\frac{1}{2}}\frac{\sqrt{\omega^2 - 1}}{8\pi\left(\sqrt{\omega^2 - 1} + \omega\right)} \tag{B.14}$$

$$\Sigma_1 P^2 = \frac{\pi^2 T^4}{30}\left(\frac{5\lambda}{2\pi^2} - 15\left(\frac{\lambda}{\pi^2}\right)^{\frac{3}{2}}\right) \tag{B.15}$$

$$\Sigma_1 (p^0)^2 = \frac{\pi^2 T^4}{30}\left(-1 + \frac{5\lambda}{4\pi^2} - \frac{15}{4}\left(\frac{\lambda}{\pi^2}\right)^{\frac{3}{2}}\right) \tag{B.16}$$

$$\Sigma_1 (PK) p^0 = \frac{\pi^2 T^4}{30}\left(-1 + \frac{5\lambda}{4\pi^2} - \frac{15}{4}\left(\frac{\lambda}{\pi^2}\right)^{\frac{3}{2}}\right)\omega k \tag{B.17}$$

$$\Sigma_1 (PK)^2 = \frac{\pi^2 T^4}{30}\left[-\frac{1}{3} - \omega^2 + \frac{5\lambda}{4\pi^2}\left(1 + \omega^2\right) - \frac{5}{4}\left(\frac{\lambda}{\pi^2}\right)^{\frac{3}{2}}\left(5 + 3\omega^2\right)\right] k^2 \tag{B.18}$$

$$\Sigma_2 (PQ)^2 = \Sigma_2 P^2 Q^2 = \frac{\pi^2 T^4}{30}\left[-5\frac{\lambda}{\pi^2} + \left(\frac{\lambda}{\pi^2}\right)^{\frac{3}{2}}\left(30 + \frac{15\sqrt{\omega^2 - 1}}{4\left(\sqrt{\omega^2 - 1} + \omega\right)}\right)\right] \tag{B.19}$$

$$\begin{aligned}
\Sigma_2(PQ)p^0q^0 &= \Sigma_2 P^2(q^0)^2 = \Sigma_2(p^0)^2Q^2 = \\
&\frac{\pi^2T^4}{30}\left[1-\frac{5\lambda}{2\pi^2}\left(1-\omega Q_0(\omega)\right)+\right. \\
&\left.\frac{15}{2}\left(\frac{\lambda}{\pi^2}\right)^{\frac{3}{2}}\left(1-\omega Q_0(\omega)-\frac{\omega}{2\sqrt{\omega^2-1}}\right)\right] &\text{(B.20)} \\
\Sigma_2(PQ)p^0(QK) &= \Sigma_2(PQ)(PK)q^0 = \Sigma_2 P^2(QK)q^0 = \Sigma_2(PK)p^0Q^2 = \\
&\frac{\pi^2T^4}{30}\left[1-\frac{15}{4}\left(\frac{\lambda}{\pi^2}\right)^{\frac{3}{2}}\right]\omega k &\text{(B.21)} \\
\Sigma_2(PQ)(PK)(QK) &= \Sigma_2 P^2(QK)^2 = \Sigma_2(PK)^2Q^2 = \\
&\frac{\pi^2T^4}{30}\left[\frac{1}{3}+\omega^2-\frac{5\lambda}{2\pi^2}+\right. \\
&\left.\frac{5}{4}\left(\frac{\lambda}{\pi^2}\right)^{\frac{3}{2}}\left(11-3\omega^2\right)\right]k^2 &\text{(B.22)} \\
\Sigma_2(p^0q^0)^2 &= \frac{\pi^2T^4}{30}\left[\frac{1}{2}-2\omega Q_0(\omega)+\right. \\
&\frac{\lambda}{\pi^2}\left(\frac{15}{8}+\frac{5}{4\left(\omega^2-1\right)}\right)- \\
&\left.\left(\frac{\lambda}{\pi^2}\right)^{\frac{3}{2}}\left(\frac{45}{8}+\frac{15}{4\left(\omega^2-1\right)}+\frac{5\omega}{4\left(\omega^2-1\right)^{\frac{3}{2}}}\right)\right] &\text{(B.23)} \\
\Sigma_2(p^0)^2q^0(QK) &= \Sigma_2 p^0(PK)(q^0)^2 = \\
&\frac{\pi^2T^4}{30}\left[-\frac{3}{2}+\frac{15\lambda}{8\pi^2}-\frac{45}{8}\left(\frac{\lambda}{\pi^2}\right)^{\frac{3}{2}}\right]\omega k &\text{(B.24)} \\
\Sigma_2(PK)(QK)p^0q^0 &= \Sigma_2(PK)^2(q^0)^2 = \Sigma_2(p^0)^2(QK)^2 = \\
&\frac{\pi^2T^4}{30}\left[\frac{1}{2}-\frac{3\omega^2}{2}-\frac{5\lambda}{8\pi^2}\left(1-3\omega^2\right)+\right. \\
&\left.\frac{15}{8}\left(\frac{\lambda}{\pi^2}\right)^{\frac{3}{2}}\left(1-3\omega^2\right)\right]k^2 &\text{(B.25)} \\
\Sigma_2(PK)p^0(QK)^2 &= \Sigma_2(PK)^2(QK)q^0 = \\
&\frac{\pi^2T^4}{30}\left[\frac{5}{6}-\frac{3\omega^2}{2}-\frac{5\lambda}{8\pi^2}\left(1-3\omega^2\right)+\right. \\
&\left.\frac{5}{8}\left(\frac{\lambda}{\pi^2}\right)^{\frac{3}{2}}\left(1-9\omega^2\right)\right]\omega k^3 &\text{(B.26)}
\end{aligned}$$

$$
\begin{aligned}
\Sigma_2 (PK)^2 (QK)^2 &= \frac{\pi^2 T^4}{30}\left[\frac{1}{2}\left(3\omega^2+1\right)-\frac{15\lambda}{8\pi^2}\left(1+\omega^2\right)+\right. \\
&\left.\frac{15}{8}\left(\frac{\lambda}{\pi^2}\right)^{\frac{3}{2}}\left(5+3\omega^2\right)\right]\left(1-\omega^2\right)k^4 \qquad \text{(B.27)}
\end{aligned}
$$

$$
\begin{aligned}
\Sigma_2 p^0 q^0 &= \frac{T^2}{12}\left[\frac{1}{2}-\omega Q_0(\omega)+\right. \\
&\left.\left(\frac{3}{2}\left(\frac{\lambda}{\pi^2}\right)^{\frac{1}{2}}-\frac{9}{4}\frac{\lambda}{\pi^2}+\frac{27}{16}\left(\frac{\lambda}{\pi^2}\right)^{\frac{3}{2}}\right)\frac{\omega}{\sqrt{\omega^2-1}}\right] \qquad \text{(B.28)} \\
\Sigma_2 (PQ) &= \frac{T^2}{12}\left[1-\left(3\left(\frac{\lambda}{\pi^2}\right)^{\frac{1}{2}}-\frac{9\lambda}{2\pi^2}+\right.\right. \\
&\left.\left.\frac{27}{8}\left(\frac{\lambda}{\pi^2}\right)^{\frac{3}{2}}\right)\left(1+\frac{\sqrt{\omega^2-1}}{2\left(\sqrt{\omega^2-1}+\omega\right)}\right)\right] \qquad \text{(B.29)} \\
\Sigma_2 (PK)(QK) &= \frac{T^2}{12}\left[\frac{1}{2}-\frac{3}{2}\left(\frac{\lambda}{\pi^2}\right)^{\frac{1}{2}}+\frac{9}{4}\frac{\lambda}{\pi^2}-\right. \\
&\left.\frac{27}{16}\left(\frac{\lambda}{\pi^2}\right)^{\frac{3}{2}}\right]\left(1-\omega^2\right)k^2 \qquad \text{(B.30)} \\
\Sigma_2 p^0 (QK) &= \Sigma_2 (PK) q^0 = \frac{T^2}{12}\left[-\frac{1}{2}+\frac{3}{2}\left(\frac{\lambda}{\pi^2}\right)^{\frac{1}{2}}-\right. \\
&\left.\frac{9}{4}\frac{\lambda}{\pi^2}+\frac{27}{16}\left(\frac{\lambda}{\pi^2}\right)^{\frac{3}{2}}\right]\omega k \qquad \text{(B.31)}
\end{aligned}
$$

Appendix C

Recursion relations

To solve Eqs. (4.1) – (4.4), (4.6) and (4.7) the metric potentials $\Phi, \Phi_{\rm rp}, \Pi, \Psi$, and H are expanded into (generalized) power series. As mentioned in section 4.1 regular and singular solutions can be derived in such a way. Since the latter equations conserve the parity of the metric potentials, the regular solutions are calculated for the even and the odd part separately.

The recursion relations have been implemented in a *Mathematica* [69] code to calculate the first 60 coefficients and to plot the solutions in Figs. 4.1–4.10.

C.1 Scalar perturbations

The metric potentials are expanded into power series:

$$\Phi = \sum_{n=0}^{\infty}(-1)^n \frac{x^{2n}}{(2n)!}\left(\phi_n^{\rm even} + \frac{x}{(2n+1)}\phi_n^{\rm odd} + x^{\sigma^{(0)}}\phi_n^{\rm sing}\right) , \quad \text{(C.1)}$$

$$\Pi = \sum_{n=0}^{\infty}(-1)^n \frac{x^{2n}}{(2n)!}\left(\pi_n^{\rm even} + \frac{x}{(2n+1)}\pi_n^{\rm odd} + x^{\sigma^{(0)}}\pi_n^{\rm sing}\right) , \quad \text{(C.2)}$$

$$\Phi_{\rm cll} = \sum_{n=0}^{\infty}(-1)^n \frac{x^{2n}}{(2n)!}\left(q_n^{\rm even} + \frac{x}{(2n+1)}q_n^{\rm odd} + x^{\sigma^{(0)}}q_n^{\rm sing}\right) . \quad \text{(C.3)}$$

For simplicity $e_n := 2(\phi_n + \pi_n)$ (for regular even and odd solutions and for the singular solution) is defined. From Eq. (4.4), the relations

$$3(2n+1)\phi_n^{\rm even} = 3\phi_0^{\rm even} - e_0^{\rm even} - 3e_n^{\rm even} - \sum_{l=1}^{n-1}(2l+4)e_l^{\rm even} \quad \text{(C.4)}$$

$$3(2n+2)\phi_n^{\rm odd} = 2(3\phi_0^{\rm odd} - e_0^{\rm odd}) - 3e_n^{\rm odd} - \sum_{l=1}^{n-1}(2l+5)e_l^{\rm odd} \quad \text{(C.5)}$$

$$\begin{aligned}3(\sigma^{(0)}+2n+1)\phi_n^{\text{sing}} &= \frac{(2n)!\Gamma(\sigma^{(0)}+2)}{\Gamma(\sigma^{(0)}+2n+1)}(3\phi_0^{\text{sing}}-e_0^{\text{sing}})-3e_n^{\text{sing}}- \\ &\quad -\frac{(2n)!}{\Gamma(\sigma^{(0)}+2n+1)}\times \\ &\quad \sum_{l=1}^{n-1}\frac{\Gamma(\sigma^{(0)}+2l+1)(\sigma^{(0)}+2l+4)}{(2l)!}e_l^{\text{sing}} \qquad (C.6)\end{aligned}$$

determine Φ, with $n \geq 1$. For the odd regular solutions $2\phi_0^{\text{odd}} = -e_0^{\text{odd}}$ and the singular solutions obey $(\sigma^{(0)}+1)\phi_0^{\text{sing}} = -e_0^{\text{sing}}$. Together with $(n \geq 0)$

$$\begin{aligned}(2n+2)(2n+1)\pi_n^{\text{even}} &= -6\alpha\sum_{l=0}^{n-1}\frac{2l+2}{(2l+3)(2l+5)}e_{n-l}^{\text{even}}+ \\ &\quad +6\alpha(-1)^n\left[(2n+2)!\sum_{l=0}^{n+1}\frac{(-1)^l\beta_{2n-2l+2}^{(0)}}{(2l)!!(4n-2l+5)!!}+\right. \\ &\quad \left.+\,3(2n+4)!\sum_{l=0}^{n+2}\frac{(-1)^l\beta_{2n-2l+4}^{(0)}}{(2l)!!(4n-2l+9)!!}\right], \qquad (C.7) \\ (2n+3)(2n+2)\pi_n^{\text{odd}} &= -6\alpha\sum_{l=0}^{n}\frac{2l+2}{(2l+3)(2l+5)}e_{n-l}^{\text{odd}}+ \\ &\quad +6\alpha(-1)^n\left[(2n+3)!\sum_{l=0}^{n+1}\frac{(-1)^l\beta_{2n-2l+3}^{(0)}}{(2l)!!(4n-2l+7)!!}+\right. \\ &\quad \left.+3(2n+5)!\sum_{l=0}^{n+2}\frac{(-1)^l\beta_{2n-2l+5}^{(0)}}{(2l)!!(4n-2l+11)!!}\right], \qquad (C.8) \\ (2n+2)(2n+1)\pi_n^{\text{sing}} &= -6\alpha\frac{(2n+2)!}{\Gamma(\sigma^{(0)}+2n+3)}\times \\ &\quad \sum_{l=0}^{n}\frac{\Gamma(\sigma^{(0)}+2n-2l+1)(2l+2)}{(2n-2l)!(2l+3)(2l+5)}e_{n-l}^{\text{sing}} \qquad (C.9)\end{aligned}$$

from Eq. (4.3), Φ and Π can be calculated. The condition (4.13) has to be satisfied to gain regular solutions. The collisionless part of Φ, Φ_{rp}, is determined by Eq. (4.2). From the constant term of the latter equation

$$\phi_0^{\text{even}} + 2\pi_0^{\text{even}} = -4\beta_0^{(0)}$$

follows for the initial values. The higher terms give the relations $(n \geq 0)$:

$$\begin{aligned}(2n+2)(2n+1)q_n^{\text{even}} &= 6\alpha\left[\phi_{n+1}^{\text{even}}-e_{n+1}^{\text{even}}+\right. \qquad (C.10) \\ &\quad \left.\sum_{l=0}^{n}\left(\frac{1}{2l+1}+\frac{3}{(2l+3)(2n+3)}\right)e_{n-l+1}^{\text{even}}\right]+\end{aligned}$$

$$
\begin{aligned}
& +12\alpha(-1)^n \left[(2n+2)! \sum_{l=0}^{n+1} \frac{(-1)^l \beta^{(0)}_{2n-2l+2}}{(2l)!!(4n-2l+5)!!} - \right. \\
& \left. -3(2n+2)!(2n+4) \sum_{l=0}^{n+2} \frac{(-1)^l \beta^{(0)}_{2n-2l+4}}{(2l)!!(4n-2l+9)!!}\right] ,
\end{aligned}
$$

$$
\begin{aligned}
(2n+3)(2n+2)q_n^{\mathrm{odd}} &= 6\alpha \left[\phi^{\mathrm{odd}}_{n+1} - e^{\mathrm{odd}}_{n+1} + \right. \qquad \text{(C.11)} \\
& \left. \sum_{l=0}^{n+1} \left(\frac{1}{2l+1} + \frac{3}{(2l+3)(2n+4)}\right) e^{\mathrm{odd}}_{n-l+1}\right] + \\
& +12\alpha(-1)^n \left[(2n+3)! \sum_{l=0}^{n+1} \frac{(-1)^l \beta^{(0)}_{2n-2l+3}}{(2l)!!(4n-2l+7)!!} - \right. \\
& \left. -3(2n+3)!(2n+5) \sum_{l=0}^{n+2} \frac{(-1)^l \beta^{(0)}_{2n-2l+5}}{(2l)!!(4n-2l+11)!!}\right] ,
\end{aligned}
$$

$$
\begin{aligned}
(2n+2)(2n+1)q_n^{\mathrm{sing}} &= 6\alpha \left[\phi^{\mathrm{sing}}_{n+1} - e^{\mathrm{sing}}_{n+1} + \frac{(2n+2)!}{\Gamma(\sigma^{(0)}+2n+3)} \times \right. \qquad \text{(C.12)} \\
& \times \sum_{l=0}^{n+1} \left(\frac{1}{2l+1} + \frac{3}{(2l+3)(\sigma^{(0)}+2n+3)}\right) \times \\
& \left. \times \frac{\Gamma(\sigma^{(0)}+2n-2l+3)}{(2n-2l+2)!} e^{\mathrm{sing}}_{n-l+1}\right] .
\end{aligned}
$$

The perfect fluid component is provided by $\Phi_{\mathrm{pf}} = \Phi - \Phi_{\mathrm{rp}}$.

C.2 Vector perturbations

Analogously, the metric potential Ψ is split up:

$$
\Psi = \sum_{n=0}^{\infty} (-1)^n \frac{x^{2n}}{(2n)!} \left(\psi^{\mathrm{even}}_n + \frac{x}{(2n+1)} \psi^{\mathrm{odd}}_n + x^{\sigma^{(1)}} \psi^{\mathrm{sing}}_n\right) . \qquad \text{(C.13)}
$$

The regular even solutions are defined by

$$
\begin{aligned}
\left[(2n+2)(2n+1) + \frac{8\alpha}{5}\right] \psi^{\mathrm{even}}_n &= -24\alpha \sum_{l=1}^{n} \frac{\psi^{\mathrm{even}}_{n-l}}{(2l+3)(2l+5)} + \\
&+ 12\alpha(-1)^n \left[(2n+2)! \sum_{l=0}^{n+1} \frac{(-1)^l \beta^{(1)}_{2n-2l+2}}{(2l)!!(4n-2l+5)!!} + \right. \\
&+ \left. (2n+4)! \sum_{l=0}^{n+2} \frac{(-1)^l \beta^{(1)}_{2n-2l+4}}{(2l)!!(4n-2l+9)!!}\right] , \qquad \text{(C.14)}
\end{aligned}
$$

for $n \geq 0$. The solution for the regular odd part is provided for $n \geq 0$ by

$$\begin{aligned}
\left[(2n+3)(2n+2)+\frac{8\alpha}{5}\right]\psi_n^{\text{odd}} &= -24\alpha\sum_{l=1}^{n}\frac{\psi_{n-l}^{\text{odd}}}{(2l+3)(2l+5)}+ \\
&+ 12\alpha(-1)^n\left[(2n+3)!\sum_{l=0}^{n+1}\frac{(-1)^l\beta_{2n-2l+3}^{(1)}}{(2l)!!(4n-2l+7)!!}+\right. \\
&+ \left.(2n+5)!\sum_{l=0}^{n+2}\frac{(-1)^l\beta_{2n-2l+5}^{(1)}}{(2l)!!(4n-2l+11)!!}\right] . \qquad \text{(C.15)}
\end{aligned}$$

Additionaly the conditions (4.16) and (4.17) have to be satisfied. Singular solutions are fixed by ψ_0^{sing} and

$$\begin{aligned}
\left[n(2n+3)+2n\sigma^{(1)}\right]\psi_n^{\text{sing}} = -12\alpha\frac{(2n)!}{\Gamma(\sigma^{(1)}+2n+1)}\times \\
\times\sum_{l=1}^{n}\frac{\Gamma(\sigma^{(1)}+2n-2l+1)}{(2n-2l)!}\frac{\psi_{n-l}^{\text{sing}}}{(2l+3)(2l+5)} , \qquad \text{(C.16)}
\end{aligned}$$

for $n \geq 1$.

C.3 Tensor perturbations

For the metric potential H the ansatz

$$H=\sum_{n=0}^{\infty}(-1)^n\frac{x^{2n}}{(2n)!}\left(h_n^{\text{even}}+\frac{x}{(2n+1)}h_n^{\text{odd}}+x^{\sigma^{(2)}}h_n^{\text{sing}}\right) \qquad \text{(C.17)}$$

is made. Regular even solutions are defined by

$$\begin{aligned}
\left[(2n+1)2n+\frac{8\alpha}{5}\right]h_n^{\text{even}} &= 2n(2n-1)h_{n-1}^{\text{even}}-24\alpha\sum_{l=1}^{n-1}\frac{h_{n-l}^{\text{even}}}{(2l+1)(2l+3)(2l+5)}+ \\
&+ 3\alpha(-1)^n\left[(2n)!\sum_{l=0}^{n}\frac{(-1)^l\beta_{2n-2l}^{(2)}}{(2l)!!(4n-2l+1)!!}+\right. \\
&+ 2(2n+2)!\sum_{l=0}^{n+1}\frac{(-1)^l\beta_{2n-2l+2}^{(2)}}{(2l)!!(4n-2l+5)!!}+ \\
&+ \left.(2n+4)!\sum_{l=0}^{n+2}\frac{(-1)^l\beta_{2n-2l+4}^{(2)}}{(2l)!!(4n-2l+9)!!}\right] , \qquad \text{(C.18)}
\end{aligned}$$

for $n \geq 1$. The initial value $h_0^{\rm even}$ specifies the regular solution together with the inhomogeneous terms. The latter have to respect the condition (4.18). The solution for the regular odd part is provided for $n \geq 0$ by

$$\begin{aligned}\left[(2n+2)(2n+1)+\frac{8\alpha}{5}\right] h_n^{\rm odd} &= (2n+1)2nh_{n-1}^{\rm odd} \\ &- 24\alpha \sum_{l=1}^{n} \frac{h_{n-l}^{\rm odd}}{(2l+1)(2l+3)(2l+5)} + \\ &+ 3\alpha(-1)^n \left[(2n+1)! \sum_{l=0}^{n} \frac{(-1)^l \beta_{2n-2l+1}^{(2)}}{(2l)!!(4n-2l+3)!!} + \right. \\ &+ 2(2n+3)! \sum_{l=0}^{n+1} \frac{(-1)^l \beta_{2n-2l+3}^{(2)}}{(2l)!!(4n-2l+7)!!} + \\ &+ \left. (2n+5)! \sum_{l=0}^{n+2} \frac{(-1)^l \beta_{2n-2l+5}^{(2)}}{(2l)!!(4n-2l+11)!!}\right] . \quad \text{(C.19)}\end{aligned}$$

Singular solutions are fixed by $h_0^{\rm sing}$ and

$$\begin{aligned}\left[n(2n+1)+2n\sigma^{(2)}\right] h_n^{\rm sing} &= n(2n-1)h_{n-1}^{\rm sing} - \quad \text{(C.20)} \\ -12\alpha \frac{(2n)!}{\Gamma(\sigma^{(2)}+2n+1)} \sum_{l=1}^{n} &\frac{\Gamma(\sigma^{(2)}+2n-2l+1)}{(2n-2l)!} \frac{h_{n-l}^{\rm sing}}{(2l+1)(2l+3)(2l+5)} ,\end{aligned}$$

for $n \geq 1$.

Bibliography

[1] M. J. Geller and J. P. Huchra, Science **246** (1989) 897.

[2] P. J. E. Peebles, *The Large-Scale Structure of the Universe* (Princeton University Press, Princeton, 1980).

[3] P. J. E. Peebles, *Principles of Physical Cosmology* (Princeton University Press, Princeton, 1993).

[4] E. W. Kolb and M. S. Turner, *The Early Universe* (Addison-Wesley, Redwood City, 1990).

[5] J. Lequeux, in *Physical Cosmology*, Eds. R. Balian et al. (North-Holland, Amsterdam, 1980).

[6] J. C. Mather et al., Astrophys. J. **420** (1994) 439.

[7] G.F. Smoot et al., Astrophys. J. **396**, L1 (1992); C. L. Bennett et al., *Cosmic temperature fluctuations from two year of COBE DMR*, preprint astro-ph/9401012 (1994).

[8] D. Bailin and A. Love, Rep. Prog. Phys. **50** (1987) 1087.

[9] S. W. Hawking and G. F. R. Ellis, *The lage scale structure of space-time* (Cambridge University Press, Cambridge, 1980).

[10] G. F. R. Ellis, Gen. Rel. Grav. **2** (1971) 7.

[11] G. Börner, *The Early Universe: Facts and Fiction* (Springer, Berlin, 1993).

[12] J. I. Kapusta, *Finite-temperature field theory*, (Cambridge University Press, Cambridge, 1989).

[13] N. P. Landsman and Ch. G. van Weert, Phys. Rep. **145**, 141 (1987).

[14] C. W. Misner, Phys. Rev. Lett. **22**, 1071 (1969); V. A. Belinskii, I. M. Khalatnikov and E. M. Lifshitz, Adv. Phys. **19**, 525 (1970).

[15] V. N. Lukash, I. D. Novikov and A. A. Starobinskii, Sov. Phys. - JETP **42**, 757 (1976).

[16] J. Jeans, Philos. Trans. R. Soc. London A **199**, 491 (1902).

[17] P. Mészáros, Astron. Astrophys. **37**, 225 (1974).

[18] Y. B. Zeldovich and I. D. Novikov, *Relativistic Astrophysics Vol. 2: The Structure and Evolution of the Universe*, (The Univesity of Chicago Press, Chicago, 1983).

[19] E. R. Harrison, Phys. Rev. D **1**, 2726 (1970), Ya. B. Zel'dovich, Mon. Not. R. Astr. Soc. **160**, 1P (1972).

[20] E. Lifshitz, Zh. Eksp. Teor. Fiz. **16**, 587 (1946); E. Lifshitz and I. Khalatnikov, Adv. Phys. **12**, 185 (1963).

[21] G. F. R. Ellis and M. Bruni, Phys. Rev. D **40**, 1804 (1989); G. F. R. Ellis, J. Hwang, and M. Bruni, ibid. **40**, 1819 (1989); M. Bruni, P. K. S. Dunsby, and G. F. R. Ellis, Astrophys. J. **395**, 34 (1992).

[22] W. H. Press and E. T. Vishniac, Astrophys. J. **239**, 1 (1980).

[23] J. M. Stewart, Astrophys. J. **176**, 323 (1972).

[24] C. P. Ma and E. Bertschinger, *Cosmological perturbation theory in the synchronous vs conformal Newtonian gauge*, preprint astro-ph/9401007 (1994).

[25] B. Rose, S. Rahmstorf, and H. Dehnen, Gen. Rel. Grav. **20**, 1193 (1988); B Rose and H. Dehnen, ibid. **21**, 705 (1989); B. Rose and M. Corona-Galindo, ibid. **23**, 1317 (1991); B. Rose, ibid. **25**, 503 (1993).

[26] J. M. Bardeen, Phys. Rev. D **22**, 1882 (1980).

[27] V. F. Mukhanov, H. A. Feldman, and R. H. Brandenberger, Phys. Rep. **215**, 203 (1992).

[28] J. M. Stewart and M. Walker, Proc. R. Soc. Lond. A **341**, 49 (1974).

[29] J. M. Stewart, Class. Quantum Grav. **7**, 1169 (1990); L. Bombelli, W. E. Couch, and R. J. Torrence, ibid. **11**, 139 (1994).

[30] H. Kodama and M. Sasaki, Prog. Theor. Phys. Suppl. **78**, 1 (1984).

[31] R. Durrer and N. Straumann, Helv. Phys. Acta **61**, 1027 (1988).

[32] R. Durrer, *Gauge Invariant Cosmological Perturbation Theory*, Report No. ZU-TH14/92, 1993.

[33] L. F. Abbott and M. B. Wise, Nucl. Phys. **B237**, 226 (1984).

[34] P. J. E. Peebles and J. T. Yu, Astrophys. J. **162**, 815 (1970).

[35] J. Ehlers, in *General Relativity and Gravitation*, edited by R. K. Sachs (Academic Press, New York, 1971); J. M. Stewart, *Non-equilibrium Relativistic Kinetic Theory*, (Springer-Verlag, New York, 1971).

[36] P. J. E. Peebles, Astrophys. J. **180**, 1 (1973).

[37] A. V. Zakharov, Zh. Eksp. Teor. Fiz. **77**, 434 (1979).

[38] E. T. Vishniac, Astrophys. J. **257**, 456 (1982).

[39] J. R. Bond and A. S. Szalay, Astrophys. J. **274**, 443 (1983)

[40] M. Kasai and K. Tomita, Phys. Rev. D **33**, 1576 (1986).

[41] U. Kraemmer and A. Rebhan, Phys. Rev. Lett. **67**, 793 (1991).

[42] A. Rebhan, Nucl. Phys. **B351**, 706 (1991).

[43] See, e.g., O. A. Fonarev, Class. Quant. Grav. **11**, 2597 (1994); J. Math. Phys. **35**, 2105 (1994); K. Pirk and G. Börner, Class. Quant. Grav. **6**, 1855 (1989).

[44] D. J. Schwarz, Int. J. Mod. Phys. D **3**, 265 (1994).

[45] A. Rebhan, Nucl. Phys. **B369**, 479 (1992); in *Relativistic Astrophysics and Cosmology*, S. Gottlöber, J. P. Mücket, and V. Müller (eds.), (World Sci., Singapore, 1992) p. 137.

[46] A. Rebhan, Astrophys. J. **392**, 385 (1992).

[47] A. K. Rebhan and D. J. Schwarz, Phys. Rev. D **50**, 2541 (1994).

[48] D. J. Schwarz, *Exact solutions for cosmological perturbations with collisionless matter*, preprint gr-qc/9407007 (1994).

[49] H. Nachbagauer, A. K. Rebhan, and D. J. Schwarz, Phys. Rev. D **51**, R2504 (1995).

[50] H. Nachbagauer, A. K. Rebhan, and D. J. Schwarz, in preperation (1995).

[51] R. Durrer, Astron. Astrophys. **208**, 1 (1989).

[52] R. K. Schaefer, Int. J. Mod. Phys. A **6**, 2075 (1991).

[53] D. J. Gross, M. J. Perry, and L. G. Yaffe, Phys. Rev. D **25**, 330 (1982); Y. Kikuchi, T. Moriya, and H. Tsukahara, Phys. Rev. D **29**, 2220 (1984); P. S. Gribosky, J. F. Donoghue, and B. R. Holstein, Ann. Phys. (N.Y.) **190**, 149 (1989).

[54] J. Frenkel and J. C. Taylor, Z. Phys. C **49**, 515 (1991); F. T. Brandt, J. Frenkel, and J. C. Taylor, Nucl. Phys. **B374**, 169, (1992); F. T. Brandt and J. Frenkel, Phys. Rev. D **47**, 4688 (1992); **48**, 4980 (1993).

[55] A. P. de Almeida, F. T. Brandt, and J. Frenkel, Phys. Rev. D **49**, 4196 (1994).

[56] I. E. Dzyaloshinski, Zh. Eksp. Teor. Fiz. **42**, 1126 (1962); R. D. Pisarski, Nucl. Phys. **B309**, 476 (1988); J. Frenkel and J. C. Taylor, Nucl. Phys. **B334**, 199 (1990).

[57] E. D. Carlson, M. E. Machacek, and L. J. Hall, Astrophys. J. **398**, 43 (1992).

[58] A. A. de Laix, R. J. Scherrer, and R. K. Schaefer, *Constraints on self-interacting dark matter*, preprint astro-ph/9502087 (1994).

[59] E. Braaten and R. D. Pisarski, Nucl. Phys. **B337**,569 (1990).

[60] U. Kraemmer, A. K. Rebhan, and H. Schulz, Ann. Phys. (N.Y.) 238, 286 (1995).

[61] R. W. Linquist, Ann. Phys. (N.Y.) **37**, 487 (1966).

[62] J. Bernstein, *Kinetic Theory in the Expanding Universe*, (Cambridge University Press, Cambridge, 1988).

[63] S. R. de Groot, W. A. van Leeuwen, and Ch. G. van Weert, *Relativistic Kinetic Theory*, (North-Holland Publishing Company, Amsterdam, 1980).

[64] B. J. T. Jones, Rev. Mod. Phys. **48**, 107 (1976).

[65] B. Davies, *Integral Transforms and Their Applications*, (Springer-Verlag, New York, 1978).

[66] L. P. Grishchuk, Sov. Phys. - JETP **40**, 409 (1975); Phys. Rev. D **48**, 5581 (1993); ibid. **50**, 7154 (1994) N. Deruelle and V. F. Mukhanov, *On matching conditions for cosmological perturbations*, preprint gr-qc/9503050 (1995).

[67] T. E. Perko, R. A. Matzner, and L .C. Shepley, Phys. Rev. D **6**, 969 (1972).

[68] R. B. Abbott, B. Bednarz, and S. D. Ellis, Phys. Rev. D **33**, 2147 (1986); K. Tomita and M. Den, Phys. Rev. D **34**, 3570 (1986).

[69] S. Wolfram, *Mathematica* 2nd Ed., (Addison-Wesley, Redwood City, 1991).

Curriculum Vitae

Name: Dominik Johannes Schwarz

Title: Diplom-Ingenieur (Dipl.-Ing.)

Address: Rochusgasse 6/8, A-1030 Wien

1968-01-15 birth in Vienna

1994-06-04 marriage to Dipl.-Ing. Petra Renate Lutter

General Education:

- **1974 – 1978** Volksschule
- **1978 – 1986** Bundesrealgymnasium Wien 3
- **1986-06-04** Matura (finals)

Languages: German, English

Scientific Education:

- **1986 – 1991** studies of "Technische Physik" at the Vienna University of Technology
- **1991-06-07** diploma examination with excellent success (diploma thesis: "R^2-Gravitation in zwei Dimensionen"); Prof. W. Kummer (supervisor) and Prof. P. Skalicky
- **1991 – 1995** Doktoratsstudium (Ph.D. studies) at the Vienna University of Technology (supervisor: Prof. A. K.-Rebhan)

Scientific Carreer:

- **1989-11-06 – 1992-09-10** Vertragsbediensteter (librarian) at the Institut für Theoretische Physik (Vienna University of Technology)
- **1991-10-1 – 1992-01-31** Tutor (teaching assistant) for fundamental courses of Mathematics at the Institut für Angewandte und Numerische Mathematik (Vienna University of Technology)
- **since 1993-10-01** Vertragsassistent (research assistant) at the Institut für Theoretische Physik (Vienna University of Technology)

1989 – 1991 spokesman of the local students-of-Physics organization

since 1992 member of the "Österreichische Physikalische Gesellschaft"